UNIVERSIDADE
ESTADUAL DE LONDRINA

PEDRO MARETI MAÇAIRA FÍGARO

MALATION E CICLOSPORINA A ALTERAM A MORFOFISIOLOGIA RENAL E HEPÁTICA EM MODELOS DE ROEDOR

Londrina
2021

PEDRO MARETI MAÇAIRA FÍGARO

MALATION E CICLOSPORINA A ALTERAM A MORFOFISIOLOGIA RENAL E HEPÁTICA EM MODELOS DE ROEDOR

Dissertação apresentada ao Programa de Pós-Graduação em Patologia Experimental da Universidade Estadual de Londrina, como requisito à obtenção do título de Mestre em Patologia Experimental.

Orientadora: Profa. Dra. Glaura Scantamburlo Alves Fernandes
Coorientador: Prof. Dr. Fábio Goulart de Andrade

Londrina
2021

Ficha de identificação da obra elaborada pelo autor, através do Programa de Geração Automática do Sistema de Bibliotecas da UEL

F437m Fígaro, Pedro Mareti Maçaira;.

Malation e Ciclosporina A alteram a morfofisiologia renal e hepática em modelos de roedor. / Pedro Mareti Maçaira; Fígaro. - Londrina, 2021.

72 f. : il.

Orientador: Glaura Scantamburlo Alves Fernandes.

Coorientador: Fábio Goulart de Andrade.

Dissertação (Mestrado em Patologia Experimental) - Universidade Estadual de Londrina, Centro de Ciências Biológicas, Programa de Pós-Graduação em Patologia Experimental, 2021.

Inclui bibliografia.

1. Nefrotoxicidade - Tese. 2. Hepatotoxicidade - Tese. 3. Morfofisiologia - Tese. 4. Estresse oxidativo - Tese. I. Fernandes, Glaura Scantamburlo Alves . II. Andrade, Fábio Goulart de . III. Universidade Estadual de Londrina. Centro de Ciências Biológicas. Programa de Pós-Graduação em Patologia Experimental. IV. Título.

CDU 616

PEDRO MARETI MAÇAIRA FÍGARO

MALATION E CICLOSPORINA A ALTERAM A MORFOFISIOLOGIA RENAL E HEPÁTICA EM MODELOS DE ROEDOR

Dissertação apresentada ao Programa de Pós-Graduação em Patologia Experimental da Universidade Estadual de Londrina, como requisito à obtenção do título de Mestre em Patologia Experimental.

BANCA EXAMINADORA

____
Orientadora: Profa. Dra Glaura
Scantamburlo Alves Fernandes
Universidade Estadual de Londrina – UEL

____
Prof. Dr. Fábio Rodriguês Ferreira Seiva
Universidade Estadual do Norte do Paraná –
Campus Luiz Meneghel - UENP

____
Profa. Dra. Adriana Souza Torsoni
Universidade Estadual de Campinas,
Faculdade de Ciências Aplicadas - UNICAMP

Londrina, 14 de junho de 2021

AGRADECIMENTOS

Agradeço a Deus por todas as oportunidades que me foram concebidas e por sempre estar ao meu lado. Agradeço a minha orientadora Prof. Dr. Glaura Scantamburlo Alves Fernandes por ter me guiado pelos melhores caminhos e por investir seu tempo durante todo este período.

Também agradeço ao meu coorientador Prof. Dr. Fábio Goulart de Andrade, por sempre estar presente e acreditar no meu potencial.

Agradeço a todos os membros do Departamento de Histologia do Centro de Ciências Biológicas. Agradeço a CNPq pela bolsa de estudos, que contribuíram muito para minha formação e dedicação à pesquisa. Agradeço a todos os meus colegas de laboratório, sem os quais a realização deste trabalho não seria possível.

Agradeço a minha namorada Maria Vitoria por estar junto a mim nos momentos mais difíceis, por me motivar e por ser minha companheira em todos os momentos. À minha família, por sempre acreditarem no meu potencial, pelo suporte financeiro e por superarem todos os obstáculos para que eu pudesse me formar. Agradeço também aos meus pais, por todo apoio e por acreditar nos meus sonhos.

FÍGARO, Pedro Mareti Maçaira; **Malation e Ciclosporina A alteram a morfofisiologia renal e hepática em modelos de roedor**. 2021. 109 páginas. Dissertação de Mestrado (Programa de Pós-Graduação em Patologia Experimental) – Universidade Estadual de Londrina, Londrina, 2021.

RESUMO

O malation e a ciclosporina A são compostos utilizados para o controle de pragas na agricultura e para evitar a rejeição de órgãos transplantados, respectivamente. No entanto, ambos apresentam histórico de toxicidade. Assim, o objetivo deste trabalho foi avaliar as possíveis alterações histológicas, funcionais e no status antioxidante em rins e fígado de roedores expostos ao malation e à ciclosporina A. Para estudo dos efeitos do malation, utilizaram-se 18 ratos machos *Wistar* adultos distribuídos em 3 grupos (n=6): controle (C), recebeu água; malation 10 mg/kg (G10); malation 50 mg/kg (G50), tratados diariamente. Após o 41º dia experimental, os animais foram anestesiados e submetidos à eutanásia. Para avaliação da exposição à Ciclosporina A, 30 camundongos *Swiss* adultos foram tratados durante 10 e 50 dias, distribuídos em 5 grupos (n= 6): o grupo controle (C) recebeu água e o grupo CsA10i recebeu 10 mg/kg de CsA, ambos submetidos à eutanásia no 11º dia experimental; o grupo CsA10r recebeu 10 mg/kg de CsA, passou por período de recuperação de 10 dias e foi submetido à eutanásia no 21º dia experimental. Com relação ao período de 50 dias, o grupo CsA50i recebeu 10 mg/kg de CsA, e foi submetido à eutanásia no 51º dia experimental; o grupo CsA50r recebeu 10 mg/kg de CsA, passou por período de recuperação de 50 dias e foi submetido à eutanásia no 101º dia experimental. Em ambos experimentos, foram coletados: plasma, para as dosagens das concentrações de AST, ALT, ureia e creatinina; rins e fígado, para análise histopatológica e avaliação de biomarcadores de estresse oxidativo. A exposição ao malation causou aumento no diâmetro glomerular no grupo 50M e redução do espaço de Bowman no grupo 10M. No córtex renal, houve diminuição de glicogênio em ambas dosagens. No fígado, foi observado aumento das reservas de glicogênio na região periportal e centrolobular, nos grupos 10M e 50M. Referente à nefrotoxicidade e à hepatotoxicidade, os animais do grupo 50M apresentaram aumento das concentrações de AST, ALT e creatinina. Também foi observado aumento da atividade de GST hepática e da catalase renal, além de diminuição da atividade de SOD nos rins. Referente à exposição à CsA, verificou-se diminuição apenas no espaço de Bowman no grupo CsA10r e CsA50r. No fígado, houve aumento no diâmetro médio das vênulas centrolobulares nos grupos CsA10i e CsA10r, e da vênula porta, apenas no grupo CsA10r. Houve diminuição no diâmetro médio dos ductos biliares no grupo CsA50i, e dilatação dos sinusoides periportais e vênulas centrolobulares nos grupos CsA10i e CsA10r. A concentração de ureia aumentou no grupo CsA50r e as dosagens de ALT diminuíram no grupo CsA10i. A lipoperoxidação renal e hepática aumentou no grupo CsA50r, enquanto a GST renal diminuiu em todos os grupos tratados e no fígado houve diminuição apenas nos grupos CsA50i e CsA50r. Houve diminuição de SOD renal nos grupos CsA10i, CsA10r e CsA50i. Conclui-se que a exposição as doses de 10 mg/kg e 50 mg/kg de malation e 10 mg/kg de ciclosporina A provoca hepatotoxicidade e nefrotoxicidade em roedores machos.

Palavras-chave: Nefrotoxicidade. Hepatotoxicidade. Morfofisiologia. Estresse oxidativo

FÍGARO, Pedro Mareti Maçaira. **Malathion and Cyclosporin A alters renal and hepatic morphophysiology in rodent models**. 2021. 109 pages. Master's degree (Postgraduate Program in Experimental Pathology) – State University of Londrina, Londrina, 2021.

ABSTRACT

Malathion and cyclosporine A are compounds used to control pests in agriculture and to prevent rejection of transplanted organs, respectively. However, both have a history of toxicity. Thus, the objective of this work was to evaluate the possible histological, functional and antioxidant status changes in kidneys and liver of rodents exposed to malathion and cyclosporine A. To study the effects of malathion, 18 adult male Wistar rats were used, divided into 3 groups (n=6): control (C), received water; malation 10 mg / kg (G10); malation 50 mg / kg (G50), treated daily. After the 41st experimental day, the animals were anesthetized and euthanized. To assess the exposure to Cyclosporin A, 30 adult Swiss mice were treated for 10 and 50 days, divided into 5 groups (n=6): the control group (C) received water and the CsA10i group received 10 mg / kg of CsA, both subjected to euthanasia on the 11th experimental day; the CsA10r group received 10 mg/kg of CsA, went through a 10-day recovery period and was euthanized on the 21st experimental day. Regarding the 50-day period, the CsA50i group received 10 mg / kg of CsA and was euthanized on the 51st experimental day; the CsA50r group received 10 mg / kg of CsA, underwent a 50-day recovery period and was euthanized on the 101st experimental day. In both experiments, plasma was collected for the measurement of AST, ALT, urea and creatinine concentrations, kidneys, and liver, for histopathological analysis and evaluation of oxidative stress biomarkers. Exposure to malation caused an increase in the glomerular diameter in the 50M group and a reduction in Bowman's space in the 10M group. In the renal cortex, there was a decrease in glycogen at both dosages. In the liver, an increase in glycogen reserves was observed in the periportal and centrilobular regions, in the 10M and 50M groups. Regarding nephrotoxicity and hepatotoxicity, the animals in the 50M group showed increased concentrations of AST, ALT and creatinine. Increased activity of hepatic GST and renal catalase has also been observed, in addition to decreased activity of SOD in the kidneys. Regarding exposure to CsA, there was a decrease only in Bowman's space in the CsA10r and CsA50r group. In the liver, there was an increase in the average diameter of the centrilobular venules in the CsA10i and CsA10r groups, and of the portal venule, only in the CsA10r group. There was a decrease in the mean diameter of the bile ducts in the CsA50i group, and dilation of the periportal sinusoids and centrilobular venules in the CsA10i and CsA10r groups. The urea concentration increased in the CsA50r group, and the ALT measurements decreased in the CsA10i group. Renal and hepatic lipoperoxidation increased in the CsA50r group, while renal GST decreased in all treated groups and in the liver, there was a decrease only in the CsA50i and CsA50r groups. There was a decrease in renal SOD in the CsA10i, CsA10r and CsA50i groups. It is concluded that exposure to doses of 10 mg/kg and 50 mg/kg of malathion and 10 mg/kg of cyclosporin A causes hepatotoxicity and nephrotoxicity in male rodents.

Key words: Nephrotoxicity. Hepatotoxicity. Morphophysiology. Oxidative stress

LISTA DE ILUSTRAÇÕES

LISTA DE ABREVIATURAS E SIGLAS

CsA	Ciclosporina A
AST	Aspartato Aminotransferase
ALT	Alanina Aminotransferase
ERO	Espécies reativas de oxigênio
SOD	Superóxido dismutase
GST	Glutationa S-transferase
TBARS	Substâncias reativas ao ácido tiobarbitúrico

SUMÁRIO

1 INTRODUÇÃO

Estudos apontam que o malation é um dos principais inseticidas da classe dos organofosforados, responsável por intoxicações na vida adulta. Os efeitos tóxicos que estes pesticidas podem provocar no organismo estão diretamente relacionados à sua elevada utilização na agricultura, principalmente, nos indivíduos envolvidos no processo de aplicação do inseticida na lavoura ou que entram em contato de forma indireta com este químico. O período peripuberal é um importante marco no desenvolvimento pós-natal de vários órgãos, e pouco se sabe sobre os prejuízos causados aos indivíduos expostos a este pesticida durante esta etapa. Assim, é relevante verificar as alterações que o malation pode promover nos rins e fígado durante este período.

A Ciclosporina A (CsA) é um medicamento imunossupressor utilizado no tratamento de doenças autoimunes e para evitar rejeição de órgãos transplantados. Estudos apontam a sua possível utilização como contraceptivo masculino, dada sua capacidade em inibir a calcineurina, proteína que está diretamente associada a regulação da espermatogênese. No entanto, a CsA apresenta um histórico de toxicidade hepática e renal, dificultando seu uso para este propósito. Assim, para que este medicamento seja pesquisado para esta finalidade no futuro, faz-se necessária sua administração em baixa dose, para que não haja resposta imunossupressora e efeitos adversos, visto que sua toxicidade é dose dependente. Desta forma, torna-se relevante analisar as características renais e hepáticas, decorrentes da exposição à baixa dose de CsA.

Visando atingir os objetivos acima propostos, esta dissertação de mestrado foi elaborada em conformidade com as normas vigentes do Programa de Pós-Graduação em Patologia Experimental da Universidade Estadual de Londrina, sendo constituída por uma Revisão Bibliográfica e 2 artigos científicos baseados nas pesquisas experimentais realizadas. A estrutura geral deste trabalho está em conformidade com as normas da Associação Brasileira de Normas Técnicas (ABNT) para apresentação de trabalhos acadêmicos[1].

---

[1] ABNT - ASSOCIAÇÃO BRASILEIRA DE NORMAS TÉCNICAS. NBR 14724: informações e documentação - trabalhos acadêmicos - apresentação. Rio de Janeiro: ABNT, 2011.

2 REVISÃO BIBLIOGRÁFICA

2.1 Morfofisiologia Renal e Hepática

2.1.1 Aspectos histofisiológicos dos rins

O sistema urinário é composto por dois rins, dois ureteres, bexiga e uretra. Os rins são responsáveis pela filtração do sangue, removendo os dejetos metabólicos, apresentando grande importância na regulação da composição e do volume do líquido extracelular e do equilíbrio acidobásico (MOORTHY; BLICHFELDT, 2009; GARTNER; HIATT, 2017; JUNQUEIRA; CARNEIRO, 2017; RADI, 2019; VERSCHUREN et al., 2020). Além disso, são responsáveis por produzir a urina, inicialmente denominada ultrafiltrado, o qual é modificado por reabsorção seletiva e secreção específica. A urina em seu estado final contém água e eletrólitos, bem como ureia, ácido úrico, creatinina e outros produtos oriundos do metabolismo celular (KRICHEVSKY, 2005; ALLEN, 2008; VERSCHUREN et al., 2020).

Atividades endócrinas também são realizadas pelos rins, como a síntese de eritropoietina, responsável por regular a formação das hemácias em resposta à diminuição da tensão de oxigênio no sangue. Além disso, os rins produzem renina, enzima envolvida no controle da pressão arterial, do volume sanguíneo e na hidroxilação da vitamina D3 (MOORTHY; BLICHFELDT, 2009; ROSS, PAWLINA, 2016; GARTNER; HIATT, 2017).

Internamente, os rins são divididos em lobos, e cada um apresenta uma região cortical e uma região medular, nas quais o principal constituinte é denominado túbulo urinífero. O túbulo urinífero (Fig. 1), unidade funcional do rim, é uma estrutura envolvida por uma lâmina basal e altamente enovelada, a qual modifica o fluído que passa em seu interior, formando a urina como produto. Em seu trajeto pela região cortical, o túbulo urinífero é constituído pelo corpúsculo renal, túbulos contorcidos proximais e distais, enquanto na região medular são encontrados a alça de Henle e os ductos e túbulos coletores (ALLEN, 2008; GARTNER; HIATT, 2017; NAWATA; PANNABECKER, 2018).

Figura 1. Representação esquemática de túbulo urinífero

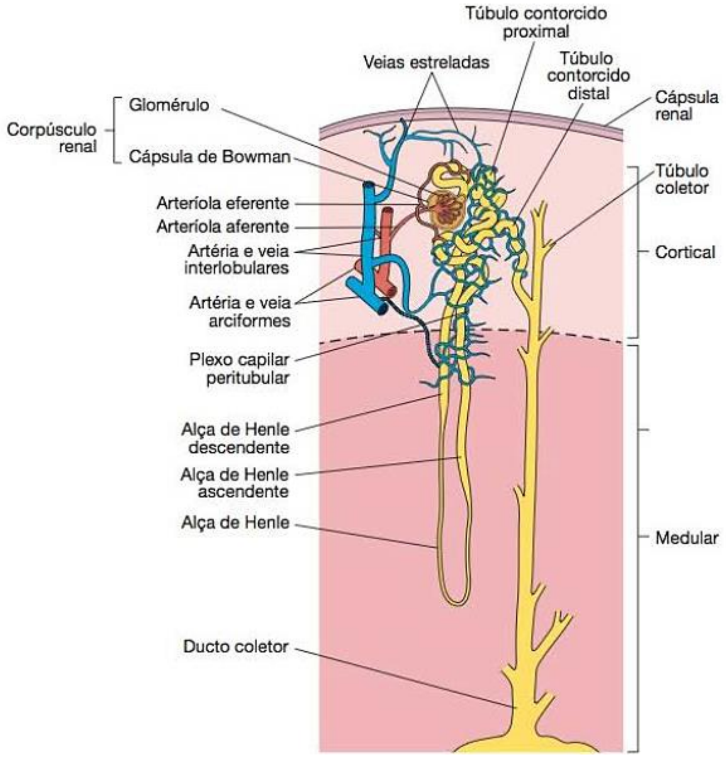

Fonte: JUNQUEIRA; CARNEIRO (2017).

Os néfrons são a unidade responsável pela filtração sanguínea, formados por uma parte dilatada – composta pelo corpúsculo renal ou de Malpighi –, pelo túbulo contorcido proximal, pelas partes delgada e espessa da alça de Henle e pelo túbulo contorcido distal (MOORTHY; BLICHFELDT, 2009; GARTNER; HIATT, 2017; JUNQUEIRA; CARNEIRO, 2017).

Os corpúsculos renais são estruturas esféricas, com aproximadamente 200 μm de diâmetro, que constituem o seguimento inicial do néfron. Cada corpúsculo renal tem um polo vascular pelo qual penetra a arteríola aferente e parte a arteríola eferente, e um polo urinário, no qual tem início o túbulo contorcido proximal. Ao penetrar o corpúsculo renal, a arteríola aferente divide-se em vários capilares, que constituem as alças glomerulares, constituintes do glomérulo (KRICHEVSKY, 2005; ALLEN, 2008; DUMAS et al., 2021). Os glomérulos apresentam um aglomerado de capilares compostos por 10 a 20 alças capilares, circundadas pela de cápsula de Bowman, constituída por um epitélio simples pavimentoso, que se apoia na lâmina basal a partir de uma fina camada de fibras reticulares.

A parte interna desta camada é chamada de folheto visceral, e é constituída por células especializadas, denominadas de podócitos. Estas células possuem um grande corpo celular, de onde se projetam numerosos prolongamentos que se interpenetram e se ancoram à lâmina basal dos capilares. Entre estes prolongamentos existem espaços denominados de fendas de filtração, cobertos por uma fina membrana de aproximadamente 6 nm de espessura, constituída por colágeno do tipo IV, glicocálice dos podócitos e a proteína nefrina, o que dificulta a passagem de moléculas aniônicas. (ALLEN, 2008; ROSS, PAWLINA, 2016; JUNQUEIRA; CARNEIRO, 2017). Além disso, nos glomérulos há células mesangiais, que são contráteis e possuem receptores para angiotensina II, cuja ativação promove a redução no fluxo sanguíneo glomerular. As células mesangiais também garantem o suporte estrutural ao glomérulo, sintetizam matriz extracelular e fagocitam e digerem substâncias que são retidas pela barreira de filtração, além de produzir prostaglandinas e endotelinas (KRICHEVSKY, 2005; ROSS, PAWLINA, 2016; RADI, 2019).

O túbulo contorcido proximal é o principal local onde ocorre a reabsorção (67% a 80% da água, sódio e cloreto, além de 100% das proteínas), recebendo o ultrafiltrado do espaço urinário da cápsula de Bowman. As células cúbicas deste túbulo possuem várias mitocôndrias alongadas em seu citoplasma e diversos microvilos, aumentando a sua superfície de contato e formando uma orla em escova. Estas estruturas estão diretamente envolvidas na absorção e no transporte de líquidos, sendo responsáveis pela reabsorção de Na^+, que cria um gradiente osmótico no interstício, favorecendo a reabsorção de água neste segmento do néfron (ALLEN, 2008; ROSS, PAWLINA, 2016; VERSCHUREN et al., 2020).

A alça de Henle é o segmento do néfron em forma de U que participa diretamente da retenção de água pelos rins. Esta estrutura é constituída por um ramo descendente e outro ascendente, sendo que cada ramo é formado por um segmento espesso e outro delgado. O lúmen desta região do néfron é largo, pois a sua parede é formada por um epitélio simples pavimentoso. Sua função é criar um gradiente de hiper osmolaridade no interstício medular, que influencia a concentração da urina, à medida em que passa pelos ductos coletores (ALLEN, 2008; ROSS, PAWLINA, 2016; RADI, 2019).

Após um curto trajeto na região cortical, o segmento espesso da alça de Henle torna-se tortuoso e constitui o túbulo contorcido distal. As células dos túbulos distais apresentam invaginações da membrana basolateral, onde se encontram inúmeras mitocôndrias. Além disso, estas células apresentam receptores para aldosterona, que atuam aumentando a reabsorção de Na^+ e de água, bem como a secreção de K^+ para o ultrafiltrado, com consequente elevação do volume sanguíneo e da pressão arterial. Neste local, também ocorre a reabsorção de íons bicarbonato, com secreção concomitante de íons hidrogênio, levando a uma maior acidificação da urina. (GARTNER; HIATT, 2017; JUNQUEIRA; CARNEIRO, 2017; VERSCHUREN et al., 2020).

Ao passar dos túbulos contorcidos distais para os túbulos coletores, a urina desemboca em tubos mais calibrosos, os ductos coletores, que se dirigem em direção às papilas renais. Em sua extensão, os túbulos coletores são formados por células pobres em organelas, porém repletas de pequenas mitocôndrias e vários canais de água, regulados pelo hormônio antidiurético. Desta forma, estes canais realizam a reabsorção de água, e contribuem diretamente para mudança de concentração da urina (JUNQUEIRA; CARNEIRO, 2017; NAWATA; PANNABECKER, 2018).

2.1.2 Aspectos histofisiológicos do fígado

O fígado é anatomicamente dividido em quatro lobos: direito, esquerdo, quadrado e caudado; apresenta superfície superior convexa e uma reentrância em sua região inferior, onde está localizada o hilo hepático (GARTNER, 2017; DANGELO; FATINI, 2007). Esta região é o local de entrada da veia porta e das artérias hepáticas (direita e esquerda), e saída do ducto biliar, de vasos linfáticos e da veia hepática (GARTNER, 2017; ROSS; PAWLINA, 2016).

O fígado participa do metabolismo proteico, com a produção de proteínas plasmáticas (albumina, globulina e fibrinogênio) e síntese de aminoácidos não essenciais (AIRES, 2012). Também participa do metabolismo dos ácidos graxos, do colesterol, de carboidratos, da síntese de ureia, de corpos cetônicos e é responsável pela produção da bile, que posteriormente será armazenada na vesícula biliar (KARANTH et al., 2018). Além disso, é capaz de inativar diversos hormônios, como a cortisona, a adrenalina e a noradrenalina. Também armazena substâncias como ferro, hemoglobina e vitaminas (JUNQUEIRA; CARNEIRO, 2017).

O fígado apresenta irrigação sanguínea dupla, uma vez que aproximadamente 70 a 80% do sangue que chega ao órgão provém da veia porta, e o restante através da artéria hepática (GUICCIARDI et al., 2013; MATHEW; VENKATESH, 2018). Estes vasos ramificam-se em estruturas de menor calibre: as vênulas portas interlobulares e as arteríolas hepáticas interlobulares, responsáveis por irrigarem os hepatócitos através de uma rede de capilares sinusoides. O sangue, então, é drenado às vênulas centrolobulares para que possa desembocar na veia cava inferior, alcançando outras regiões do organismo. (ROSS, PAWLINA, 2016; JUNQUEIRA; CARNEIRO, 2017; MAK; PNG, 2020).

O fígado é constituído por lóbulos (Fig. 2). Estas estruturas apresentam formatos poliédricos adjacentes, contendo uma vênula em posição central, denominada centrolobular e espaços-porta nos vértices. Os hepatócitos ficam dispostos em forma de cordões entre os espaços-porta e as vênulas centrolobulares, e por entre eles passam os capilares sinusoidais (KIERSZEMBAUM, 2004; ROSS, PAWLINA, 2016; KRUEPUNGA et al., 2019; MAK; PNG, 2020). Estes capilares possuem uma camada de células endoteliais fenestradas, separadas dos cordões de hepatócitos por um espaço conhecido como espaço de Disse, onde ocorre as trocas entre o sangue e estas células (ROSS, PAWLINA, 2016; JUNQUEIRA; CARNEIRO, 2017; WANG et al., 2017).

Figura 2. Representação da estrutura do lóbulo hepático

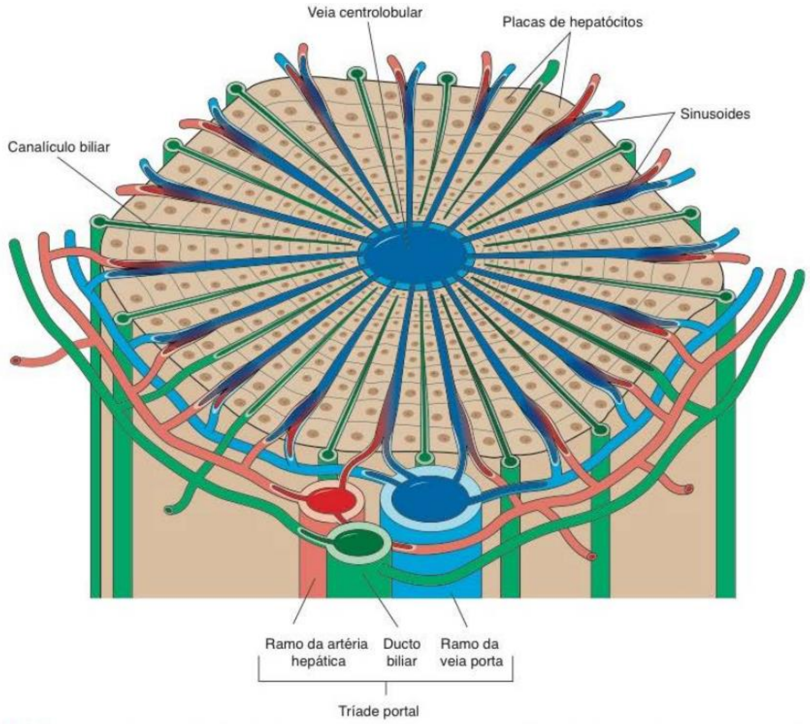

Fonte: JUNQUEIRA; CARNEIRO (2017).

Os hepatócitos constituem a unidade morfofuncional do fígado e representam cerca de 80% da população de células deste órgão. Por serem células muito ativas metabolicamente, apresentam núcleo grande e arredondado e citoplasma rico em organelas, com abundante retículo endoplasmático liso e rugoso e grande quantidade de mitocôndrias (LOWE; ANDERSON, 2015; JUNQUEIRA; CARNEIRO, 2017; WANG et al., 2017).

Os hepatócitos são capazes de degradar toxinas e xenobióticos, além de possuírem grande diversidade de enzimas responsáveis pelo metabolismo de fármacos. Estas enzimas modificam quimicamente os compostos, tornando-os inativos e facilitando a excreção. Esse processo é denominado biotransformação e ocorre em duas fases (GEBHARDT; MATZ-SOJA, 2014). A fase I ou fase de oxidação/redução ocorre no retículo endoplasmático liso e nas mitocôndrias dos hepatócitos. Consiste em processos de oxidação e redução que modificam a estrutura química. A reação oxidativa mais frequente é a hidroxilação (adição de um grupo hidroxila). Estas reações bioquímicas envolvem uma família de proteínas conhecidas como citocromo P450. A fase II ou fase de conjugação/hidrólise consiste na hidrólise ou conjugação do fármaco com moléculas grandes e polares, como o glicuronato, o sulfato, a glutationa e o acetato. Estas duas fases têm o objetivo de tornar os compostos hidrossolúveis para que os rins possam excretá-los (GOLAN, 2009; GEBHARDT; MATZ-SOJA, 2014).

No parênquima hepático, podem ser identificadas as células de Kupffer, macrófagos residentes que se situam na superfície das células endoteliais dos sinusoides, suas principais funções são realizar a fagocitose e a imunorregulação. Além disso, existem as células de Ito, responsáveis por realizarem o armazenamento de vitamina A. No entanto, em situações de doença hepática estas células se diferenciam e apresentam características de miofibroblastos, dando início à síntese de colágeno e promovendo a manutenção da fibrose no órgão. (ROSS; PAWLINA, 2016; JUNQUEIRA; CARNEIRO, 2017).

2.1.3 Estresse oxidativo

A geração de radicais livres constitui, um processo contínuo e fisiológico, que está associado a funções importantes no organismo. Durante os processos metabólicos, esses radicais atuam como mediadores para a transferência de elétrons em diversas reações bioquímicas. Sua produção, em proporções adequadas, possibilita a síntese de ATP, por meio da cadeia transportadora de elétrons; fertilização do ovócito II; ativação de genes e participação de mecanismos de defesa durante o processo de infecção. No entanto a produção excessiva pode promover danos oxidativos nos tecidos afetados (BARBOSA et al., 2010).

O organismo humano sofre ação constante das espécies reativas de oxigênio (ERO), sendo que as principais se distribuem em dois grupos, os radicalares: hidroxila (HO•), superóxido (O2 •−), peroxila (ROO•) e alcoxila (RO•); e os não-radicalares: oxigênio, peróxido de hidrogênio e ácido hipocloroso. Dentre estes elementos, alguns podem ser reativos nos tecidos, promovendo alterações em lipídios, proteínas e DNA (CZERSKA et al., 2015; PIZZINO et al., 2017). A contínua produção de ERO durante os processos metabólicos promove o desenvolvimento de mecanismos de defesa antioxidante em nosso organismo, os quais são compostos pelo sistema enzimático e sistema não-enzimático. O sistema enzimático (Fig. 3) é composto pela Superóxido Dismutase (SOD), Catalase (CAT) e Glutationa Peroxidase (GPx). Além disso, o sistema não-enzimático inclui compostos de origem dietética, como vitaminas, minerais e compostos fenólicos. Estes mecanismos, apresentam o objetivo de limitar os níveis intracelulares desses elementos oxidantes e controlar os possíveis danos causados por estas moléculas. O início do processo de estresse oxidativo decorre da existência de um desequilíbrio entre compostos oxidantes e antioxidantes, em favor da geração excessiva de ERO ou em detrimento da velocidade de remoção dos mesmos. Este processo conduz à oxidação de biomoléculas com consequente perda de suas funções biológicas ou desequilíbrio homeostático, cuja manifestação é o dano oxidativo potencial contra células e tecido (BARBOSA et al., 2010; PENG et al., 2014; PIZZINO et al., 2017).

Figura 3. Sistema de defesa enzimático

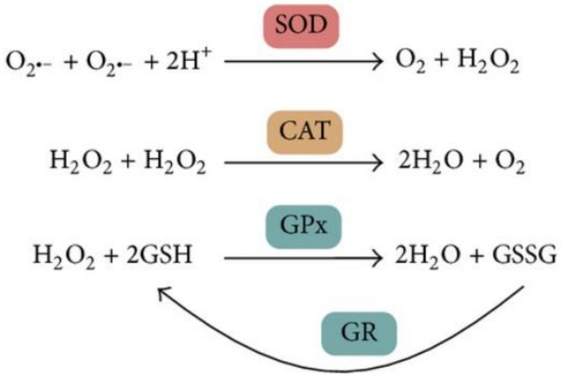

Fonte: PENG et al., (2014)

2.2 Malation

2.2.1 Características gerais

Durante os últimos 70 anos, os agrotóxicos são utilizados na lavoura com o objetivo de melhorar a produtividade, minimizando as perdas causadas por pragas (OZSOY et al., 2016). No entanto, sua utilização não é totalmente segura, uma vez que os resíduos dos agrotóxicos contaminam fontes de água, devido ao escoamento de campos agrícolas e efluentes industriais, alterando de forma direta ou indiretamente a flora e a fauna aquática, causando eventualmente efeitos tóxicos à saúde humana (ULLAH et al., 2018). Em razão do manuseio inadequado do produto, os trabalhadores rurais também são expostos aos danos causados pelos agrotóxicos, através das vias dérmicas, respiratórias ou orais (MUÑOZ-QUEZADA et al., 2014). De acordo com o Sistema Nacional de Informações Tóxico-Farmacológicas (SINITOX), em 2017 foram registrados 3.379 casos de intoxicação pelo uso de agrotóxicos, tanto no meio agrícola quanto doméstico, com indivíduos entre trinta e trinta e nove anos de idade constituindo a faixa etária mais comprometida, representando um contingente de 15,86% do total. Em seguida estão os indivíduos entre 20 a 29 anos, com uma porcentagem de 15,62% (SINITOX, 2020).

Os organofosforados são compostos sintéticos, insolúveis em água, e amplamente utilizados na agricultura como inseticidas devido ao seu baixo custo e sua grande efetividade no controle de pragas agrícolas (VIJAYA KUMAR et al., 2010). Sua degradação ocorre de maneira rápida em condições naturais, sendo considerado uma boa alternativa para praguicidas organoclorados, conhecidos pelos seus efeitos tóxicos para o meio ambiente devido ao fenômeno da bioacumulação (SELMI et al., 2018; SIDHU et al., 2019).

No entanto, mesmo sendo utilizados amplamente nas plantações, os organofosforados são extremamente nocivos para o organismo, sendo responsáveis pelo maior número de intoxicações do que qualquer outra classe de agrotóxicos. Seu processo de toxicidade decorre da inibição da acetilcolinesterase, enzima responsável por hidrolisar a acetilcolina nas sinapses colinérgicas e nas junções neuromusculares através de ligação covalente de radicais de fosfato com o sítio ativo da enzima. Sua inibição promove o acúmulo de acetilcolina e resulta na estimulação exacerbada de receptores colinérgicos, muscarínicos e nicotínicos, tanto nos músculos, como no sistema nervoso central, periférico e autônomo. Esta exposição causa uma ampla gama de manifestações tóxicas colinérgicas, podendo promover o bloqueio da ação neuromuscular (SOLTANINEJAD; ABDOLLAHI, 2009; SIDHU et al., 2019). Além destas alterações, a exposição aos organofosforados induz a produção de espécies reativas de oxigênio (ERO), favorecendo o processo de peroxidação lipídica e a degradação de fosfolipídios (MEHRI et al., 2016).

No corpo humano, diversos órgãos podem ser acometidos pela toxicidade dos organofosforados e isto ocorre devido às suas propriedades lipofílicas e à sua rápida assimilação intestinal. Dentre as alterações, podem ser citados o comprometimento do sistema imunológico, o desenvolvimento de pancreatite, de doença hepática, distúrbios hematológicos, doença renal, diminuição da fertilidade e problemas no sistema nervoso (SELMI et al., 2018).

Diversos inseticidas estão presentes no grupo dos organofosforados, como o Clorpirifós, o Diazinon e o malation, os quais vêm ganhando muita atenção devido a sua grande utilização na agricultura. O Clorpirifós, um dos praguicidas mais amplamente utilizados no mundo devido ao seu baixo custo e sua alta eficácia contra insetos e pragas (SANDOVAL et al., 2019). Assim como, o Diazinon um organofosforado comum, altamente tóxico e amplamente utilizado para o controle de pragas no meio ambiente. (DEHGHANI et al., 2019) Durante anos, foi um dos inseticidas mais utilizado nos EUA para controle de pragas residenciais e agrícolas (USEPA, 2008).

O malation, por sua vez, é um inseticida não sistêmico de amplo espectro da classe dos organofosforados. Introduzido na década de 1950, tornou-se mundialmente conhecido pela sua efetividade no controle de pragas, sendo um dos praguicidas mais utilizados na lavoura, além de ser um dos primeiros inseticidas amplamente utilizados no campo, na veterinária e na indústria (ESPINOZA-NAVARRO; PONCE-LAROSA; BUSTOS-OBREGÓN, 2017; ULLAH et al., 2018). Derivado do ácido ditionofosfórico o malation é considerado pouco tóxico (pertencente a classe III dos organofosforados), o que reforça a sua ampla utilização (BACONI et al., 2013). No entanto, seu uso generalizado leva à poluição ambiental e aumenta a extensão dos danos, permitindo que diversos indivíduos sejam expostos através de diferentes meios (JENSEN; WHATLING, 2010).

Sua absorção ocorre rapidamente pelo organismo, através da ingestão de água e alimentos contaminados, contato com a pele e exposição respiratória por meios ocupacionais e não ocupacionais (OZSOY et al., 2016). Posteriormente, o organismo realiza a biotransformação deste composto, que será eliminado, principalmente, através da urina (76 – 88%), bem como pelas fezes, em menor quantidade (7 – 11%). O malation e os seus metabólitos acumulam em quantidades extremamente baixas nos tecidos (menor que 1%), principalmente no fígado, pele e trato gastrointestinal. Sugere-se que a metabolização deste composto ocorra pelas carboxilesterases plasmáticas. Desta forma, o processo de metabolização é caracterizado pela hidrólise das ligações éster para formar o ácido monocarboxílico do malation e o malation dicarboxílico (JENSEN; WHATLING, 2010). Posteriormente, estes compostos quando em baixas concentrações, são catalisados pelas enzimas hepáticas do citocromo P450, tanto a CYP1A2, como a 2B6. No entanto, quando em altas concentrações, há também a atuação da CYP3A4 (BURATTI; TESTAI, 2006). Estes membros do citocromo P450 são responsáveis por formar o malaoxon, considerado 40 vezes mais tóxico do que o próprio malation (JENSEN; WHATLING, 2010).

Após as carboxilesterases metabolizarem o malation, tanto o ácido monocarboxilíco como o ácido dicarboxilico, competem com o malaoxon pelo citocromo P-450. Sendo assim, um fator que agrava a toxicidade relacionada a este inseticida, é a presença de diversos contaminantes nas formulações comerciais de malation, que muitas vezes atuam como potentes inibidores das carboxilesterases, mudando assim o equilíbrio para um aumento significativo na formação de malaoxon (BURATTI; TESTAI, 2006).

Diversos estudos apontam que a toxicidade do malation esteja relacionada com a disfunção de vários órgãos, como rim (JALILI et al., 2018), fígado (ESEN; UYSAL, 2018), pâncreas (EKREMOĞLU et al., 2020), testículos (MORIDI et al., 2018) e cérebro (SÁNCHEZ-SANTED; COLOMINA; HERRERO HERNÁNDEZ, 2016). Algumas das características destas alterações são: inibição da acetilcolinesterase, estresse oxidativo, indução de resposta inflamatória, apoptose, genotoxicidade e imunomodulação. No entanto, a toxicidade depende de vários fatores, como a duração, o nível e o meio em que ocorreu a exposição, além do estado de saúde e a idade do indivíduo (LIU; ERIN, 2014; SÁNCHEZ-SANTED; COLOMINA; HERRERO HERNÁNDEZ, 2016; BADR, 2020).

Como o principal mecanismo relacionado aos efeitos tóxicos do malation é a inibição da acetilcolinesterase (ESEN; UYSAL, 2018), na intoxicação aguda, os sintomas mais característicos estão associados à excitação dos receptores muscarínicos, causando salivação, lacrimejamento, micção e defecação, dispneia, vômito e bradicardia. Outros sintomas, porém, relacionados ao tecido muscular também podem ocorrem e são provocados pela estimulação excessiva dos receptores nicotínicos, proporcionando fraqueza muscular, tremores, rigidez, convulsões, paralisia e em alguns casos depressão respiratória (KWONG, 2002; TAKAHASHI; HASHIZUME, 2014).

Recentemente foi descrito que o estresse oxidativo é um dos principais fatores envolvidos nos efeitos tóxicos causados pela exposição ao malation. Isto ocorre, devido a suas características lipofílicas, que permitem que o inseticida interaja com a bicamada lipídica presente nas membranas celulares, causando distúrbios estruturais, peroxidação lipídica e induza a produção de espécies reativas de oxigênio (OZSOY et al., 2016). Além disso, o malation pode prejudicar ou diminuir as defesas antioxidantes celulares, como a glutationa reduzida (GSH) e a superóxido dismutase (SOD), causando alterações no equilíbrio redox do organismo (FRANCO et al., 2009).

Em razão das ERO afetarem diretamente a integridade das membranas, alterações no funcionamento mitocondrial podem ocorrer, bem como a indução da oxidação de moléculas, como proteínas e DNA (AGARWAL; SAID, 2005; FOUAD; BADR; ATTIA, 2019).

O período peripuberal é um importante marco no desenvolvimento pós-natal de vários órgãos do organismo. Assim, ele corresponde a uma janela para a ação de efeitos de xenobióticos sobre o desenvolvimento pós natal do indivíduo, de modo que o desenvolvimento de órgãos pode ser alterado (OJEDA et al., 1980). É conhecido que o malation altera o desenvolvimento pós natal em modelos experimentais (SELMI et al., 2018; ERTHAL et al., 2020). Considerando a teoria DOHAD (Developmental Origins of Health and Disease) a qual estuda o papel da exposição pré-natal e perinatal a fatores ambientais, como desnutrição, na determinação do desenvolvimento de doenças (SILVEIRA et al., 2007), tem-se o malation como um potencial fator interferente neste período.

2.2.2 Toxicidade renal e hepática relacionada ao malation

Dentre os diversos tecidos afetados pelo malation, os rins são um dos principais órgãos acometidos pela sua toxicidade. Dentre as alterações promovidas pelo inseticida, são identificadas aumento das dosagens de ureia e creatinina, que sugerem insuficiência tubular renal e filtração glomerular deficiente (ZIDAN, 2015; KHALIFA; ALKHALAF, 2020). Segundo o estudo de caso conduzido por YOKOTA et al., (2017), após a exposição ao malation, ocorreram esclerose glomerular, inchaço dos podócitos e das células epiteliais da cápsula de Bowman, dilatação irregular dos túbulos contorcidos distais, artérias interlobulares com acentuado espessamento fibroso da túnica íntima e edema endotelial focal, caracterizando o processo de necrose tubular aguda.

Também foi relatada degeneração dos glomérulos, das cápsulas de Bowman e das estruturas dos túbulos renais, com diminuição no tamanho dos glomérulos, e aumento do espaço de Bowman. Além disso, mudanças nas concentrações plasmáticas de ácido úrico foram apontadas, decorrentes de alterações em sua reabsorção nos túbulos proximais do néfron (SELMI et al., 2018).

Além disso, alterações devidas ao estresse oxidativo também foram identificadas, similares aos dados descritos para o fígado. Assim, a exposição ao malation causa diminuição da expressão no mRNA de GPx-3 nos rins (SELMI et al., 2018), redução nas concentrações da catalase, GSH, Glutationa Peroxidase e SOD, o que colabora para uma diminuição no balanço antioxidante deste órgão e possibilita o aumento das espécies reativas de oxigênio, favorecendo o processo de peroxidação lipídica. Mudanças nos padrões histológicos também foram encontradas, como alterações degenerativas renais, incluindo inchaço turvo, descamações celulares, bem como inchaço e pleomorfismo mitocondrial (AL-ATTAR, 2010; COBAN et al., 2015).

O fígado também é afetado pela toxicidade proveniente da exposição ao malation. Diversos estudos apontam que a exposição a este inseticida causa danos, sendo que os achados mais comuns são o aumento da atividade das enzimas hepáticas, aspartato aminotransferase (AST) e alanina aminotransferase (ALT), assim como alterações nas concentrações dos fatores oxidantes e antioxidantes (LASRAM et al., 2014; MEHRI et al., 2016; ABOUBAKR et al., 2019; GUPTA et al., 2020).

Ratos *Wistar* machos adultos expostos a 150 mg/kg de malation por 1 semana tiveram aumento da peroxidação e esse aumento foi relacionado com a produção excessiva de ERO. Em razão do processo de lipoperoxidação prejudicar a integridade das membranas celulares, sua interação com as células ocasiona na liberação de enzimas citoplasmáticas, que promovem o recrutamento de células inflamatórias e, consequentemente iniciam o processo de inflamação local. Além destas alterações, também foram encontradas mudanças nas concentrações plasmáticas de AST e ALT, que estavam aumentadas após a exposição ao inseticida (MEHRI et al., 2016).

Referente aos achados histológicos, o estudo, de ABDEL-SALAM et al., (2018) utilizando a dose de 150 mg/kg de malation em ratos *Sprague–Dawley* machos adultos, com eutanásia quatro horas após sua administração, identificou diversas alterações estruturais, como dilatação das veias porta e sinusoides, sinais de degeneração vacuolar, cariólise, cariorrexe, picnose e focos necróticos.

Semelhante a estes dados, em outro estudo utilizando ratos *Sprague–Dawley* machos adultos, com a dose de 40 mg/kg e eutanasiados ao término da administração, foram identificados congestão das veias centro lobulares, infiltrados inflamatórios e degeneração hidrópica (NUR et al., 2018). Do mesmo modo, foram identificados efeitos similares no estudo de AL-ATTAR., (2010) o qual utilizou a dose de 100 mg/kg de malation diariamente durante o período de um mês em ratos *Wistar* machos.

Além destes fatores, há um aumento expressivo da inflamação hepática, que se dá através da expressão de algumas citocinas como interferon-γ, interleucina 1-β, fator de necrose tumoral-α e fator nuclear-κB (NF-kB). Estes mediadores promovem o recrutamento e ativação de células do sistema imune, podendo provocar lesões hepáticas, como esteatose e apoptose (FUJII; KAWADA, 2012; LASRAM et al., 2014; INCE et al., 2017).

Além destas alterações, redução nas concentrações plasmáticas de albumina também foi descrita em roedores expostos ao malation, sugerindo possível alteração no metabolismo de proteínas e aminoácidos em ratos *Wistar* machos adultos (AKBEL et al., 2018). Também foram encontradas alterações no metabolismo de lipídios, sendo caracterizadas pelo aumento do colesterol total, da lipoproteína de baixa densidade (LDL) e dos triglicerídeos, bem como pela redução da lipoproteína de alta densidade (HDL).

2.3 Ciclosporina A

2.3.1 Características gerais

A ciclosporina A (CsA) é conhecida por ser um undecapeptídeo cíclico lipofílico neutro isolado a partir do fungo *Tolypocladium inflatum* (BEAUCHESNE; CHUNG; WASAN, 2007). Sua descoberta ocorreu em 1976 durante um estudo que buscava novas substâncias antibióticas. Primeiramente, foi utilizada com um amplo espectro de atividades biológicas, incluindo efeitos antiparasitários, fungicidas e antiinflamatórios. No entanto, em estudos posteriores foi descoberto ser um poderoso agente imunossupressor (BOREL et al., 1994). Dentre as diversas variações que a ciclosporina possui, a CsA é uma das mais conhecidas e utilizadas. Este medicamento faz parte de um grupo de imunossupressores inibidores da calcineurina, e a sua principal função está associada à prevenção da rejeição de órgãos transplantados, como rins, coração, pâncreas e fígado, levando à diminuição da morbidade (BOREL et al., 1994; FLORES et al., 2019; MOON; KIM, 2019). Além disso, a CsA também é utilizada como tratamento de diversas doenças autoimunes, como psoríase, síndrome nefrótica idiopática e artrite reumatoide (KOROLCZUK et al., 2013; ZHU et al., 2016). Sua atividade celular é restrita a um subconjunto de células T e, como resultado, é um forte inibidor da inflamação crônica, não apresentando efeito na inflamação aguda mediada pelo sistema imunológico (BOREL et al., 1996).

A CsA atua no organismo ao se ligar em seu alvo endógeno (SCHREIBER; CRABTREE, 1992), uma proteína presente no citosol, denominada ciclofilina. Seu mecanismo de ação ocorre, devido à formação de um complexo de alta afinidade, que age através da inibição da calcineurina (COLOMBO; AMMIRATI, 2011).

A calcineurina, ou proteína fosfatase 3, é um heterodímero, dependente de Ca^{2}+, que apresenta duas subunidades. A subunidade “A”, considerada o centro catalítico da enzima e a subunidade “B”, que regula a ligação com o Ca^{2}+. Ambas estão fortemente ligadas e sofrem dissociação apenas por desnaturação ou em situações extremas de baixa quantidade do Ca^{2}+, estando envolvida no crescimento e desenvolvimento muscular e neuronal, na apoptose e no reparo do DNA (MUSSON; SMIT, 2011).

Além disso, a calcineurina é essencial na produção de citocinas necessárias para ativação do receptor das células T (TCR) (CAMPISTOL; SACKS, 2000). Estas células são ativadas pelo reconhecimento de antígenos através TCR, gerando uma cascata de sinalização que culmina na ativação da tirosina quinase. Desta forma, permite fosforilar várias proteínas adaptadoras e enzimas situadas próximas ao TCR. As proteínas adaptadoras se ligam e ativam fosfolipases, como a PLC Y. Este processo, gera um subproduto denominado IP3, que por sua vez estimula a liberação de Ca^{2}+ do retículo endoplasmático (MUSSON; SMIT, 2011). O aumento na concentração de Ca^{2}+ no citosol culmina na abertura de canais na membrana plasmática, promovendo influxo deste íon. Assim, o Ca^{2}+ se liga à calmodulina, formando um complexo que ativa a calcineurina. Esta fosfatase é responsável por retirar o grupo fosfato do fator nuclear de células T ativadas, tornando possível sua migração para o núcleo, onde irá ativar genes promotores de interleucina 2, um dos fatores de crescimento de linfócitos T (ABBAS; LICHTMAN; PILLAI, 2015).

Sendo assim, ao ser administrada, a CsA liga-se à ciclofilina, seu receptor citoplasmático e o complexo CsA-ciclofilina liga-se à calcineurina, inibindo sua capacidade de desfosforilar fatores nucleares presentes no citosol, o que, por sua vez, impede a produção de citocinas envolvidas no processo de ativação dos linfócitos T (HO, 2004).

A CsA administrada por via oral apresenta baixa absorção, que ocorre principalmente no intestino delgado, nas regiões do jejuno e íleo (BEAUCHESNE; CHUNG; WASAN, 2007). Este medicamento apresenta o efeito de primeira passagem de aproximadamente 59% e sua biodisponibilidade de cerca de 30% em pacientes saudáveis. Sua concentração máxima no sangue pode ser encontrada em 1 até 8 horas após a administração oral (FAULDS; GOA; BENFIELD, 1993).

A concentração plasmática máxima de CsA é de 240 a 1,250 ug/ml, atingida entre 2 a 4 h após a administração oral de uma dose de 600 mg (BLOCK; SUTTER; MIHATSCH, 1983). Sua distribuição ocorre rapidamente entre os componentes sanguíneos, onde 58% está presente nos eritrócitos, 5% ligado aos linfócitos, 4% aos granulócitos e 33% à fração plasmática, ligando-se principalmente as lipoproteínas (BEAUCHESNE; CHUNG; WASAN, 2007). Deste modo, este medicamento se correlaciona com os níveis teciduais de ciclofilina e lipídios, apresentando concentrações maiores nos órgãos ricos em leucócitos e em órgãos com quantidade acentuada de tecido adiposo (BLOCK; SUTTER; MIHATSCH, 1983).

Sua metabolização ocorre principalmente nos hepatócitos, através do metabolismo de fase I pela subfamília CYP3A, um tipo de sistema do citocromo P450 (CYP450). Grande parte deste metabolismo será realizado a partir de dois membros desta subfamília, a CYP3A4 e CYP3A5, presentes em grandes quantidades tanto no fígado como no intestino (WANG et al., 2018).

A CsA é excretada principalmente por metabólitos, com menos de 1% sendo fármaco inalterado. Sua liberação ocorre de maneira bifásica, sendo 6% eliminado na urina e 70% a 80% eliminado nas fezes, uma vez que a sua principal via de excreção se dá, através do sistema biliar, devido a CsA ser absorvida pelas micelas formadas pela bile (LINDHOLM, 1991; BEAUCHESNE; CHUNG; WASAN, 2007).

2.3.2 Nefrotoxicidade induzida pela Ciclosporina A

Os danos renais causados pela exposição a CsA podem ser citados em duas formas distintas: a nefrotoxicidade aguda e a nefrotoxicidade crônica. A nefrotoxicidade aguda é caracterizada por alterações hemodinâmicas e ausência de lesão permanente nos tecidos, de modo que as células lesadas retornam ao estado normal com a diminuição ou parada na utilização do medicamento. Em relação à nefrotoxicidade crônica, sua principal característica é a fibrose intersticial progressiva dos rins, podendo progredir para doença renal crônica (BURDMANN et al., 2003).

As alterações hemodinâmicas identificadas na lesão aguda são caracterizadas pelo desequilíbrio nos mediadores de vasoconstrição renal. Este processo é caracterizado pela ativação do sistema renina-angiotensina, causando vasoconstrição arteriolar aferente intensa, diminuição do fluxo sanguíneo renal e na taxa de filtração glomerular (MURRAY; PALLER; FERRIS, 1985; BURDMANN et al., 2003; MOON; KIM, 2019; SHIROLIKAR et al., 2020). A ativação do sistema renina-angiotensina pode acontecer de duas formas, através de um efeito direto nas células justaglomerulares, aumentando a secreção de renina (KURTZ; DELLA BRUNA; KUHN, 1988), e de forma indireta através da vasoconstrição arterial e diminuição do fluxo plasmático renal (SHIROLIKAR et al., 2020).

O processo de vasoconstrição que ocorre pela exposição à CsA, pode ser acompanhado de hipóxia, e está associado ao aumento da expressão de endotelina -1 (ET-1), um potente vasoconstritor, que exerce sua função na célula alvo por meio de dois receptores, ETA e ETB. A ativação do receptor ETA é o principal responsável pela vasoconstrição, proliferação celular, proteinúria e indução de fibrose renal. A enzima de conversão de endotelina (ECE -1), responsável por gerar a ET-1, sofre regulação positiva via fator induzível por hipóxia (HIF). Ou seja, a CsA atua aumentando a expressão de ET-1 diretamente, assim como contribuindo indiretamente para o aumento de ECE-1 devido a presença do HIF (CAIRES et al., 2018; HEYMAN et al., 2018).

Disfunções tubulares são uma das maiores manifestações da nefrotoxicidade aguda da CsA (ADU et al., 1983). Um dos mecanismos associado a estas alterações é o aumento da permeabilidade para o cloreto nos túbulos distais, o que propicia o aumento na reabsorção de íons e do volume de sangue dentro dos vasos. (KAMEL et al., 1992). Além disso, em um estudo utilizando células MDCK I, foi possível identificar que a CsA causa alterações na montagem das proteína presentes nas junções comunicantes, e consequentemente altera a permeabilidade nos túbulos renais (LEE et al., 2011).

Com relação à nefrotoxicidade crônica, alterações como fibrose intersticial e glomerulosclerose podem ser identificadas. Estas alterações são observadas pela presença de algumas características como: atrofia tubular, acúmulo de matriz extracelular (MEC) e espessamento da membrana basal, o que resulta em perda da função das estruturas renais (SLATTERY et al., 2005; ZHAO, 2019).

As células mesangiais renais ativadas são as principais produtoras de MEC glomerular, e são essenciais para a plasticidade estrutural (DE CHIARA et al., 2017). No entanto, a exposição à CsA pode induzir a ativação destas células através da cascata de sinalização profibrogênica TGF-β/Smad, causando elevada produção de fibras colágenas (AKOOL et al., 2012).

Um outro fator associado à fibrose renal é o processo de transição epitelial-mesenquimal (TEM), caracterizado pela perda de características celulares, como a polaridade apical-basal, ligação célula-célula e marcadores epiteliais dos túbulos renais (SCHELLING, 2016). As células que passam por esta mudança fenotípica, produzem uma quantidade excessiva de componentes da matriz extracelular, influenciando diretamente o processo de fibrose renal (SLATTERY et al., 2005; LIU et al., 2017). Estudos apontam que a CsA pode aumentar a secreção de TGF-β1 (WAISER et al., 2002; CHEN et al., 2019), e mediar o processo de TEM, por estimular a síntese de componentes da matriz extracelular e reduzir a produção de colagenase (WOLF, 2006).

2.3.3 Hepatotoxicidade induzida pela Ciclosporina A

A CsA é um dos medicamentos mais importantes relacionados a agentes imunossupressores para transplantes de órgãos e doenças autoimunes. No entanto, diversos efeitos tóxicos para o organismo são identificados, os quais acometem principalmente o fígado e os rins (HAGAR, 2004; LEE et al., 2011; DE ARRIBA et al., 2013; KOROLCZUK et al., 2013; MOON; KIM, 2019).

Os danos hepáticos são, caracterizados por alterações estruturais e funcionais (HAGAR, 2004; KOROLCZUK et al., 2013; AKOOL, 2015). Com relação às alterações estruturais, podem ser destacados: a presença de degeneração hidrópica, focos necróticos, perda de organelas e diminuição dos espaços sinusoidais. Também foram encontrados focos de congestão tecidual, edema dos tratos portais, alargamento do seio hepático, ativação das células de Kupffer, infiltrado inflamatório, hiperplasia do ducto biliar e redução do glicogênio intracelular (YÜCE; ATEŞŞAHIN; ÇERIBAŞI, 2008; AHMED FETOUH; AL SHAHAT, 2013). No entanto, muitas destas alterações foram encontradas principalmente quando os animais são expostos à altas doses de CsA, visto que a sua toxicidade é dose-dependente (BINGUL et al., 2019).

As alterações funcionais estão relacionadas com o aumento dos níveis séricos de transaminases hepáticas, fosfatase alcalina, colestase, aumento da produção de sais biliares e comprometimento da secreção de lipídios (DE FREITAS et al., 2015; KOROLCZUK et al., 2016). Além disso, também são identificados aumento na atividade da gama-glutamil transferase (GGT), bilirrubina total (TBIL) e colesterol total (LEE et al., 2019).

O aumento da GGT indica que a exposição à CsA causa lesões do trato biliar, e um alto nível de TBIL pode indicar doença hepática e bloqueio dos dutos biliares. Estes danos estão envolvidos no desenvolvimento de um estado hipermetabólico e estão relacionados com a inibição do transporte de bilirrubina e sais biliares através das membranas dos hepatócitos (LEE et al., 2019).

O mecanismo exato que leva ao processo de hepatotoxicidade pela CsA não é totalmente conhecido. No entanto, diversos estudos apontam que o estresse oxidativo seja um dos principais fatores envolvidos (WOLF et al., 1997; HAGAR, 2004; AKOOL, 2015).

Alterações mitocondriais estão entre as principais mudanças causadas pelo estresse oxidativo, e ocorrem devido exposição prolongada à CsA. Este processo, induz o aumento de Ca^{2+} no interior das mitocôndrias, levando à produção de espécies reativas de oxigênio (ERO), causando inibição do metabolismo de glicose e a produção de ATP (KOROLCZUK et al., 2016). Outro fator que está associado com a hepatotoxicidade é o aumento na atividade da caspase 3. Vários estudos apontam que estas alterações ocorrem, em razão da despolarização das membranas mitocondriais, promovendo a liberação do citocromo c pró-apoptótico e a proteína Smac / Diablo. Este mecanismo ocorre, devido abertura de poros de transição de permeabilidade mitocondrial causados pela exposição a CsA, dando início ao processo de apoptose nos hepatócitos (RONCHI; VERCESI; CASTILHO, 2011; KOROLCZUK et al., 2016).

2.3.4 Estresse oxidativo nos rins e fígado

Diversos artigos apontam que os danos causados pela CsA, tanto nos rins como no fígado, estão diretamente relacionados com a produção de espécies reativas de oxigênio (ERO) (HAGAR, 2004; AKOOL, 2015; BALAH; EZZAT; AKOOL, 2018; YOUSEF et al., 2020).

Para evitar que estas alterações aconteçam, as células possuem mecanismos associados ao uso de enzimas antioxidantes, sendo que os principais são, a catalase, a superóxido dismutase (SOD) e a glutationa (GSH). A catalase é uma enzima antioxidante que promove a decomposição do H_2O_2, que pode formar um radical hidroxila altamente reativo na presença do ferro. Em relação a GSH e a GSH-Px, ambas convertem o H_2O_2 e peróxidos lipídicos em produtos que não são lesivos para a célula. A superóxido dismutase (SOD), é a primeira enzima de desintoxicação e o antioxidante mais poderoso da célula. Seu papel é atuar no sistema de defesa de primeira linha contra espécies reativas do metabolismo do oxigênio (ERO). Responsável por catalisar a dismutação de duas moléculas de ânion superóxido, ($^*O_2$) em peróxido de hidrogênio (H_2O_2) e oxigênio molecular (O_2), consequentemente tornando o ânion superóxido menos prejudicial para o organismo (IGHODARO; AKINLOYE, 2018).

A atividade reduzida destes sistemas, devido aos efeitos causados pela exposição a CsA, induz o processo de estresse oxidativo o qual pelo aumento da peroxidação lipídica pode induzir o processo de hepatotoxicidade e nefrotoxicidade (KOWALTOWSKI; CASTILHO; VERCESI, 2001; HAGAR, 2004).

As ERO estão associadas a vários danos nos túbulos renais, como em casos de isquemia, glomerulonefrite e obstrução uretral. Um dos precursores para estas alterações é o H_2O_2, considerado um importante mediador de lesão oxidativa. Estudos utilizando culturas de células apontaram que a CsA aumenta a morte celular apoptótica e necrótica, através da presença de H_2O_2 nas células epiteliais dos túbulos proximais (MOON; KIM, 2019). Foi identificado que a CsA induz a síntese de ERO, causando redução do potencial de membrana mitocondrial e formação de poros de transição de permeabilidade. Este processo induz a liberação do citocromo c, acompanhado da ativação das caspase-9 e 3, levando ao processo de morte celular (KOWALTOWSKI; CASTILHO; VERCESI, 2001; RONCHI; VERCESI; CASTILHO, 2011; DE ARRIBA et al., 2013; YU et al., 2016). Junto a este fator, quando em baixas concentrações de NAD+ intracelular e na presença dos poros de transição de permeabilidade a enzima nuclear PARP-1 pode provocar a morte celular (ALANO;

YING; SWANSON, 2004). A exposição à CsA também pode induzir o estresse oxidativo no retículo endoplasmático, causando alterações no dobramento de proteínas (PALLET et al., 2008; CHONG; SHASTRI; ERI, 2017).

Os danos encontrados no fígado, referente ao estresse oxidativo estão diretamente relacionados à peroxidação lipídica e ao aumento de seus produtos, malondialdeído (MDA) e 4-hidroxialquenais (4HAE). Este processo, promove alterações mitocondriais, as quais resultam em redução na produção de ATP (KOROLCZUK et al., 2016).

O tratamento utilizando a CsA além de aumentar os níveis de oxidantes, também age diminuindo os níveis de antioxidantes. Desta forma, os rins e o fígado se tornam mais suscetíveis ao estresse oxidativo, podendo resultar em um processo de toxicidade (GHAZNAVI et al., 2007).

De acordo com estes dados, o estudo conduzido por Wolf et al (1997), verificou que em altas doses, a CsA diminui as concentrações dos fatores antioxidantes, favorecendo o status pró-oxidativo das células. No entanto, quando administrada em baixa dose, o estresse oxidativo não é identificado, indicando que a toxicidade induzida pela CsA é dose-dependente e está diretamente relacionada com o aumento das ERO (WOLF et al., 1997).

3 OBJETIVOS

3.1 Gerais

Visto a grande utilização de ambos compostos e a falta de informações sobre a toxicidade do malation no período peripuberal e a toxicidade da ciclosporina em baixa dose, os objetivos deste estudo foram: (1) Identificar os efeitos do inseticida malation sobre a morfofisiologia renal e hepática de ratos machos *Wistar* durante o período peripuberal; (2) Avaliar as possíveis alterações histológicas, bioquímicas e no status antioxidante dos rins e fígado de camundongos expostos a uma baixa dose de CsA considerada sem efeito imunossupressor.

3.2 Específicos

- Avaliar a morfologia e função renal e hepática de ratos expostos ao malation nas doses de 10 mg/kg e 50 mg/kg no período peripuberal e de camundongos expostos a Ciclosporina A em baixa dose

-Quantificar os biomarcadores de estresse oxidativo e nos rins e fígado de ratos expostos ao malation nas doses de 10 mg/kg e 50 mg/kg no período peripuberal e de camundongos expostos a Ciclosporina A em baixa dose

-Determinar as concentrações de glicogênio e colágeno nos rins e fígado de ratos expostos ao malation nas doses de 10 mg/kg e 50 mg/kg no período peripuberal e de camundongos expostos a Ciclosporina A em baixa dose

-Contribuir com mais dados sobre a toxicidade provocada pelo Malation no período peripuberal e pela Ciclosporina A em baixa dose nos rins e fígado

4 ARTIGOS

Este trabalho foi desenvolvido no Laboratório de Toxicologia e Distúrbios Metabólicos da Reprodução, da Universidade Estadual de Londrina (UEL) e no Laboratório de Analise Histopatológica, da Universidade Estadual de Londrina (UEL). Os resultados obtidos serão publicados em dois artigos científicos:

1) **Malathion causes renal and hepatic damage in male *Wistar* rats during the peripuberal period**. Pedro Mareti Maçaira Figaro; Lorena Coelho; Gabriel Smolak Sobieski; Maylla Cardoso de Oliveira; Ivana Regina Costa; Rafaela Pires Erthal; Suellen Ribeiro da Silva; Fábio Goulart de Andrade; Glaura Scantamburlo Alves Fernandes.

2) **Cyclosporine A alteres renal and hepatic morphophysiology in *Swiss* mice**. Pedro Mareti Maçaira Figaro; Danielle Ramos; Gabriel Smolak Sobieski e Silva; Maylla Cardoso de Oliveira; Ivana Regina Costa; Suellen Ribeiro da Silva Scarton; Glaucia de Lion Siervo; Fábio Goulart de Andrade; Glaura Scantamburlo Alves Fernandes.

As formatações dos artigos seguem as normas das revistas *Acta Histochemica* (Fator de impacto: 2.107; Qualis Capes Medicina II: A4) e *Human & Experimental Toxicology* (Fator de impacto: 2.067; Qualis Capes Medicina II: B1), respectivamente.

Artigo 1

Malathion causes renal and hepatic damage in male *Wistar* rats during the peripuberal period

Artigo será submetido à revista —"Acta Histochemica"

ISSN: 0065-1281;

F.I. 2020: 2.107

Qualis CAPES 2013-2019 (Medicina II): A4

4.1 MALATHION CAUSES RENAL AND HEPATIC DAMAGE IN MALE *WISTAR* RATS DURING THE PERIPUBERAL PERIOD

Pedro Mareti Maçaira Fígaro[1,2,3], Lorena Coelho[2], Gabriel Smolak Sobieski e Silva [2], Maylla Cardoso de Oliveira [2], Ivana Regina Costa [1], Rafaela Pires Erthal[2], Suellen Ribeiro da Silva Scarton[2,3], Fábio Goulart de Andrade[2], Glaura Scantamburlo Alves Fernandes[1]*

1 – Department of General Biology, Biological Sciences Center, State University of Londrina – UEL, Londrina, Paraná, Brazil, Rodovia Celso Garcia Cid, PR 445, Postal code: 86057-970
2 – Department of Histology, Biological Sciences Center, State University of Londrina – UEL, Londrina, Paraná, Brazil, Rodovia Celso Garcia Cid, PR 445, Postal code: 86057-970
3 – Department of General Pathology, Biological Sciences Center, State University of Londrina – UEL, Londrina, Paraná, Brazil, Rodovia Celso Garcia Cid, PR 445, Postal code: 86057-970

***Corresponding author**
Glaura Scantamburlo Alves Fernandes
Tel.: +55 43 33714417
E-mail address: glaura@uel.br (G. S. A. Fernandes)

HIGHLIGHTS

- Malathion alters renal morphology during the peripubertal period.
- Renal function is impaired due to exposure to malathion.
- Malathion promoted an increase in the activity of antioxidant enzymes.

ABSTRACT

Malathion is an organophosphate insecticide, which is effective against several insects, widely used in agriculture. However, its use is not completely safe since its residues can remain in the environment and reach water sources. The peripubertal period is a large vulnerability window to the action of toxic agents, and the renal and hepatic tissues may be compromised. Thus, the objective of this study was to identify the effects of malathion on the renal and hepatic morphophysiology of male *Wistar* rats during the peripubertal period. The study included male *Wistar* rats at postnatal day 21 (PND 21) divided into three experimental groups (n = 6 animals/group). Two of these groups received daily malathion doses of 10 mg/kg (10M) and 50 mg/kg (50M). The control group received only the vehicle. After 41 PND, the animals were anesthetized and euthanized for blood, kidney, and liver collection. The plasma obtained was used to analyze aspartate transaminase (AST), alanine aminotransferase (ALT), urea, and creatinine levels. The kidneys and liver of the rats were used to evaluate oxidative stress biomarkers and were processed for histopathological evaluation using hematoxylin and eosin, periodic acid-Schiff, Heidenhain's AZAN trichrome, and picrosirius red staining methods. The results showed that malathion decreased the Bowman's space (10M) and increased the glomerular diameter (50M). In addition, glycogen was decreased in the renal cortex with both doses. In the liver, both doses increased glycogen reserves in the portal and centrilobular venules, and 50 mg/kg of malathion dose increased AST, ALT, and creatinine levels and decreased urea levels. As for the oxidative stress, increased hepatic glutathione and renal catalase activity were detected, and decreased superoxide dismutase activity was detected in the kidneys. Exposure to low doses of malathion during the peripubertal period causes hepatotoxicity and nephrotoxicity in male rats.

Keywords: Insecticide; liver; kidney; peripuberty

INTRODUCTION

The use of insecticides has increased over the years, becoming one of the main causes of severe chronic poisoning in humans (Soltaninejad and Abdollahi, 2009). Insecticide poisoning with organophosphates is associated with a high mortality rate, besides being the cause of most hospital admissions for poisoning (Espinoza-Navarro et al., 2017; Vijaya kumar et al., 2010). Malathion is an example of this class of insecticides, which is used worldwide to control pests and is considered of low toxicity. It is widely used in agriculture (Baconi et al., 2013; Espinoza-Navarro et al., 2017).

This insecticide can be absorbed through the skin, digestive tract, and airways (Lasram et al., 2009). It is deposited mainly in the liver, kidney, and adipose tissue and excreted mainly by the urinary route (Naraharisetti et al., 2009). The lipophilic character of this insecticide is considered a facilitating factor for its interaction with cell membranes, increasing the possibility of lesions in the cell structure of most visceral organs (Selmi et al., 2015). The liver is the main target organ for the toxic effect of organophosphates. Malathion affects hepatic metabolic pathways, and interferes with protein, lipid, and carbohydrate metabolism (Karami-Mohajeri et al., 2017; Karami-Mohajeri and Abdollahi, 2011). The main pathophysiological mechanism of this insecticide is associated with the inhibition of acetylcholinesterase enzyme, which is responsible for the hydrolysis of acetylcholine into choline in the synaptic cleft (Joshi and Sharma, 2011). Thus, acetylcholine accumulates at the site, consequently blocking neuromuscular action (Soltaninejad and Abdollahi, 2009; Vijaya kumar et al., 2010).

In addition, there is a direct effect of oxidative stress caused by malathion exposure. Lipophilic characteristics allow its interaction with the lipid bilayer present in the cell membranes, causing lipid peroxidation, structural disturbances, and increased production of reactive oxygen species (Ozsoy et al., 2016). The process of lipid peroxidation is facilitated because malathion decreases the activity of antioxidant enzymes present in the cells, such as glutathione S-transferase (GST) and superoxide dismutase (SOD); hence, changing the antioxidant balance of the body (Franco et al., 2009).

Thus, since the peripubertal period is a large vulnerability window to the action of toxic agents and there is a scarce amount of information on the effects of malathion on the liver and kidney tissues in the peripubertal period, the objective of this study was to evaluate the effects of low doses of malathion on the kidney and liver morphophysiology of male *Wistar* rats during the peripubertal period.

MATERIAL AND METHODS

Animals and experimental conditions

Male *Wistar* rats (n=18), at postnatal day 21 (PND21) were supplied by the Animal House of Biological Sciences Centre, State University of Londrina (CCB - UEL), and were acclimated to the new environment at the Laboratory of Toxicology and Metabolic Dysfunction of Reproduction with controlled temperature conditions (23 °C) and lighting (photoperiod of 12h light/12h dark). Before the start of the experimental period, the rats were acclimated to the new environment for 4 days. The animals were allocated into polypropylene cages with laboratory-grade pine shavings as bedding during the entire experiment and received rat chow and filtered tap water *ad libitum*. Animal care and handling procedures were in accordance with the National Institutes of Health guide for the care and use of Laboratory animals (Nih et al., 2011), and with the approval of the Ethics Committee on Animal Use of State University of Londrina (OF. CIRC. CEUA/UEL nº 137/2016).

Experimental design

The animals were randomly assigned to three experimental groups (n= 6/group): In groups 10M and 50M, animals received malathion via gavage in doses of 10 and 50 mg / kg of body weight, respectively, diluted in 0.9% saline solution. In the control group (C), the animals received only the vehicle. The animals were treated daily for 40 consecutive days (PND25 a PDN65), which corresponds to the juvenile and peripuberal periods established for rats (Ojeda et al., 1980).

Malathion doses were administered according to Mansour et al. (2008), which demonstrated renal and hepatic disorders in adult male *Wistar* rats exposed to 36 mg / kg p.c. of malathion. The average of doses used in the present study represents the dosimetric adjustment of the AOEL dose of 0.03 mg/bw/day in humans (European Commission) with an added security factor of 10 considering intraspecies variability (Erthal et al., 2020; Nielsen et al., 2008).

Malathion

Malathion (dietil-dimetoxitiofosforiltio; CAS no. 121-75-5; Cheminova) was obtained from Dominus Quimica (Jandaia do Sul, Brazil). The compound was diluted in 0.9% saline daily as vehicle.

Kidney and Liver collection

At the end of the experimental period, the rats were anesthetized intraperitoneally with a combination of ketamine (75 mg/kg b.w. - Sedomin® 10%, Avellaneda, Argentina) and xylazine (10 mg/kg b.w. - Anasedan®, Paulínia, Brazil) and euthanized via cardiac puncture. Blood was collected in the presence of anticoagulant heparin (Hemofol®, São Paulo, Brazil) for the determination of plasma concentrations of aspartate aminotransferase (AST), alanine aminotransferase (ALT), urea and creatinine. The kidneys were collected and used for histopathological analysis (left kidney) and assessment of oxidative stress biomarkers (right kidney). The liver was collected, weighed, sectioned, and destined for histopathological analysis (right lobe) and dosages of oxidative stress biomarkers (left lobe).

Histopathological analysis

Kidneys and liver were fixed in aqueous Bouin's solution for 48 hours and subsequently sent to the histopathological analysis laboratory (LAHip) of Londrina State University. After fixation, the organs were dehydrated in an increasing series of ethanol, clarified in xylol and embedding in histological paraffin. The 7 µm thick cuts were made in a semi-automatic microtome (CUT 5062 SLEE medical GmbH, Germany) and the slides were stained with hematoxylin and eosin; Schiff's periodic acid (PAS); Azan trichrome and Picrosirius Red (Bancroft and Gamble, 2002). Observations and photo documentation were performed at 400x magnification, in a Moticam image capture system (Motic, Xiamen, China), attached to the light microscope.

Hematoxylin and Eosin (H&E) for morphometric analysis

In the kidneys, 10 images of the cortical region and 10 images of the medullary region per animal were analyzed. In the cortical region, the diameter of the renal corpuscles, Bowman's space and diameters of the proximal and distal convoluted tubules were determined. In the medullary region, the diameter of the collecting tubules was measured (Imafidon et al., 2016; Olatunji et al., 2015).

In the liver, 10 images of the periportal region and 10 images of the centrilobular region were analyzed, per animal. In the periportal region, the diameters of 10 portal venules, 10 bile ducts and 10 sinusoids were determined. In the centrilobular region, the diameters of 10 centrilobular venules and 10 sinusoids were measured. In both regions, the leukocytes adhered to the endothelium of the venules were quantified (Nirmal et al., 2020).

Periodic acid Schiff reaction (PAS) for detection of neutral glycoconjugates

In the kidneys, 5 images of the cortical region and 5 images of the medullary region were analyzed, while in the liver, 5 images of the periportal region and 5 images of the centrilobular region were analyzed, per animal. In each image, using the image-Pro Plus® software (Media Cybernetics, Maryland, USA) the proportion of the purple pixels was determined, indicating positive marking for neutral glycoconjugates (Bancroft and Gamble, 2002).

Azan trichrome to determine the percentage of total collagen

In the kidneys, 5 images of the cortical region and 5 images of the medullary region were analyzed, while in the liver, 5 images of the periportal region and 5 images of the centrilobular region were analyzed, per animal. In each image, using the image-Pro Plus® software (Media Cybernetics, Maryland, USA) the proportion of the blue pixels presented by the collagen fibers in the histological sections was determined (Adisa et al., 2016).

Picrosirius Red for quantification of type I and type III collagen

In observation under polarized light, 5 images of the cortical region and 5 images of the medullary region were captured in the kidneys, while 5 images of the periportal region and 5 images of the centrilobular region were analyzed per animal in the liver. In each image, using the image-Pro Plus® software (Media Cybernetics, Maryland, USA), the proportion of the red (type I collagen) and green (type III collagen) pixels was determined (Pupim et al., 2017).

Assessment of renal function and liver toxicity

To assess renal function, plasma urea and creatinine concentrations were determined using commercial kits, according to the manufacturer's instructions. (Labtest® Diagnóstico S.A., Lagoa Santa, MG, Brazil). The results were presented in milligrams per deciliter (mg / dL) of plasma urea or creatinine.

To assess hepatotoxicity, plasma samples were processed following manufacturer’s instructions to determine the concentrations of aspartate aminotransferase (ALT) and alanine aminotransferase (AST) using commercial kits (Labtest® Diagnóstico S.A., Lagoa Santa, MG, Brazil). The results were presented as U / L of ALT or plasma AST.

Analysis of oxidative stress biomarkers in the kidney and liver

Sample processing

The fragments of the kidneys and livers were homogenized in PBS (pH 7.2), and the homogenate was centrifuged at 3,000 rpm for 20 minutes. The supernatant was separated and diluted at a ratio of 1:100. The quantification of proteins in the sample was determined using the Bradford biochemical method. A standard curve, consisting of white, 0.06; 0.12; 0.25; 0.5 and 1 mg BSA per mL, was pipetted in triplicate into a 96-well plate. Then, 10μL of the diluted samples were also pipetted in triplicate, following the standard curve. 250μL of the Bradford reagent was added and absorbance was measured at 595 nm. From the data obtained, calculations were performed for the dilution of the samples to have a final protein concentration of 1 mg/mL.

Determination of thiobarbituric acid reactive substances (TBARS)

For this analysis, 50 μL of the sample in triplicate was pipetted into a 96-well microplate, 5 μl of iron chloride (FeCl3) (1M), 5 μl of ascorbic acid (0.5M), 50 μl of trichloroacetic acid (TCA) (2.8%) and 50 μl of thiobarbituric acid (TBA) (1%). The microplates were kept in a water bath for 15 minutes and the absorbances were read at 535 and 572 nm. (Buege and Aust, 1978)

Glutathione s-transferase activity (GST)

In this analysis, 20 μL of the samples and potassium phosphate buffer (0.1 M) were pipetted, in triplicate, in a 96-well microplate. Subsequently, 180 μL of a mixture composed of reduced glutathione (GSH), 1-chloro-2,4-dinitrobenzene (CDNB) and potassium phosphate buffer were pipetted in all wells. Sample absorbances were measured at 340 nm at 40-second intervals for 5 minutes (Keen et al., 1976). (Ferreira and Matsubara, 1997; Hayes et al., 2005).

Catalase activity (CAT)

To determine the catalase activity, 3 μL of the samples were used, then 297 μL of the reaction was pipetted, containing Tris-HCl buffer, ethylene diamine tetra-acetic acid (EDTA) and hydrogen peroxide (H2O2), in the wells that contained samples. Sample absorbances were measured at 240 nm at 15-second intervals for 1 minute (Aebi, 1984).

Superoxide dismutase activity (SOD)

The activity of superoxide dismutase (SOD) was evaluated according to the method originally proposed by (Crouch et al., 1981). The principle of this analysis was to quantify the complex formed between superoxide and nitrotetrazolium blue (NBT), measured at 560 nm over a period of 1 hour. An aliquot of 0.75 mg.mL-1 of protein in 25% ethanol was prepared in a total volume of 800 µL. The samples were centrifuged at 13,680 g at 4ºC for 20 minutes, and supernatant was pipetted in triplicate, in a 96-well microplate; the final 200µL volume contained: 0.1 mg protein.mL-1, 0.09 mM NBT, 0.015 mM EDTA, 34.78 mM hydroxylamine sulfate and 79 mM sodium carbonate buffer (pH 10,2). The activity values of the antioxidant enzymes were expressed in U. mg protein-1.

Statistical analysis

For statistical analysis, the IBM SPSS® software was used (SPSS Inc, Chicago, Illinois, USA) and the results were expressed as mean ± SD. One-way analysis of variance (ANOVA) was used, followed by Dunnett's post-test for parametric data. Nonparametric results were compared by Kruskal-Wallis and Dunn's post-test. Differences were considered statistically significant when $P < 0.05$.

RESULTS

Kidney and liver morphometry

Compared to the control group, there was an increased glomerular diameter (Figure 1A) in the 50M group and decreased Bowman’s space (Figure 1B) in the 10M group. The diameters of the proximal (Figure 1C), distal (Figure 1D), and collecting tubules (Figure 1E) presented no change after exposure to malathion. As for the liver, the 10M and 50M groups showed no differences compared to the control group (Figure 2). However, despite not being statistically significant, malathion caused a 13.07% (Figure 2A) dilation in the portal venule in the 10M group and 17.8% in the 50M group compared to the control group. The biliary ducts (Figure

2B) showed no significant diameter changes in the 10M and 50M groups. The centrilobular venule (Figure 2C) presented dilation of 14.18% in the 10M group and of 17.13% in the 50M group compared to the control group. The number of cells adhered to the portal (Figure 2D) and centrilobular venules (Figure 2E) and the diameter of hepatic sinusoids around the portal (Figure 2F) and centrilobular venules (Figure 2G) showed no significant changes in the 10M and 50M groups compared to the control group.

Neutral glycoconjugate analysis

Malathion exposure resulted in lower neutral glycoconjugate labeling in the cortical region of the kidneys (Figure 3A) compared to the control group. Liver tissue presented increased labeling both in the periportal (Figure 4A) and centrilobular regions (Figure 4B) in the 10M and 50M groups compared to the control group.

Type I, III, and total collagen quantification

Exposure to both doses of malathion did not change mean total collagen percentages in the kidney (Figure 3C and D) and liver (Figure 4C and D) of the male *Wistar* rats in 10M and 50M groups compared to the control group. Additionally, the three experimental groups showed a prevalence of type I collagen in relation to type III collagen in the renal (Figure 3E and F) and hepatic (Figure 4E and F) tissues.

Hepatotoxicity and nephrotoxicity

Plasma urea concentrations in the 10M and 50M groups (Figure 5A) showed no significant change compared to the control group. However, the 50M group showed increased plasma creatinine (Figure 5B), aspartate transaminase (AST) (Figure 5C), and alanine aminotransferase (ALT) levels (Figure 5D) compared to the control group.

Oxidative stress biomarkers

Lipid peroxidation results evidenced by thiobarbituric acid reactive substances (TBARS) levels in the kidneys (Figure 6A) and liver (Figure 6B) showed statistical similarity between the three experimental groups. GST activity increased only in the liver (Figure 6D) of the rats exposed to the highest dose of malathion (50M group) compared to the control group. However, both treatment groups presented increases catalase (CAT) activity in the kidneys (Figure 6E) compared to the control group. SOD activity decreased in the kidneys (Figure 6G) of rats in the 50M group compared to the control group. However, the liver tissues showed no significant SOD activity changes (Figure 6H) between the three experimental groups.

DISCUSSION

This study showed that exposure to malathion during the peripubertal period damaged the kidneys and liver as there were significant changes in the morphology and function of these organs.

The decreased Bowman's space in animals receiving the lowest insecticide dose corroborates with the findings reported by Jalili et al. (2018). These authors reported that a malathion dose of 27 mg/kg via gavage decreased the Bowman's space and increased urea and serum creatinine levels in male *Wistar* rats. This event may indicate impaired ultrafiltrate production in animals exposed to malathion. According to the study conducted by Vijaya kumar et al. (2010), ultrafiltrate production failure is one of the characteristics of organophosphate nephrotoxicity, which may lead to renal failure, the main kidney damage caused by pesticides of this class. Although no changes were identified in the proximal and distal convoluted tubules and collecting tubules, Al-Attar, (2010) reported that a dose of 100 mg/kg of malathion administered by gavage in male *Wistar* rats for one month caused several ultrastructural changes in the renal tubule cells and identified vacuoles with damaged outer membrane and swollen and pleomorphic mitochondria. This result indicates that exposure to a dose higher than the ones used in this study causes more severe renal damage than that observed in this study.

The increased glomerular diameter after exposure to malathion in the 50M group indicates the process of hypertensive nephropathy, which precedes glomerular arteriosclerosis. A previous study by Baiomy et al. (2015), using a dose of 50 mg/kg of malathion via gavage in male *Wistar* rats for 30 days, identified glomerular capillary dilation and glomerular degeneration. Selmi et al. (2018) used 200 mg/kg of malathion via gavage in male mice in the peripubertal period for 30 days and reported glomerular shrinkage and degeneration, and Bowman's capsule and renal tubule degeneration. This indicates that exposure to higher malathion doses increases renal structure damage.

The absence of changes in the liver tissues indicates that the dose used was not enough to cause morphological changes in this tissue. However, the study by Baconi et al. (2013) identified that exposure to malathion at 42.5 and 85 mg/kg doses via gavage in male and female *Wistar* rats for 35 days caused vasodilation, microvacuoles, and granular dystrophy. Similar data were found by El-Gharieb et al. (2010), who reported portal venule dilatation in addition to other tissue changes, such as pyknosis and inflammatory infiltrate. Naraharisetti et al. (2009) reported centrilobular venule dilatation as one of the effects of malathion in 1-month-old chickens treated with the insecticide (500 ppm) for 28 days. These authors reported that this change may cause imbalance in the hepatic vascular pattern, changing the blood supply to the organ. Furthermore, malathion exposure changes hepatic blood perfusion, causing hypoxia not only in the liver, but also in the heart (Vijaya kumar et al., 2010).

The decrease glycogen reserves observed in the renal tissue indicate that the function of the organ is increased, promoting greater glycogen consumption by the cells. However, these data contradict the results presented by Kaya et al. (2018). These authors treated *Wistar* rats with 0.8 mg/kg of Fenthion, an organophosphate, observing increased glycogen stores in the kidneys of these animals 24 hours after treatment. Therefore, despite the lack of consensus regarding this result, it is evident that malathion affects renal glycogen levels. Contrary to this effect on the renal tissue, the liver tissue responded in the opposite manner to malathion exposure. Thus, the increased quantification of neutral glycoconjugates present in the liver is explained by the process of hepatic glycogenolysis and gluconeogenesis, responsible for promoting glycogen depletion. This change is corrected by the body through glycogen synthesis under the effect of hyperinsulinemia, which increases hepatic glycogen deposition (Flehi-Slim et al., 2015). Rezg et al. (2007) reported that subchronic exposure via gavage to 100 mg/kg malathion in male *Wistar* rats decreases liver proteins and lipids. Furthermore, the results reported by Abdollahi et al. (2004) indicate that the process of gluconeogenesis is stimulated by the increased activity of the hepatic gluconeogenic enzyme phosphoenolpyruvate carboxykinase in response to 100, 200, and 400 ppm of malathion exposure in male *Wistar* rats for 4 weeks. According to Flehi-Slim et al. (2015), male *Wistar* rats exposed to 137, 13.7, or 1.3 mg/kg of malathion for 30 days presented increased glycogen stores in the liver in a dose-dependent manner. These data are consistent with the research by Joshi and Rajini, (2009), who demonstrated increased glycogen deposition in the liver of male *Wistar* rats treated with 140 mg/kg of acephate, an insecticide of organophosphate class. Malathion can inactivate the enzyme glycogen phosphorylase, decreasing glycogen conversion into glucose and increasing glycogen stores in the liver (Lasram et al., 2014).

However, despite these hypotheses regarding the effects of malathion on the liver and kidney function, the maintenance in the amount of type I, III, and total collagen in the kidneys and liver of animals exposed to malathion indicates no tissue damage in these organs. In an inflammatory process, type I collagen is removed and type III collagen fibers are produced, being later replaced by type I collagen fibers (Medeiros and Dantas-Filho, 2017). However, doses higher than those used in this study lead to irreversible tissue damage processes, such as fibrosis. Exposure to 200 mg/kg of malathion via gavage for a period of 30 days in *Wistar* rats induced liver inflammation and fibrosis (El-Bini Dhouib et al., 2015).

The evaluation of AST and ALT enzyme levels indicates the quality of liver tissue. Thus, increased plasma levels of these enzymes may indicate cellular injury with changes in the membrane permeability of hepatocytes, allowing the extravasation of intracellular contents (Gowda et al., 2009). In this study, the increased AST and ALT plasma levels corroborate with those reported in the previous studies. Kalender et al. (2010) identified increased liver enzymes (AST and ALT) after exposure to 27 mg/kg of malathion via gavage in male *Wistar* rats for 4 weeks. Gupta et al. (2020) also reported increased AST and ALT enzyme levels in male *Wistar* rats exposed to 29 mg/kg of malathion for 2 weeks. These studies indicate that exposure to malathion even at lower doses causes liver toxicity.

Plasma urea and creatinine levels are the main indicators of renal function by assessing the glomerular filtration rate (Abensur, 2011). In this study, the increased plasma creatinine level in the group of animals exposed to the highest dose of malathion indicates nephrotoxicity. A significantly increased serum creatinine level may occur owning to impaired glomerular function and tubular damage in the kidneys (Mansour and Mossa, 2010). Thus, this change in creatinine level is directly associated with glomerular dilatation since creatinine is directly related to the glomerular filtration process.

As for lipid peroxidation, the results show that this process did not occur in the kidneys and liver of the animals exposed to malathion, since no significant change in TBARS levels was noted. This result relates to increased antioxidant defenses represented by GST activity in the liver and CAT activity in the kidneys of animals exposed to the highest malathion dose. This indicates that these tissues could protect themselves from the damage caused by malathion; thus, preventing lipid peroxidation. However, renal SOD was decreased in the group exposed to the highest dose of malathion, indicating the beginning of a possible imbalance in renal tissue antioxidant defense. These data indicate that exposure to malathion for a longer period could increase reactive oxygen species formation and cause lipid peroxidation in the kidneys. Previous studies, such as the one by Abdel-Salam et al. (2018) that used higher doses of malathion (150 mg/kg) than those used in this study, identified increased oxidative stress levels owning to decreased antioxidant levels and evident lipid peroxidation process in the liver of male Sprague Dawley rats. Corroborating these data, Selmi et al. (2015) reported decreased activity of antioxidant enzymes, such as SOD and CAT, and increased lipid peroxidation in the kidneys and liver of infant *Wistar* rats nursed by mother *Wistar* rats exposed to 200 mg/kg of malathion.

This study shows that the kidney and liver are affected by exposure to malathion in a specific and independent way, with the kidney being more sensitive to the effects of this insecticide. In both the organs, the changes found cannot be associated with oxidative stress biomarkers since certain changes did not affect this process.

CONCLUSION

Malathion exposure during the peripubertal period causes significant renal tissue damage, changing its morphology and function, besides causing liver damage. It is evident that the kidneys are more sensitive to the action of malathion, without any relation with oxidative stress biomarkers.

ACKNOWLEDGMENTS

This article is part of the master's thesis of PMM Figaro (State University of Londrina, PR, Brazil) under the supervision of GSA Fernandes.

This study was partially funded by the Coordination for the Improvement of Higher Education Personnel (CAPES) - Financial Code 001. The authors thank CAPES/PROEX for the scholarship granted to PMM Figaro and for the financial support.

CONFLICT OF INTEREST

The authors declare no conflict of interests.

REFERENCES

Abdel-Salam, O.M., Sleem, A.A., Youness, E.R., Morsy, F.A., 2018. Preventive effects of cannabis on neurotoxic and hepatotoxic activities of malathion in rat. https://doi.org/10.4103/1995-7645.231467

Abdollahi, M., Donyavi, M., Pournourmohammadi, S., Saadat, M., 2004. Hyperglycemia associated with increased hepatic glycogen phosphorylase and phosphoenolpyruvate carboxykinase in rats following subchronic exposure to malathion. Comp. Biochem. Physiol. - C Toxicol. Pharmacol. 137, 343–347. https://doi.org/10.1016/j.cca.2004.03.009

Abensur, H., 2011. Biomarcadores na Nefrologia.

Adisa, A., Udeabor, S., Kubesch, A., Barbeck, M., Ghanaati, S., 2016. The utility of azan trichrome staining in Ameloblastoma. Niger. Postgrad. Med. J. 23, 44. https://doi.org/10.4103/1117-1936.180187

Aebi, H., 1984. Catalase in Vitro. Methods Enzymol. 105, 121–126. https://doi.org/10.1016/S0076-6879(84)05016-3

Al-Attar, A.M., 2010. Physiological and Histopathological Investigations on the Effects of α-Lipoic Acid in Rats Exposed to Malathion. J. Biomed. Biotechnol. 2010. https://doi.org/10.1155/2010/203503

Baconi, D.L., Bârcă, M., Manda, G., Ciobanu, A.M., Bălălău, C., 2013. Investigation of the toxicity of some organophosphorus pesticides in a repeated dose study in rats. Rom. J. Morphol. Embryol. 54, 349–356.

Baiomy, A.A., Attia, H.F., Soliman, M.M., Makrum, O., 2015. Protective effect of ginger and zinc chloride mixture on the liver and kidney alterations induced by malathion toxicity. Int. J. Immunopathol. Pharmacol. 28, 122–128. https://doi.org/10.1177/0394632015572083

Bancroft, J.D., Gamble, M., 2002. Theory and Practice of Histological Techniques, 5th ed. ed. Churchill Livingstone, Edinburgh.

Buege, J.A., Aust, S.D., 1978. Microsomal Lipid Peroxidation. Methods Enzymol. 52, 302–310. https://doi.org/10.1016/S0076-6879(78)52032-6

Crouch, R.K., Gandy, S.E., Kimsey, G., Galbraith, R.A., Galbraith, G.M., Buse, M.G., 1981. The inhibition of islet superoxide dismutase by diabetogenic drugs. Diabetes 30, 235–241. https://doi.org/10.2337/diab.30.3.235

El-Bini Dhouib, I., Lasram, M.M., Annabi, A., Gharbi, N., El-Fazaa, S., 2015. A comparative study on toxicity induced by carbosulfan and malathion in Wistar rat liver and spleen. Pestic. Biochem. Physiol. 124, 21–28. https://doi.org/10.1016/j.pestbp.2015.03.012

El-Gharieb, M.A., El-Masry, T.A., Emara, A.M., Hashem, M.A., 2010. Potential hepatoprotective effects of vitamin E and Nigella sativa oil on hepatotoxicity induced by chronic exposure to malathion in human and male albino rats. Toxicol. Environ. Chem. 92, 391–407. https://doi.org/10.1080/02772240902955719

Erthal, R.P., Staurengo-Ferrari, L., Fattori, V., Luiz, K.G., Cunha, F.Q., Pescim, R.R., Cecchini, R., Verri, W.A., Guarnier, F.A., Alves Fernandes, G.S., 2020. Exposure to low doses of malathion during juvenile and peripubertal periods impairs testicular and sperm parameters in rats: Role of oxidative stress and testosterone. Reprod. Toxicol. 96, 17–26. https://doi.org/10.1016/j.reprotox.2020.05.013

Espinoza-Navarro, O., Ponce-LaRosa, C., Bustos-Obregón, E., 2017. Organophosphorous Pesticides: Their Effects on Biosentinel Species and Humans. Control and Application in Chile. Int. J. Morphol. 35, 1069–1074. https://doi.org/10.4067/s0717-95022017000300041

Ferreira, A.L., Matsubara, L.S., 1997. Free radicals: concepts, associated diseases, defense system and oxidative stress. Rev. Assoc. Med. Bras. https://doi.org/10.1590/S0104-42301997000100014

Flehi-Slim, I., Chargui, I., Boughattas, S., El Mabrouk, A., Belaïd-Nouira, Y., Neffati, F., Najjar, M.F., Haouas, Z., Cheikh, H. Ben, 2015. Malathion-induced hepatotoxicity in male Wistar rats: biochemical and histopathological studies. Environ. Sci. Pollut. Res. 22, 17828–17838. https://doi.org/10.1007/s11356-015-5014-5

Franco, J.L., Posser, T., Mattos, J.J., Trevisan, R., Brocardo, P.S., Rodrigues, A.L.S., Leal, R.B., Farina, M., Marques, M.R.F., Bainy, A.C.D., Dafre, A.L., 2009. Zinc reverses malathion-induced impairment in antioxidant defenses. Toxicol. Lett. 187, 137–143. https://doi.org/10.1016/j.toxlet.2009.02.015

Gowda, S., Desai, P.B., Hull, V. V, Math, A.A.K., Vernekar, S.N., Kulkarni, S.S., 2009. A review on laboratory liver function tests. Pan Afr. Med. J. 3, 17. https://doi.org/10.11604/pamj.2009.3.17.125

Gupta, V.K., Kumar, A., Pereira, M. de L., Siddiqi, N.J., Sharma, B., 2020. Anti-Inflammatory and Antioxidative Potential of Aloe vera on the Cartap and Malathion Mediated Toxicity in Wistar Rats. Int. J. Environ. Res. Public Health 17, 5177. https://doi.org/10.3390/ijerph17145177

Hayes, J.D., Flanagan, J.U., Jowsey, I.R., 2005. Glutathione transferases. Annu. Rev. Pharmacol. Toxicol. https://doi.org/10.1146/annurev.pharmtox.45.120403.095857

Imafidon, E.C., Akomolafe, R.O., Oladele, A.A., 2016. Sexually dimorphic proteinuria in Wistar rats: Relevance to clinical models. Pathophysiology 23, 51–59. https://doi.org/10.1016/j.pathophys.2016.02.001

Jalili, C., Roshankhah, S., Moradi, Y., Salahshoor, M., 2018. Resveratrol attenuates malathion-induced renal damage by declining oxidative stress in rats. Int. J. Pharm. Investig. 8, 192. https://doi.org/10.4103/jphi.jphi_7_19

Joshi, A.K.R., Rajini, P.S., 2009. Reversible hyperglycemia in rats following acute exposure to acephate, an organophosphorus insecticide: Role of gluconeogenesis. Toxicology 257, 40–45. https://doi.org/10.1016/j.tox.2008.12.006

Joshi, S.C., Sharma, P., 2011. Male reproductive toxicity of organophosphorous compounds: A review. Toxicol. Environ. Chem. https://doi.org/10.1080/02772248.2011.581874

Kalender, S., Uzun, F.G., Durak, D., Demir, F., Kalender, Y., 2010. Malathion-induced hepatotoxicity in rats: The effects of vitamins C and E. Food Chem. Toxicol. 48, 633–638. https://doi.org/10.1016/j.fct.2009.11.044

Karami-Mohajeri, S., Abdollahi, M., 2011. Toxic influence of organophosphate, carbamate, and organochlorine pesticides on cellular metabolism of lipids, proteins, and carbohydrates: A systematic review. Hum. Exp. Toxicol. https://doi.org/10.1177/0960327110388959

Karami-Mohajeri, S., Ahmadipour, A., Rahimi, H.R., Abdollahi, M., 2017. Adverse effects of organophosphorus pesticides on the liver: A brief summary of four decades of research. Arh. Hig. Rada Toksikol. https://doi.org/10.1515/aiht-2017-68-2989

Kaya, Y., Bas, O., Hanci, H., Cankaya, S., Nalbant, I., Odaci, E., Avni Uydu, H., Aslan, A., 2018. Acute renal involvement in organophosphate poisoning: histological and immunochemical investigations. Ren. Fail. 40, 410–415. https://doi.org/10.1080/0886022X.2018.1489289

Keen, J.H., Habig, W.H., Jakoby, W.B., 1976. Mechanism for the Several Activities of the Glutathione S-Transferases, THE JOURNAL or BIOLOGICAL CHEMISTRY.

Lasram, M.M., Annabi, A.B., Elj, N. El, Selmi, S., Kamoun, A., El-Fazaa, S., Gharbi, N., 2009. Metabolic disorders of acute exposure to malathion in adult Wistar rats. J. Hazard. Mater. 163, 1052–1055. https://doi.org/10.1016/j.jhazmat.2008.07.059

Lasram, M.M., Dhouib, I.B., Bouzid, K., Lamine, A.J., Annabi, A., Belhadjhmida, N., Ahmed, M. Ben, Fazaa, S. El, Abdelmoula, J., Gharbi, N., 2014. Association of inflammatory response and oxidative injury in the pathogenesis of liver steatosis and insulin resistance following subchronic exposure to malathion in rats. Environ. Toxicol. Pharmacol. 38, 542–553. https://doi.org/10.1016/j.etap.2014.08.007

Mansour, S.A., Heikal, T.M., Mossa, A.T.H., 2008. Biochemical and histopathological effects of formulations containing Malathion and Spinosad in rats. Toxicol. Int. 15, 71–78.

Mansour, S.A., Mossa, A.H., 2010. Adverse effects of lactational exposure to chlorpyrifos in suckling rats. Hum. Exp. Toxicol. 29, 77–92. https://doi.org/10.1177/0960327109357276

Medeiros, A.C., Dantas-Filho, A.M., 2017. Cicatrização das feridas cirúrgicas. J. Surg. Clin. Res. 7, 87. https://doi.org/10.20398/jscr.v7i2.11438

Naraharisetti, S.B., Aggarwal, M., Ranganathan, V., Sarkar, S.N., Kataria, M., Malik, J.K., 2009. Effects of simultaneous repeated exposure at high levels of arsenic and malathion on hepatic drug-biotransforming enzymes in broiler chickens. Environ. Toxicol. Pharmacol. 28, 213–218. https://doi.org/10.1016/j.etap.2009.04.006

Nielsen, E., Østergaard, G., Larsen, J.C., 2008. Toxicological risk assessment of chemicals. A practical guide.

Nih, Od, Oer, Olaw, 2011. GUIDE LABORATORY ANIMALS FOR THE CARE AND USE OF Eighth Edition Committee for the Update of the Guide for the Care and Use of

Laboratory Animals Institute for Laboratory Animal Research Division on Earth and Life Studies.

Nirmal, N.K., Awasthi, K.K., John, P.J., 2020. Hepatotoxicity of graphene oxide in Wistar rats. Environ. Sci. Pollut. Res. https://doi.org/10.1007/s11356-020-09953-0

Ojeda, S.R., ANDREWS, W.W., ADVIS, J.P., WHITE, S.S., 1980. Recent Advances in the Endocrinology of Puberty. Endocr. Rev. 1, 228–257. https://doi.org/10.1210/edrv-1-3-228

Olatunji, S., Adewole, O., Ayannuga, O., Taiye, A., Adedayo, A., Sesan, O., 2015. Microanatomy and histomorphometry analysis of the effects of *Moringa oleifera* leaf extract on lead-induced kidney damage in adult wistar rats. Int. J. Biol. Chem. Sci. 9, 1599. https://doi.org/10.4314/ijbcs.v9i3.39

Ozsoy, A.Z., Uysal, M., Alici, O., Butun, I., Tas, U., Delibas, I.B., 2016. Protective effect of intravenous lipid emulsion treatment on malathion-induced 2425–2434.

Rezg, R., Mornagui, B., Kamoun, A., El-Fazaa, S., Gharbi, N., 2007. Effect of subchronic exposure to malathion on metabolic parameters in the rat. Comptes Rendus - Biol. 330, 143–147. https://doi.org/10.1016/j.crvi.2006.11.002

Selmi, S., El-Fazaa, S., Gharbi, N., 2015. Oxidative stress and alteration of biochemical markers in liver and kidney by malathion in rat pups. Toxicol. Ind. Health 31, 783–788. https://doi.org/10.1177/0748233713475507

Selmi, S., Rtibi, K., Grami, D., Sebai, H., Marzouki, L., 2018. Malathion, an organophosphate insecticide, provokes metabolic, histopathologic and molecular disorders in liver and kidney in prepubertal male mice. Toxicol. Reports 5, 189–195. https://doi.org/10.1016/j.toxrep.2017.12.021

Soltaninejad, K., Abdollahi, M., 2009. Current opinion on the science of organophosphate pesticides and toxic stress: A systematic review. Med. Sci. Monit. 15, 75–90.

Vijaya kumar, S., Fareedullah, M., Sudhakar, Y., Venkateswarlu, B., Ashok Kumar, E., 2010. Current review on organophosphorus poisoning. Arch. Appl. Sci. Res. 2, 199–215.

FIGURES AND FIGURE LEGENDS

Fig. 1. Renal morphometric evaluation of the animals in the groups: control (C), Malathion 10 mg/kg b.w. (10M) and Malathion 50 mg/kg b.w. (50M). (A) Average glomerular diameter. (B) Bowman's space. (C) Mean diameter of the proximal contorted tubules. (D) Mean diameter of distal contorted tubules. (E) Average diameter of the collecting tubule. Values expressed as mean ± SD; One-way ANOVA, Dunnett's test (*P<0,05).

Fig. 2. Hepatic morphometric evaluation of the animals in the groups: control (C), Malathion 10 mg/kg b.w. (10M) and Malathion 50 mg/kg b.w. (50M). (A) Mean diameter of the portal venule. (B) Average diameter of the bile ducts. (C) Mean diameter of the centrilobular venule. (D) Average of cells adhered (leukocytes) to the portal venules. (E) Average of adhered cells (leukocytes) to centrilobular venules. (F) Diameter of the sinusoids around the portal venule. (G) Diameter of the sinusoids around the centrilobular venule. Values expressed as mean ± SD; One-way ANOVA, Dunnett's test (*P<0,05).

Fig. 3. Renal histochemical evaluation of animals in the groups: control (C), Malathion 10 mg/kg b.w. (10M) and Malathion 50 mg/kg b.w. (50M). (A) Average percentage of neutral glycoconjugates present in the cortical region. (B) Average percentage of neutral glycoconjugates present in the medullary region. (C) Percentage of total collagen in the cortical region. (D) Percentage of total collagen in the medullary region. (E) Percentage of type I and III collagen in the cortical region. (F) Percentage of type I and III collagens in the medullary region. Values expressed as mean ± SD; One-way ANOVA, Dunnett's test (*P<0,05).

Fig. 4. Histochemical evaluation of the liver of the animals in the groups: control (C), Malathion 10 mg/kg b.w. (10M) and Malathion 50 mg/kg b.w. (50M). (A) Average percentage of neutral glycoconjugates present in the portal venule region. (B) Average percentage of neutral glycoconjugates present in the region of the centrilobular venule. (C) Percentage of total collagen in the region of the portal venule. (D) Percentage of total collagen in the region of the centrilobular venule. (E) Percentage of type I and III collagen in the region of the portal venule. (F) Percentage of type I and III collagens in the region of the centrilobular venule. Values expressed as mean ± SD; One-way ANOVA, Dunnett's test (*P<0,05).

Fig. 5. Assessment of renal function and liver toxicity of the animals in the groups: control (C), Malathion 10 mg/kg b.w. (10M) and Malathion 50 mg/kg b.w. (50M). (A) Plasma concentration of urea. (B) Plasma concentration of creatinine. (C) Plasma concentrations of AST. (D) Plasma concentration of ALT. Values expressed as mean ± SD; One-way ANOVA, Dunnett's test (*P<0,05).

Fig. 6. Effects of malathion on markers of oxidative stress in kidney and liver of animals in the groups: control (C), Malathion 10 mg/kg b.w. (10M) and Malathion 50 mg/kg b.w. (50M). (A) Dosage of TBARS in the kidneys. (B) Liver TBARS dosage. (C) Evaluation of renal GST activity. (D) Evaluation of hepatic GST activity. (E) Renal catalase activity. (F) Hepatic catalase activity. (G) Renal SOD activity. (H) Hepatic SOD activity. Values expressed as mean ± SD; One-way ANOVA, Dunnett's test (*P<0,05).

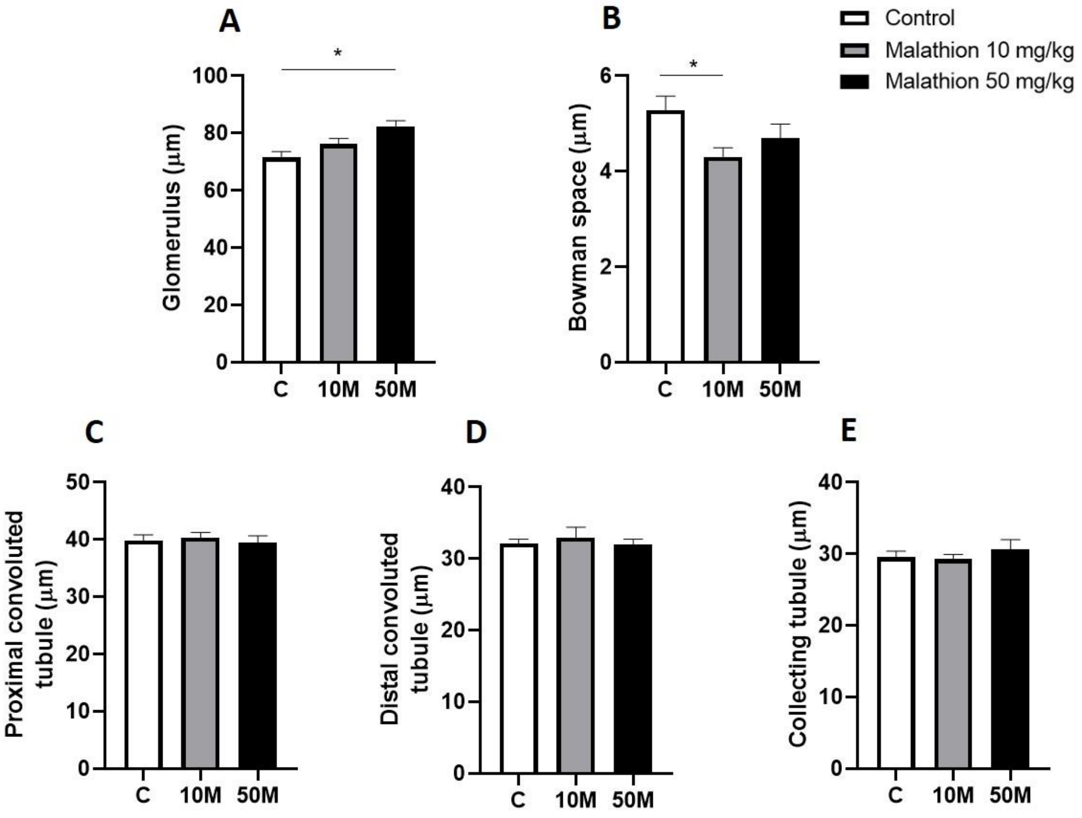
A
B
Control
Malathion 10 mg/kg
Malathion 50 mg/kg
*
Glomerulus (μm)
0
20
40
60
80
100
C
10M
50M
*
Bowman space (μm)
0
2
4
6
C
10M
50M
C
D
E
Proximal convoluted tubule (μm)
0
10
20
30
40
50
C
10M
50M
Distal convoluted tubule (μm)
0
10
20
30
40
C
10M
50M
Collecting tubule (μm)
0
10
20
30
40
C
10M
50M

Fig. 1.

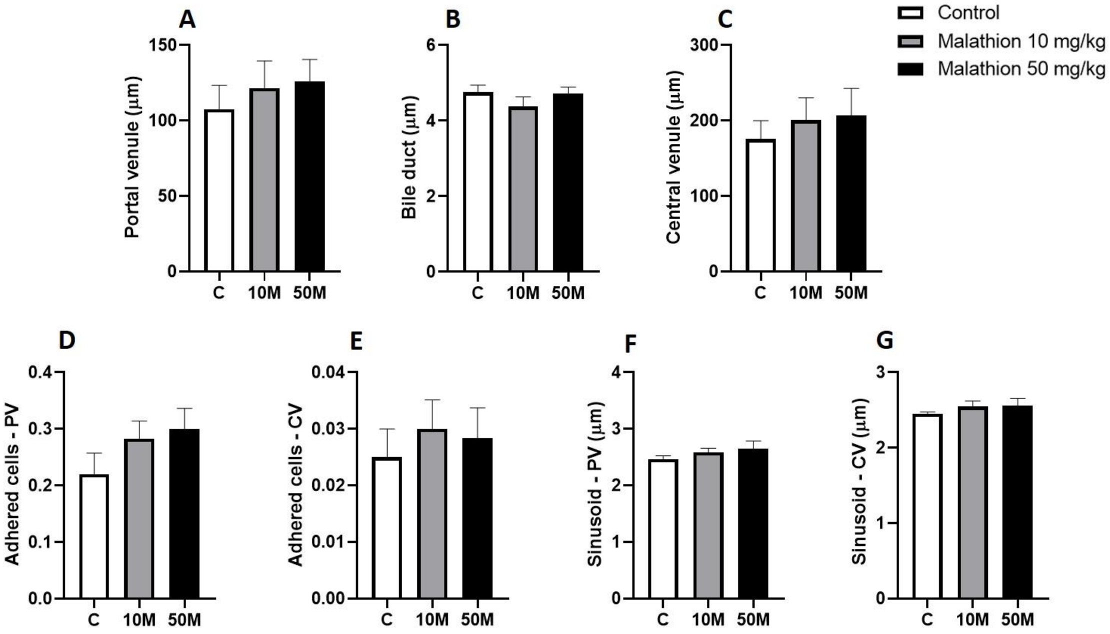
A
B
C
Control
Malathion 10 mg/kg
Malathion 50 mg/kg
Portal venule (μm)
150
100
50
0
Bile duct (μm)
6
4
2
0
Central venule (μm)
300
200
100
0
C
10M
50M
D
E
F
G
Adhered cells - PV
0.4
0.3
0.2
0.1
0.0
Adhered cells - CV
0.04
0.03
0.02
0.01
0.00
Sinusoid - PV (μm)
4
3
2
1
0
Sinusoid - CV (μm)
3
2
1
0

Fig. 2.

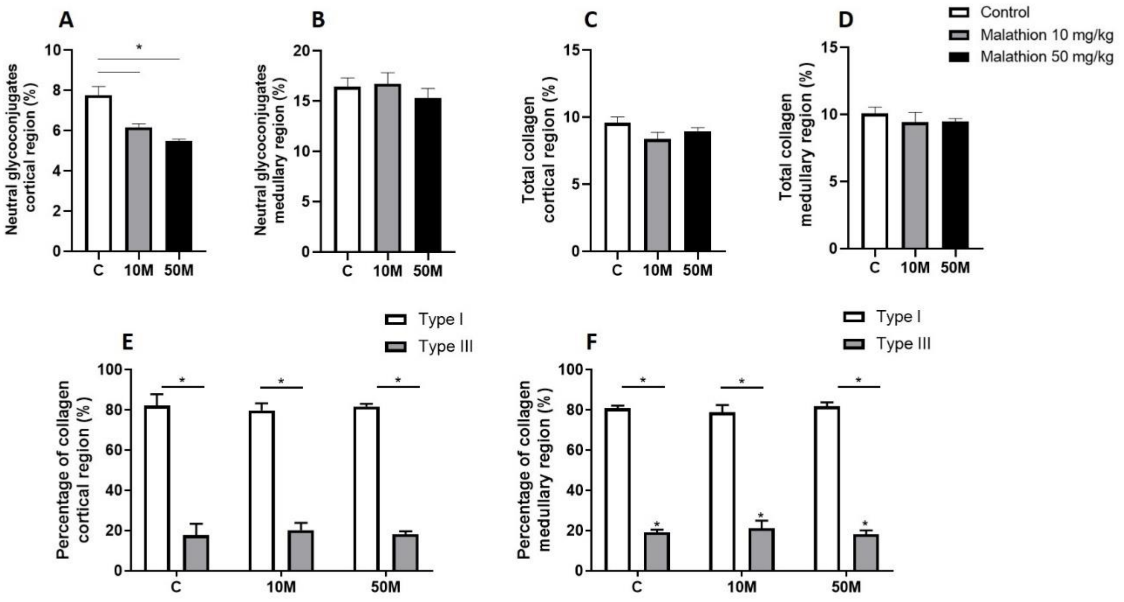
A
B
C
D
Control
Malathion 10 mg/kg
Malathion 50 mg/kg
Neutral glycoconjugates cortical region (%)
Neutral glycoconjugates medullary region (%)
Total collagen cortical region (%)
Total collagen medullary region (%)
C
10M
50M
*
E
F
Type I
Type III
Percentage of collagen cortical region (%)
Percentage of collagen medullary region (%)
0
2
4
6
8
10
5
15
20
40
60
80
100

Fig. 3.

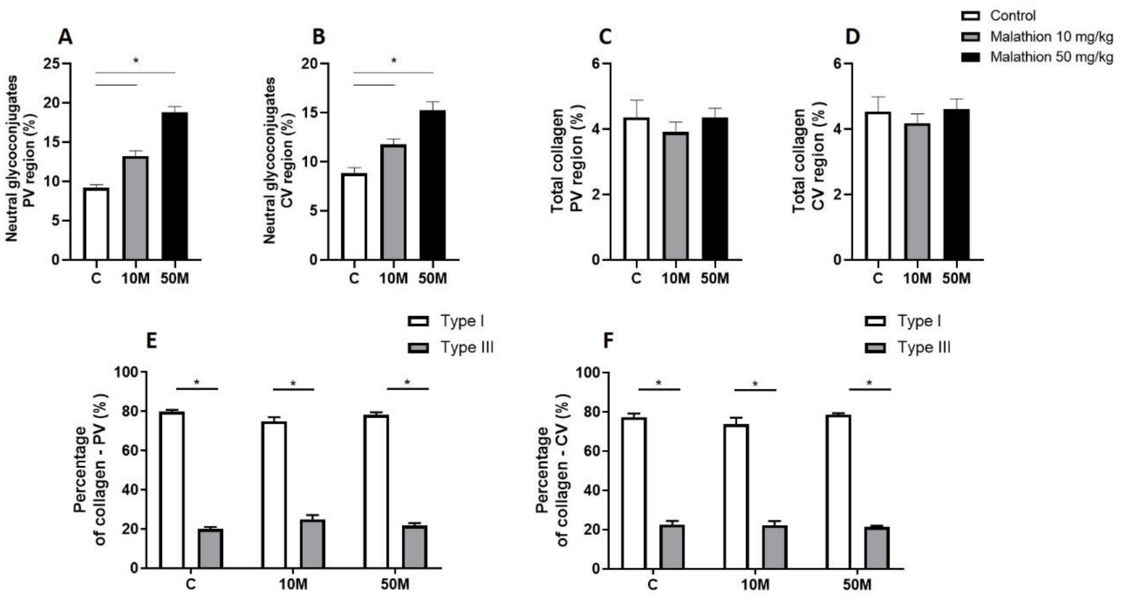
A
B
C
D
Control
Malathion 10 mg/kg
Malathion 50 mg/kg
Neutral glycoconjugates PV region (%)
Neutral glycoconjugates CV region (%)
Total collagen PV region (%)
Total collagen CV region (%)
*
25
20
15
10
5
0
6
4
2
C
10M
50M
E
F
Type I
Type III
Percentage of collagen - PV (%)
Percentage of collagen - CV (%)
100
80
60
40
20
0

Fig. 4.

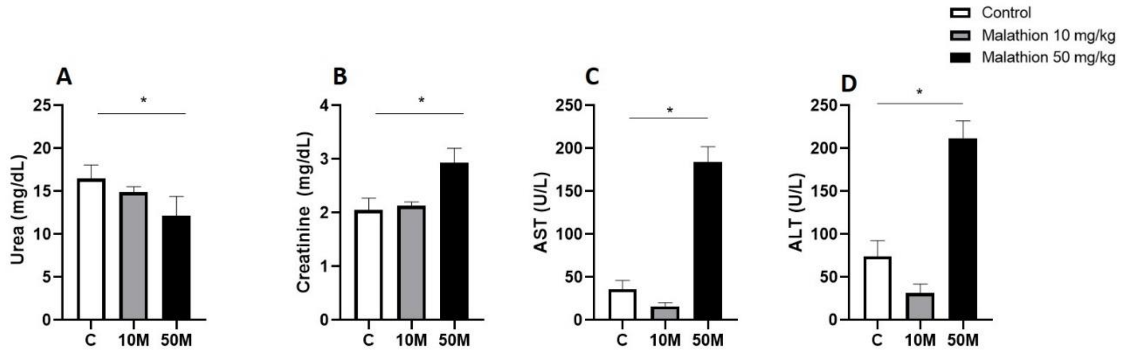
Control
Malathion 10 mg/kg
Malathion 50 mg/kg
A
Urea (mg/dL)
25
20
15
10
5
0
C
10M
50M
*
B
Creatinine (mg/dL)
4
3
2
1
0
C
10M
50M
*
C
AST (U/L)
250
200
150
100
50
0
C
10M
50M
*
D
ALT (U/L)
250
200
150
100
50
0
C
10M
50M
*

Fig. 5.

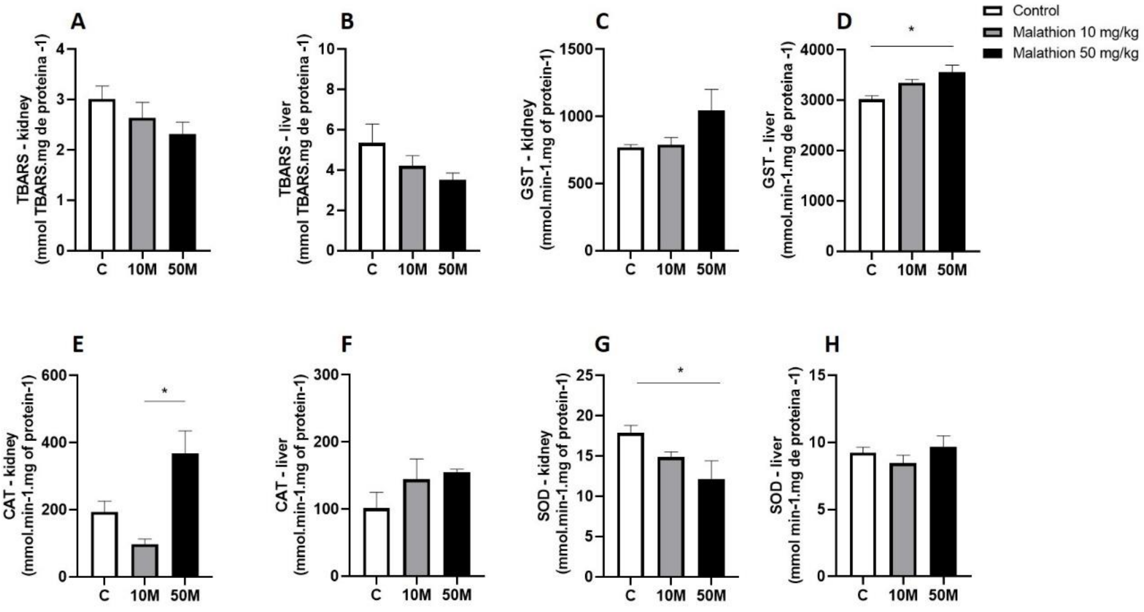
A
TBARS - kidney
(mmol TBARS.mg de proteina -1)
4
3
2
1
0
C
10M
50M
B
TBARS - liver
(mmol TBARS.mg de proteina -1)
10
8
6
4
2
0
C
10M
50M
C
GST - kidney
(mmol.min-1.mg of protein-1)
1500
1000
500
0
C
10M
50M
D
*
GST - liver
(mmol.min-1.mg de proteina -1)
4000
3000
2000
1000
0
C
10M
50M
Control
Malathion 10 mg/kg
Malathion 50 mg/kg
E
*
CAT - kidney
(mmol.min-1.mg of protein-1)
600
400
200
0
C
10M
50M
F
CAT - liver
(mmol.min-1.mg of protein-1)
300
200
100
0
C
10M
50M
G
*
SOD - kidney
(mmol.min-1.mg of protein-1)
25
20
15
10
5
0
C
10M
50M
H
SOD - liver
(mmol min-1.mg de proteina -1)
15
10
5
0
C
10M
50M

Fig. 6.

Artigo 2

Cyclosporine A alteres renal and hepatic morphophysiology in *Swiss* mice

Artigo será submetido à revista —“Human & Experimental Toxicology”

ISSN: 0960-3271;

F.I. 2020: 2.067

Qualis CAPES 2013-2019 (Medicina II): B1

4.2 CYCLOSPORINE A ALTERS RENAL AND HEPATIC MORPHOPHYSIOLOGY IN *SWISS* MICE

Pedro Mareti Maçaira Fígaro[1,2,3], Danielle Ramos da Silva[2], Gabriel Smolak Sobieski e Silva[2], Maylla Cardoso de Oliveira[2], Ivana Regina Costa[1], Suellen Ribeiro da Silva Scarton[1,3], Glaucia de Lion Siervo[1,3], Fábio Goulart de Andrade[2], Glaura Scantamburlo Alves Fernandes[1]*

1 – Department of General Biology, Biological Sciences Center, State University of Londrina – UEL, Londrina, Paraná, Brazil, Rodovia Celso Garcia Cid, PR 445, Postal code: 86057-970
2 – Department of Histology, Biological Sciences Center, State University of Londrina – UEL, Londrina, Paraná, Brazil, Rodovia Celso Garcia Cid, PR 445, Postal code: 86057-970
3 – Department of General Pathology, Biological Sciences Center, State University of Londrina – UEL, Londrina, Paraná, Brazil, Rodovia Celso Garcia Cid, PR 445, Postal code: 86057-970

***Corresponding author**
Glaura Scantamburlo Alves Fernandes
Tel.: +55 43 33714417
E-mail address: glaura@uel.br (G.S. A. Fernandes)

ABSTRACT

Cyclosporine A (CsA), an immunosuppressive drug, is used to treat autoimmune diseases and to prevent the rejection of transplanted organs. However, it demonstrates renal and hepatic toxicity. The objective of the present study was to evaluate biochemical, histological, and antioxidant changes in the kidneys and livers of mice exposed to low-dose (non-immunosuppressive) CsA. A total of 30 adult *Swiss* mice were treated for 10 and 50 days and divided into five experimental groups (n = 6). The control group (C) and the CsA10i group were administered with water and 10 mg/kg of CsA, respectively. Mice in both groups were euthanized after 11 days of commencing the experiments. The mice in the CsA10r group were administered 10 mg/kg of CsA, underwent a 10-day recovery period, and were euthanized after 21 days of commencing the experiments. The mice in the CsA50i group were administered 10 mg/kg of CsA and were euthanized after 51 days of commencing the experiments. The mice in the CsA50r group were administered 10 mg/kg of CsA, underwent a 50-day recovery period, and were euthanized after 101 days of commencing the experimental. Analysis of the renal histological features showed a decrease in the Bowman's space diameter in the CsA10r and CsA50r groups. The liver histological analysis demonstrated an increase in the mean diameter of the central venules in the CsA10i and CsA10r groups, decrease in the mean diameter of biliary ducts in the CsA50i group, and dilation of sinusoids around the portal and central venules in the CsA10i and CsA10r group. Biochemical analysis showed increased urea levels in the CsA50r group and decreased alanine aminotransferase levels in the CsA10i group. The oxidative stress analysis showed that thiobarbituric acid reactive substance levels were increased in the kidneys and liver of animals in the CsA50r group. Antioxidant enzyme, such as glutathione-S-transferase, levels were decreased in the kidneys of all treatment groups; moreover, their levels were reduced in the livers of only the CsA50i and CsA50r groups. Analysis of renal superoxide dismutase expression showed a remarkable decrease in its activity in the CsA10i, CsA10r, and CsA50i groups. We conclude that exposure to a low dose of CsA causes considerable liver damage immediately and after the recovery period, whereas damage in the kidneys was noticed only after the recovery period. Therefore, under these experimental conditions, the liver was more sensitive to CsA than the kidney, and this sensitivity was not related to oxidative stress.

Keywords: cyclosporine A; hepatotoxicity; nephrotoxicity

INTRODUCTION

Cyclosporine is a family of long-chain, cyclic, lipophilic peptides with 11 amino acids. Among them, cyclosporine A (CsA) is the most commonly used commercial drug.[1] This compound exhibits strong immunosuppressive activity via the inhibition of calcineurin, a molecule that activates nuclear factors present in the cytosol by dephosphorylating them, which, in turn, leads to the production of cytokines involved in the activation of T lymphocytes.[2–4] Calcineurin inhibitors are powerful immunosuppressants that have revolutionized organ transplantation because of their efficacy. However, they exert several toxic effects, which are dose-dependent. Renal and hepatic alterations are among the most common manifestations.[5–7]

Nephrotoxicity attributed to CsA is associated with decreased blood supply and tubular changes. Changes in blood flow are directly associated with increased vascular resistance due to activation of the sympathetic nervous system, which promotes a decrease in glomerular filtration rate.[8–11]Moreover, the vascular effects attributed to the use of CsA are also related to an increase in factors regulating vasoconstriction, including endothelin-1 (ET-1), and a decrease in factors mediating vasodilation, including prostacyclin, prostaglandin E2, and nitric oxide.[12–14]The mechanisms underlying CsA-induced hepatotoxicity remain uncharacterized. Evidence suggests that oxidative stress is the main factor involved in this process.[15,16] Thus, an increase in oxidant molecule levels attributed to CsA exposure induces mitochondrial changes in hepatocytes, such as blockade of the mitochondrial permeability transition pore, increasing the Ca^{2+} and reactive oxygen species (ROS) levels, altering the electron transport chain,[17] and inhibiting β-oxidation of fatty acids.[17,18]

Thus, the objective of the present study was to evaluate the short- and long-term effects of a safe, non-immunosuppressive dose of CsA on the kidney and liver morphology, using *Swiss* mice as an experimental model.

MATERIAL AND METHODS

Cyclosporine A

Cyclosporine A (Sandimmun Neoral ® 100mg/ml, Novartis, Delpharm Huningue S.A.S, Huningue, France) was diluted daily in the corresponding volume of water and stored protected from light until administration. The dose of 10 mg / kg was standardized from the previous study of Guada et al.[24] in which there was no immunosuppressive effect.

Animals and experimental conditions

Adult *Swiss* male mice (n=30) (Mus musculus), at postnatal day (PND 50) were supplied by the Animal House of Biological Sciences Centre, State University of Londrina (CCB - UEL), and were acclimated to the new environment at the Laboratory of Toxicology and Metabolic Dysfunction of Reproduction with controlled temperature conditions (23 °C) and lighting (photoperiod of 12h light/12h dark). Before the start of the experimental period, the rats were acclimated to the new environment for 10 days. The animals were allocated into polypropylene cages with laboratory-grade pine shavings as bedding during the entire experiment and received rat chow (standard commercial laboratory chow, Nuvilab®) and tap water *ad libitum.* All experimental protocols used were approved by the Ethics Committee on the Use of Animals at the State University of Londrina (OF. CIRC. CEUA/UEL nº 68/2017).

Experimental design

On the 60th postnatal day, 36 mice were randomly assigned to 6 groups (6 animals / group): A Control group that received only the vehicle (water) via gavage, and 4 groups that received Cyclosporine A via gavage at a dose of 10 mg / kg diluted in water for 10 or 50 days as described below:

- **10 Days experiment:** Control animals and Cyclosporine A immediate groups were treated for 10 consecutive days and euthanized immediately after treatment (11th day) (CsA10i). Animals in the cyclosporine A 10-day recovery group underwent a period of 10-day, without any treatment, being euthanized on the 21st experimental day (CsA10r).
- **50 Days experiment:** The Cyclosporine A 50-days immediate mice were treated for 50 consecutive days and euthanized immediately after treatment (51st day) (CsA50i). The animals in the Cyclosporine A 50-day recovery group underwent a 50-day period without any treatment, being euthanized on the 101st experimental day (CsA50r).

At the end of the treatment, the mice were anesthetized with isoflurane, euthanized by decapitation and the blood from the ruptured vessels was collected in a tube with heparin to obtain the plasma which was used to assess liver (AST and ALT) and renal toxicity (urea and creatinine). The kidneys and livers were collected and used for histopathological or oxidative stress analysis.

Histopathological analysis

Kidneys and liver were fixed in aqueous Bouin's solution for 48 hours and subsequently sent to the laboratory of histopathological analysis (LAHip) of the Londrina State University. After fixation, the organs were dehydrated in an increasing series of ethanol, clarified in xylol and embedding in histological paraffin. The 7 µm thick cuts were made in a semi-automatic microtome (CUT 5062 SLEE medical GmbH, Germany) and the slides were stained with hematoxylin and eosin; Schiff's periodic acid (PAS); Azan trichrome and Picrosirius Red.[20] Observations and photo documentation were performed at 400x magnification, in a Moticam image capture system (Motic, Xiamen, China), attached to the light microscope.

Hematoxylin and Eosin (H&E) for morphometric analysis

For kidney analysis, 10 images of the cortical region and 10 images of the medullary region per animal were analyzed. In the cortical region, the diameter of the renal corpuscles, Bowman's space and diameters of the proximal and distal convoluted tubules were determined. In the medullary region, the diameter of the collecting tubules was measured.[21,22]

For liver analysis, 10 images of the periportal region and 10 images of the centrilobular region were analyzed, per animal. In the periportal region, the diameters of 10 portal venules, 10 bile ducts and 10 sinusoids were determined. In the centrilobular region, the diameters of 10 centrilobular venules and 10 sinusoids were measured. In both regions, the leukocytes adhered to the endothelium of the venules were quantified.[23]

Periodic acid Schiff reaction (PAS) for the detection of neutral glycoconjugates

In the kidneys, 5 images of the cortical region and 5 images of the medullary region were analyzed, while in the liver, 5 images of the periportal region and 5 images of the centrilobular region were analyzed, per animal. In each image, using the image-Pro Plus® software (Media Cybernetics, Maryland, USA) the proportion of the purple pixels was determined, indicating positive marking for neutral glycoconjugates.[20]

Azan trichrome to determine the percentage of total collagen

In the kidneys, 5 images of the cortical region and 5 images of the medullary region were analyzed, while in the liver, 5 images of the periportal region and 5 images of the centrilobular region were analyzed, per animal. In each image, using the image-Pro Plus® software (Media Cybernetics, Maryland, USA) the proportion of the blue pixels presented by the collagen fibers in the histological sections was determined.[24]

Picrosirius Red for quantification of type I and type III collagen

In observation under polarized light, 5 images of the cortical region and 5 images of the medullary region were captured in the kidneys, while 5 images of the periportal region and 5 images of the centrilobular region were analyzed per animal in the liver In each image, using the image-Pro Plus® software (Media Cybernetics, Maryland, USA), the proportion of the red (type I collagen) and green (type III collagen) pixels was determined.[25]

Assessment of renal function and liver toxicity

To assess renal function, plasma urea and creatinine concentrations were determined using commercial kits, according to the manufacturer's instructions. (Labtest® Diagnóstico S.A., Lagoa Santa, MG, Brazil). The results were presented in milligrams per deciliter (mg / dL) of plasma urea or creatinine.

To assess hepatotoxicity, plasma samples were processed following manufacturer’s instructions to determine the concentrations of aspartate aminotransferase (ALT) and alanine aminotransferase (AST) using commercial kits (Labtest® Diagnóstico S.A., Lagoa Santa, MG, Brazil). The results were presented as U / L of ALT or plasma AST.

Analysis of oxidative stress biomarkers in the kidney and liver

Sample processing

The fragments of the kidneys and livers were homogenized in PBS (pH 7.2), and the homogenate was centrifuged at 3,000 rpm for 20 minutes. The supernatant was separated and diluted at a ratio of 1:100. The quantification of proteins in the sample was determined using the Bradford biochemical method. A standard curve, consisting of white, 0.06; 0.12; 0.25; 0.5 and 1 mg BSA per mL, was pipetted in triplicate into a 96-well plate. Then, 10µL of the diluted samples were also pipetted in triplicate, following the standard curve. 250µL of the Bradford reagent was added and absorbance was measured at 595 nm. From the data obtained, calculations were performed for the dilution of the samples to have a final protein concentration of 1mg/mL.

Determination of thiobarbituric acid reactive substances (TBARS)

In this analysis, 50 µL of the sample in triplicate was pipetted into a 96-well microplate, 5 µl of iron chloride ($FeCl3$) (1M), 5 µl of ascorbic acid (0.5M), 50 µl of trichloroacetic acid (TCA) (2.8%) and 50 µl of thiobarbituric acid (TBA) (1%). The microplates were kept in a water bath for 15 minutes and the absorbances were read at 535 and 572 nm.[26]

Glutathione s-transferase activity (GST)

For this analysis, 20 µL of the samples and potassium phosphate buffer (0.1 M) were pipetted, in triplicate, in a 96-well microplate. Subsequently, 180 µL of a mixture composed of reduced glutathione (GSH), 1-chloro-2,4-dinitrobenzene (CDNB) and potassium phosphate buffer were pipetted in all wells. Sample absorbances were measured at 340 nm at 40-second intervals for 5 minutes.[27]

Superoxide dismutase activity (SOD)

The activity of superoxide dismutase (SOD) was evaluated according to the method originally proposed by (Crouch et al., 1981). The principle of this analysis was to quantify the complex formed between superoxide and nitrotetrazolium blue (NBT), measured at 560 nm over a period of 1 hour. An aliquot of 0.75 mg.mL-1 of protein in 25% ethanol was prepared in a total volume of 800 µL. The samples were centrifuged at 13,680 g at 4ºC for 20 minutes, and supernatant was pipetted in triplicate, in a 96-well microplate; the final 200µL volume contained: 0.1 mg protein.mL-1, 0.09 mM NBT, 0.015 mM EDTA, 34.78 mM hydroxylamine sulfate and 79 mM sodium carbonate buffer (pH 10,2). The activity values of the antioxidant enzymes were expressed in U. mg protein-1.

Statistical analysis

For statistical analysis, the IBM SPSS® software was used (SPSS Inc, Chicago, Illinois, USA) and the results were expressed as mean ± SD. One-way analysis of variance (ANOVA) was used, followed by Dunnett's post-test for parametric data. Nonparametric results were compared by Kruskal-Wallis and Dunn's post-test. Differences were considered statistically significant when P <0.05.

RESULTS

Morphometric and histopathological analysis of the kidneys and livers

With respect to the histological analysis, no changes were observed in the glomerular diameter in both the “immediate” and “recovery” groups (Figure 1a). However, the Bowman's space was retracted in the CsA10r and CsA50r groups (Figure 1b) as compared to that observed in the control group. In addition, no changes in the mean diameter of the proximal (Figure 1c) and distal (Figure 1d) convoluted tubules or the collecting ducts (Figure 1e) were observed in the CsA10i, CsA50i, CsA10r, and CsA50r groups. These results were statistically similar to those observed in the control group.

Liver analysis showed an increase in the mean diameter of the portal venules in the CsA10r group (Figure 2a) and reduction in the mean diameter of the biliary ducts in the CsA50i group as compared to that observed in the control group (Figure 2b). With respect to the mean diameter of the central venules (Figure 2c), dilation was observed in the CsA10i and CsA10r groups compared to that observed in the control group. No changes were observed in the number of cells adhering to the portal venule (Figure 2d) and central venule (Figure 2e) in any of the groups; however, an increase in the diameter of the liver sinusoids located around the portal venules (Figure 2f) and central venules (Figure 2g) was observed in the CsA10i and CsA10r groups relative to that of the control group.

Determination of neutral glycoconjugates (PAS)

Staining for neutral glycoconjugates demonstrated no changes in the CsA10i, CsA10r, CsA50i, and CsA50r groups as compared to that in the control group. These findings were evaluated in the cortical (Figure 3a) and medullary (Figure 3b) regions of the kidneys and the portal (Figure 4a) and central venules (Figure 4b) in the liver.

Quantification of total collagen and collagen type I and III

The analysis of the mean percentages of total collagen in the cortical (Figure 3c) and medullary (Figure 3d) regions of the kidneys did not show significant changes in the CsA10i, CsA10r, CsA50i, and CsA50r groups as compared to those observed in the control group. In the five experimental groups, the presence of collagen type I was dominant over collagen type III in both these regions (Figures 3e and 3f). Similarly, in the liver, no alterations were observed in the percentage of total collagen in the regions of the portal (Figure 4c) and central venules (Figure 4d) as compared to those in the control group. Moreover, the presence of collagen type I was dominant over collagen type III in both regions of the liver (Figures 4e and 4f) in all groups.

Hepatotoxicity and nephrotoxicity

Serum concentrations of urea were higher in the CsA50r group (Figure 5a) than in the control group. The concentration of creatinine in the experimental groups (Figure 5b) was not significantly different from that observed in the control. In the liver, serum levels of aspartate aminotransferase (AST) (Figure 5c) observed in the CsA10i, CsA10r, CsA50i, and CsA50r groups did not differ significantly from those observed in the control; however, a decrease in the serum levels of alanine aminotransferase (ALT) was observed in the CsA10i group (Figure 5d) relative to those of the control group.

Biomarkers of oxidative stress

An increase was observed in the lipid peroxidation in the kidneys (Figure 6a) and the liver (Figure 6b) of the animals in the CsA50r group (Figure 6a) as compared to that in the control group. Although not statistically significant, an increase of 34.50% was observed in lipid peroxidation in the liver of the animals in the CsA50i group as compared to that in the control group. Glutathione-S-transferase (GST) activity was decreased in the kidneys (Figure 6c) of animals in the CsA10i, CsA10r, CsA50i, and CsA50r groups, as well as in the liver of the animals in the CsA50i and CsA50r groups (Figure 6d) compared to that observed in the control group. Superoxide dismutase (SOD) activity was reduced in the kidneys of the groups CsA10i, CsA10r, and CsA50i (Figure 6e) as compared to that observed in the kidneys of the control group. The analysis of SOD activity in the liver showed no statistically significant changes among the experimental groups, although there was a 29.08% reduction in the CsA50i group (Figure 6f) compared to that in the control group.

DISCUSSION

As demonstrated above, exposure to CsA resulted in significant liver damage in the immediate and recovery periods, whereas damage to the kidneys was only detected after the recovery period.

Although the present study did not show changes in the mean diameter of the proximal and distal tubules and collecting ducts of the animals exposed to CsA, Lu et al.[29] demonstrated that a dose of 25 mg/kg/day of CsA administered to male Sprague Dawley rats for 4 weeks caused tubular atrophy, interstitial fibrosis, and tubular apoptosis. Their findings indicated that doses higher than those used in the present study might affect renal integrity. Furthermore, continued use of CsA at a dose of 17.5 mg/kg/day in humans may induce tubular injury and focal sclerosis of the glomeruli.[30] However, retraction of the Bowman’s space observed in the CsA10r and CsA50r groups suggests that the effect of CsA is initiated after the cessation of exposure to CsA. Harb et al.[31] reported that administration of a dose of 25 mg/kg/day of CsA for 6 weeks resulted in a low glomerular retraction and mild increase of the Bowman’s space in *Wistar* rats. These finding demonstrate that histological changes are detected in the kidneys on their immediate assessment after exposure to a high dose of CsA. However, since no immediate damage was observed in the Bowman’s space in the present study, the activation of the constituents of this renal component through some unknown mechanism resulted in a latent response to CsA.

Serum concentrations of urea and creatinine are the main indicators of renal function because they measure the glomerular filtration rate.[32] Under the experimental conditions of the present study, there were no changes in serum creatinine levels but the increase in urea levels in the CsA50r group indicated that renal filtration capacity was impaired following the cessation of CsA exposure. Transplant patients treated with a dose of 3.8 mg/kg CsA for four days showed decreased serum urea and creatinine levels.[33] A study performed by administering CsA at a dose of 4.3 mg/kg for 88 days showed an increase in the serum concentrations of both renal function parameters.[34] No consensus has been established with respect to the behavior of renal functional parameters (increase or decrease) following administration of CsA at a low dose; however, the observed changes may be related to the duration of treatment. Sereno et al.[35] showed that a high dose of CsA (30 mg/kg) administered to male *Wistar* rats for three weeks increased serum urea and creatinine levels. By contrast, a dose close to that used in the said study (25 mg/kg) led to an increase in serum creatinine levels and a reduction in its clearance in male C57BL/6 mice.[36] Thus, based on the data obtained in the present study and previous studies, CsA may compromise renal function when administered at low doses for long intervals and at high doses during different periods.

Similar to the kidneys, the results of the liver analysis showed alterations in certain histological features after CsA administration. Dilation of the portal venules in the animals of the CsA10r group and in the central venules of the animals in the CsA50i and CsA50r groups, detected when determining the mean diameter of blood vessels, demonstrated a deleterious effect of CsA on these vessels observed in the immediate period and after the recovery period. Despite these alterations, no changes were observed in the number of cells (lymphocytes) adhering to these venules. Similar results were described for the diameter of liver blood vessels by Battino et al.[37] However, they treated male *Wistar* rats with 30 mg/kg of CsA for four weeks and observed dilation of the portal and central venules, with thickening of connective tissues in these regions. Kurus et al.[38] and Nacar et al.[39] administered CsA at doses of 10 and 20 mg/kg for 28 and 12 days, respectively, and reported dilation and congestion of sinusoids and apoptosis and vacuolization of hepatocytes in male rats. Hoorn et al.[40] reported that CsA promotes changes in the vascular endothelium and that the mechanism involved in these processes is still unknown. The findings of the present study corroborate these results by demonstrating alteration of vascular patterns by CsA, as shown by changes in the diameter of the portal and central venules. Furthermore, the hepatic venous system changed in response to CsA regardless of the dose and time of administration.

The increase in the diameter of liver sinusoids of the portal and central venules of the animals in the CsA10i and CsA10r group is probably an adaptation of the organ to the damage induced by CsA. Sinusoidal dilation is one of the effects associated with CsA toxicity.[41,42] Studies conducted by Böhmer et al.[43] showed dilation of liver sinusoids after the administration of CsA at doses of 25 mg/kg (for 21 days) and 15 mg/kg (for 8 weeks) in male *Wistar* rats.

In addition, the reduced diameter of the biliary ducts in the CsA50i group may be related to the excretion of CsA metabolites via the biliary system.[44] In this context, analysis of the liver function in the present study showed hepatotoxic effects associated with the dose of 10 mg/kg at the enzymatic level. The enzymes, AST and ALT, are present in large amounts in the cytoplasm of hepatocytes,[45] and serum ALT is a more sensitive diagnostic marker of liver damage, according to Srivastava et al.[46] However, Kim et al.[47] reported that hepatocellular damage results in an immediate increase in the serum level of AST. Thus, the results obtained for this enzyme show that CsA did not promote significant changes in the levels of this enzyme during any of the treatment periods or after its cessation. However, owing to a decrease in ALT levels as well as histopathological alterations in the liver it is suggested that exposure to CsA leads to changes in the liver in the immediate period.

The absence of changes in the amount of neutral glycoconjugates in the kidneys and livers in the groups exposed to CsA is in line with the results observed in the study performed by Kedzierska et al.[48] These authors treated male *Wistar* rats with 20 mg/kg of CsA for six months and observed no change in the amounts of neutral glycoconjugates in the kidneys of these animals. Akbulut et al.[49] reported a reduction in glycogen stores of the rats treated with 25 mg/kg CsA for 30 days, which may be related to the amount of neutral glycoconjugates. Thus, the data obtained in the present study suggest that treatments with CsA did not alter the distribution and quantity of neutral glycoconjugates in the kidneys and livers of mice.

The quantification of total collagen and collagen type I and III in the kidneys and livers of the animals treated with CsA showed that this drug did not alter their amounts and, therefore, did not result in the development of fibrosis-like lesions. Collagen type I and III are the main constituents of the extracellular matrix of the renal interstitium and are also part of the liver's constitution. Their proportion is not fixed and changes may be observed in the regions of the portal and central veins.[50] In a study performed with male Fischer 344 rats treated with 15 mg/kg of CsA for four weeks, there was an increase in collagen deposition in the kidneys.[51] Similarly, Rezzani et al.[52] observed an increase in the amount of collagen that resulted in the development of interstitial fibrosis in the renal tubules of mice exposed to 15 mg/kg CsA for 21 days. However, Rowshani et al.[57] demonstrated a decrease in renal fibrosis after the recovery period in the kidneys of transplant patients treated with 4 mg/kg CsA for 52 weeks. With respect to the liver, although Devarbhavi[54] reported liver fibrosis in response to methotrexate, an immunosuppressive agent, De Freitas et al.[55] did not observe this phenomenon in male *Wistar* rats administered with 15 mg/kg of CsA for 21 days. The comparison with methotrexate is justified by the fact that the study used a non-immunosuppressive dose of CsA. Because collagen plays a key role in tissue integrity,[56] the absence of changes in the present study indicates that the structures of the kidney and liver were not impaired in response to CsA.

Lim et al.[57] and Ince et al.[58] reported that the increased production of ROS and, consequently, oxidative stress are directly associated with kidney and liver damage induced by CsA exposure. This process promotes mitochondrial changes that result in disruption of $Na^+ K^+$ -ATPase activity and a concomitant reduction in ATP production.[15]

In the present study, a significant increase was observed in lipid peroxidation in the kidneys and livers of the animals in the CsA50r group, shown by the increase in levels of thiobarbituric acid reactive substances (TBARS). This data indicates that tissue damage occurs after the cessation of exposure to CsA and that it is directly related to the low antioxidant capacity of GST and SOD. This finding indicates impairment of the cellular signaling machinery associated with the antioxidant system. Although renal GST activity was reduced in all groups exposed to CsA and the liver GST levels were reduced in the CsA50i and CsA50r groups, the tissue was able to protect itself from oxidative damage induced by CsA, and no increase was observed in the lipid peroxidation in the tissues. The same interpretation can be applied to the results of renal SOD activity, which was reduced in the CsA10i and CsA10r groups. It is important to note that the normalization of SOD activity in the kidneys and liver of animals in the CsA50r group demonstrates that the organism seeks to protect itself from the harmful effects of lipid peroxidation. The reduction in the activity of antioxidant enzymes is directly associated with the increase in TBARS because the decrease in the levels of antioxidants present in the organ facilitates the process of lipid peroxidation,[42] which can lead to several alterations in the kidneys and livers.[59] In the study performed by Ghaznavi et al.[60] in which a dose of 25 mg/kg of CsA was administered to male Sprague Dawley rats, a reduction was observed in the renal antioxidant defense, which is in line with the data obtained in the present study. Similarly, Wolf et al.[18] using 25 and 50 μM of CsA in primary cultures of rat hepatocytes, detected impairment of the antioxidant system that favored the pro-oxidative processes in these cells. The present data provide evidence that oxidative stress is part of the mechanism underlying CsA-mediated toxicity in the liver and kidney cells.

In the present study, it was evident that CsA altered the kidney and liver in a specific and independent manner with respect to tissue architecture and function and that the kidneys underwent less damage in response to CsA. In both organs, these changes cannot be associated with oxidative stress because our results showed no changes in the oxidative stress biomarkers. Thus, although CsA is necessary for the treatment of a variety of disorders, it should be used with careful monitoring of the renal system and especially of the hepatic system.

CONCLUSION

We conclude that exposure to a safe (non-immunosuppressive) dose of CsA causes significant damage to the liver in the immediate and late stages following exposure, whereas damage to the kidneys was observed only after the recovery period. Therefore, under these experimental conditions, the liver is more sensitive to the action of CsA than the kidneys, and this sensitivity is not related to oxidative stress.

CONFLICTS OF INTEREST

The authors declare no potential conflicts of interest with respect to the research, authorship, and/or publication of this article.

ACKNOWLEDGMENTS

This paper is part of the master's thesis of P.M.M. Figaro (State University of Londrina - Brazil) performed under the supervision of G.S.A. Fernandes.

This study was partially funded by the Coordenação de Aperfeiçoamento de Pessoal de Nível Superior - Brazil (CAPES) - Financial Code 001. The authors thank CAPES/PROEX for the scholarship granted to P.M.M. Figaro.

ORCID iD:

Suellen Ribeiro da Silva Scarton: https://orcid.org/0000-0002-3547-6389
Gláucia de Lion Siervo: https://orcid.org/0000-0003-2084-4203
Fábio Goulart de Andrade: https://orcid.org/0000-0002-0206-4986
Glaura Scantamburlo Alves Fernandes: https://orcid.org/0000-0002-6043-1131

REFERÊNCIAS

1. Hyung S-J, Feng X, Che Y, et al. Detection of conformation types of cyclosporin retaining intramolecular hydrogen bonds by mass spectrometry. *Anal Bioanal Chem* 2014; 406: 5785–5794.
2. Ho V. The use of ciclosporin in psoriasis: A clinical review. *Br J Dermatology, Suppl* 2004; 150: 1–10.
3. Stähelin HF. The history of cyclosporin A (Sandimmune) revisited: another point of view. *Experientia* 1996; 52: 5–13.
4. Rusnak F, Mertz P. Calcineurin: Form and function. *Physiological Reviews* 2000; 80: 1483–1521.
5. Campistol JM, Sacks SH. Mechanisms Of Nephrotoxicity. 2000; SS5–SS10.
6. Damiano S, Ciarcia R, Montagnaro S, et al. Prevention of Nephrotoxicity Induced by Cyclosporine-A: Role of Antioxidants. *J Cell Biochem* 2015; 116: 364–369.
7. El-Bassossy HM, Eid BG. Cyclosporine A exhibits gender-specific nephrotoxicity in rats: Effect on renal tissue inflammation. *Biochem Biophys Res Commun* 2018; 495: 468–472.
8. Moon D, Kim J. Cyclosporin A aggravates hydrogen peroxide-induced cell death in kidney proximal tubule epithelial cells. *Anat Cell Biol* 2019; 52: 312–323.
9. Shirolikar M, Pande S, Borkar M, et al. Managing a side effect : Cyclosporine-Induced nephrotoxicity Introduction Pathophysiology of Nephrotoxicity Risk Factors for Cyclosporine Nephrotoxicity. 2020; 1–7.
10. Murray BM, Paller MS, Ferris TF. Effect of cyclosporine administration on renal hemodynamics in conscious rats. *Kidney Int* 1985; 28: 767–74.
11. Barros J, B MA, Ajzen Ti, et al. *Glomerular hemodynamics and hormonal participation on cyclosporine nephrotoxicity*. Epub ahead of print 1987. DOI: 10.1038/ki.1987.166.
12. Textor SC, Burnetit JC, Romero JC, et al. *Urinary endothelin and renal vasoconstriction with cyclosporine or FK506 after liver transplantation*. Epub ahead of print 1995. DOI: 10.1038/ki.1995.200.
13. Caires A, Fernandes GS, Leme AM, et al. Endothelin-1 receptor antagonists protect

the kidney against the nephrotoxicity induced by cyclosporine-A in normotensive and hypertensive rats. *Brazilian J Med Biol Res* 2018; 51: 1–9.

14. Heyman SN, Abassi Z, Rosenberger C, et al. Cyclosporine A induces endothelin-converting enzyme-1: Studies in vivo and in vitro. *Acta Physiol*; 223. Epub ahead of print 1 May 2018. DOI: 10.1111/apha.13033.
15. Korolczuk A, Caban K, Amarowicz M, et al. Oxidative Stress and Liver Morphology in Experimental Cyclosporine A-Induced Hepatotoxicity. *Biomed Res Int*; 2016. Epub ahead of print 2016. DOI: 10.1155/2016/5823271.
16. Wolf A, Trendelenburg CF, Diez-Fernandez C, et al. Cyclosporine A-induced oxidative stress in rat hepatocytes. *J Pharmacol Exp Ther* 1997; 280: 1328–1334.
17. Hagar HH. The protective effect of taurine against cyclosporine A-induced oxidative stress and hepatotoxicity in rats. *Toxicol Lett* 2004; 151: 335–343.
18. Illsinger S, Janzen N, Lücke T, et al. Cyclosporine A: impact on mitochondrial function in endothelial cells. *Clin Transplant* 2011; 25: 584–593.
19. Guada M, Lana H, Gil AG, et al. Cyclosporine A lipid nanoparticles for oral administration: Pharmacodynamics and safety evaluation. *Eur J Pharm Biopharm* 2016; 101: 112–118.
20. Bancroft JD, Gamble M. *Theory and Practice of Histological Techniques*. 5th ed. Edinburgh: Churchill Livingstone, https://www.worldcat.org/title/theory-and-practice-of-histological-techniques/oclc/48110455 (2002, accessed 25 March 2021).
21. Imafidon EC, Akomolafe RO, Oladele AA. Sexually dimorphic proteinuria in Wistar rats: Relevance to clinical models. *Pathophysiology* 2016; 23: 51–59.
22. Olatunji S, Adewole O, Ayannuga O, et al. Microanatomy and histomorphometry analysis of the effects of *Moringa oleifera* leaf extract on lead-induced kidney damage in adult wistar rats. *Int J Biol Chem Sci* 2015; 9: 1599.
23. Nirmal NK, Awasthi KK, John PJ. Hepatotoxicity of graphene oxide in Wistar rats. *Environ Sci Pollut Res*. Epub ahead of print 2020. DOI: 10.1007/s11356-020-09953-0.
24. Adisa A, Udeabor S, Kubesch A, et al. The utility of azan trichrome staining in Ameloblastoma. *Niger Postgrad Med J* 2016; 23: 44.
25. Pupim ACE, Campois TG, Araújo EJ de A, et al. Infection and tissue repair of experimental cutaneous candidiasis in diabetic mice. *J Med Microbiol* 2017; 66: 808–815.
26. Buege JA, Aust SD. Microsomal Lipid Peroxidation. *Methods Enzymol* 1978; 52:

302–310.

27. Keen JH, Habig WH, Jakoby WB. *Mechanism for the Several Activities of the Glutathione S-Transferases*, http://www.jbc.org/ (1976, accessed 12 January 2021).

28. Crouch RK, Gandy SE, Kimsey G, et al. The inhibition of islet superoxide dismutase by diabetogenic drugs. *Diabetes* 1981; 30: 235–241.

29. Lu Y, Li C, Ping N, et al. Hydrogen-rich water alleviates cyclosporine A-induced nephrotoxicity via the Keap1/Nrf2 signaling pathway. *J Biochem Mol Toxicol*; 34. Epub ahead of print 10 May 2020. DOI: 10.1002/jbt.22467.

30. Myers BD, Ross J, Newton L, et al. Cyclosporine-Associated Chronic Nephropathy. *N Engl J Med* 1984; 311: 699–705.

31. Harb I, Ashour H, Sabry D, et al. Nicorandil prevents the nephrotoxic effect of cyclosporine-A in albino rats through modulation of HIF-1α/VEGF /eNOS signaling. *Can J Physiol Pharmacol*. Epub ahead of print 21 August 2020. DOI: 10.1139/cjpp-2020-0012.

32. Abensur H. *Biomarcadores na Nefrologia*, http://arquivos.sbn.org.br/pdf/biomarcadores.pdf (2011, accessed 15 September 2018).

33. Laskow DA, Curtis JJ, Luke RG, et al. Cyclosporine-induced changes in glomerular filtration rate and urea excretion. *Am J Med* 1990; 88: 497–502.

34. Isnard Bagnis C, Tezenas du Montcel S, Beaufils H, et al. Long-term renal effects of low-dose cyclosporine in uveitis-treated patients: follow-up study. *J Am Soc Nephrol* 2002; 13: 2962–8.

35. Sereno HV, S. Nunes PR-P, E. Carvalho RA, et al. Cyclosporine A-induced nephrotoxicity is ameliorated by dose reduction and conversion to sirolimus in the rat. *J Physiol Pharmacol* 2015; 66: 285–299.

36. Patel L, Thaker A. The effects of A 2B receptor modulators on vascular endothelial growth factor and nitric oxide axis in chronic cyclosporine nephropathy. *J Pharmacol Pharmacother*; |. Epub ahead of print 2015. DOI: 10.4103/0976-500X.162014.

37. Battino M, Bompadre S, Leone L, et al. The effect of Cyclosporine A chronic administration on the antioxidant pattern of rat liver mitochondria: Structural and functional consequences. *BioFactors* 2003; 18: 271–275.

38. Kurus M, Esrefoglu M, Sogutlu G, et al. Melatonin Prevents Cyclosporine-Induced Hepatotoxicity in Rats. *Med Princ Pract* 2009; 18: 407–410.

39. Nacar A, Karaboğa İ, Okuyan HM, et al. Investigation of the protective effect of

erdosteine against cyclosporine-induced injury in rat liver with histological and biochemical methods. *Turkish J Med Sci* 2015; 45: 1390–1395.

40. Hoorn EJ, Walsh SB, McCormick JA, et al. Pathogenesis of calcineurin inhibitor-induced hypertension. *Journal of Nephrology* 2012; 25: 269–275.

41. Yüce A, Ateşşahin A, Çeribaşi AO. Amelioration of cyclosporine A-induced renal, hepatic and cardiac damages by ellagic acid in rats. *Basic Clin Pharmacol Toxicol* 2008; 103: 186–191.

42. Bingul I, Olgac V, Bekpinar S, et al. The protective effect of resveratrol against cyclosporine A-induced oxidative stress and hepatotoxicity. *Arch Physiol Biochem* 2019; 0: 1–6.

43. Elisa Böhmer A, Ribeiro Corrĉa AM, de Souza DG, et al. Long-term cyclosporine treatment: Evaluation of serum biochemical parameters and histopathological alterations in Wistar rats. *Exp Toxicol Pathol* 2011; 63: 119–123.

44. Beauchesne PR, Chung NSC, Wasan KM. Cyclosporine A: A review of current oral and intravenous delivery systems. *Drug Dev Ind Pharm* 2007; 33: 211–220.

45. Tian Z, Liu H, Su X, et al. Role of elevated liver transaminase levels in the diagnosis of liver injury after blunt abdominal trauma. *Exp Ther Med* 2012; 4: 255–260.

46. Srivastava AR, Kumar S, Agarwal GG, et al. Blunt abdominal injury: Serum ALT-A marker of liver injury and a guide to assessment of its severity. *Injury* 2007; 38: 1069–1074.

47. Kim WR, Flamm SL, Di Bisceglie AM, et al. Serum activity of alanine aminotransferase (ALT) as an indicator of health and disease. *Hepatology* 2008; 47: 1363–1370.

48. Kedzierska K, Sporniak-Tutak K, Kolasa A, et al. The effect of immunosuppressive therapy on renal cell apoptosis in native rat kidneys. *Histol Histopathol* 2015; 30: 105–16.

49. Akbulut S, Elbe H, Eris C, et al. Effects of antioxidant agents against cyclosporine-induced hepatotoxicity. *J Surg Res* 2015; 193: 658–666.

50. Yoshioka K, Takemura T, Akano N, et al. Distribution Of Type I Collagen In Human Kidney Diseases In Comparison With Type Iii Collagen. *J Patol* 1990; 162: 141–148.

51. Djamali A, Wilson NA, Sadowski EA, et al. Nox2 and Cyclosporine-Induced Renal Hypoxia. *Transplantation* 2017; 100: 1198–1210.

52. Rezzani R, Rodella L, Buffoli B, et al. Change in Renal Heme Oxygenase Expression in Cyclosporine A-induced Injury. *J Histochem Cytochem* 2005; 53: 105–112.

53. Rowshani AT, Scholten EM, Bemelman F, et al. No Difference in Degree of Interstitial Sirius Red-Stained Area in Serial Biopsies from Area under Concentration-over-Time Curves-Guided Cyclosporine versus Tacrolimus-Treated Renal Transplant Recipients at One Year. *J Am Soc Nephrol* 2006; 17: 305–312.

54. Devarbhavi H. An Update on Drug-induced Liver Injury. *Journal of Clinical and Experimental Hepatology* 2012; 2: 247–259.

55. De Freitas KM, Almeida JM, Monteiro JC, et al. The effects of cyclosporin A And heteropterys tomentosa on the rat liver. *An Acad Bras Cienc* 2015; 87: 369–379.

56. Rich L, Whittaker P. *Collagen and Picrosirius red Staining: A Polarized light Assessment Of Fibrillar Hue And Spatial Distribution*, http://jms.org.br/PDF/v22n2a06.pdf (2005, accessed 30 August 2018).

57. Lim SW, Hyoung BJ, Piao SG, et al. Chronic cyclosporine nephropathy is characterized by excessive autophagosome formation and decreased autophagic clearance. *Transplantation* 2012; 94: 218–225.

58. Ince S, Arslan-Acaroz D, Demirel HH, et al. Taurine alleviates malathion induced lipid peroxidation, oxidative stress, and proinflammatory cytokine gene expressions in rats. *Biomed Pharmacother* 2017; 96: 263–268.

59. Huang J, Yao X, Weng G, et al. Protective effect of curcumin against cyclosporine A-induced rat nephrotoxicity. *Mol Med Rep* 2018; 17: 6038–6044.

60. Ghaznavi R, Zahmatkesh M, Kadkhodaee M, et al. Cyclosporine Effects on the Antioxidant Capacity of Rat Renal Tissues. *Transplant Proc* 2007; 39: 866–867.

FIGURES AND FIGURE LEGENDS

Figure 1. Morphometric evaluation of the kidneys of animals exposed to CsA. Diameter of (A) glomeruli, (B) Bowman space, (C) proximal and (D) distal convoluted tubules and (E) collecting tubules. Groups: Control (c); CsA 10 days immediate (10i); CsA 10 days Recovery (10r); CsA 50 days Immediate (50i); CsA 50 days Recovery (50r). Values expressed as mean ± SD. One-way ANOVA, Tukey's post-test (*$p<0.05$).

Figure 2. Morphometric evaluation of the liver of animals exposed to CsA. Mean diameter of (A) portal venules, (B) bile ducts and (C) centrilobular venules, mean number of adherent cells (leukocytes) in (D) portal venule and (E) centrilobular venule, mean diameter of (F) sinusoids (portal venule) and (G) sinusoids (centrilobular venule). Groups: Control (c); CsA 10 days immediate (10i); CsA 10 days Recovery (10r); CsA 50 days Immediate (50i); CsA 50 days Recovery (50r). Values expressed as mean ± SD. One-way ANOVA, Tukey's post-test (*$p<0.05$).

Figure 3. Histochemical analysis of the kidneys of animals exposed to CsA. Percentage of neutral glycoconjugates (PAS) from (A) cortical and B) medullary regions. Percentage of total collagen (Azan), from (C) cortical and (D) medullary regions. Percentage of collagens I and III (Picrosirius) in the (E) cortical and (F) medullary regions. Groups: Control (c); CsA 10 days immediate (10i); CsA 10 days Recovery (10r); CsA 50 days Immediate (50i); CsA 50 days Recovery (50r). Values expressed as mean ± SD. One-way ANOVA, Tukey's post-test (*$p<0.05$).

Figure 4. Histochemical analysis of the liver of animals exposed to CsA**.** Percentage of neutral glycoconjugates (PAS) from (A) portal venule and (B) centrilobular venule regions. Total collagen (Azan), from the (C) centrilobular venule and (D) portal venule regions. Percentage of collagens I and III (Picrosirius) in the region of (E) portal venule and (F) centrilobular venule. Groups: Control (c); CsA 10 days immediate (10i); CsA 10 days Recovery (10r); CsA 50 days Immediate (50i); CsA 50 days Recovery (50r). Values expressed as mean ± SD. One-way ANOVA, Tukey's post-test (*$p<0.05$).

Figure 5. Renal toxicity and liver function of animals exposed to CsA. Evaluation of plasma biomarker concentrations for renal toxicity; (A) Urea, (B) Creatinine and for liver function (C) AST, (D) ALT. Groups: Control (c); CsA 10 days immediate (10i); CsA 10 days Recovery (10r); CsA 50 days Immediate (50i); CsA 50 days Recovery (50r). Values expressed as mean ± SD. One-way ANOVA, Tukey's post-test (*$p<0.05$).

Figure 6. Determination of oxidative stress biomarkers in kidney and liver of animals exposed to CsA. TBARS dosage in (A) kidney and (B) liver. GST activity in (C) kidney and (D) liver. SOD activity in (E) kidney and (F) liver. Groups: Control (c); CsA 10 days immediate (10i); CsA 10 days Recovery (10r); CsA 50 days Immediate (50i); CsA 50 days Recovery (50r). Values expressed as mean ± SD. One-way ANOVA, Tukey's post-test (*$p<0.05$).

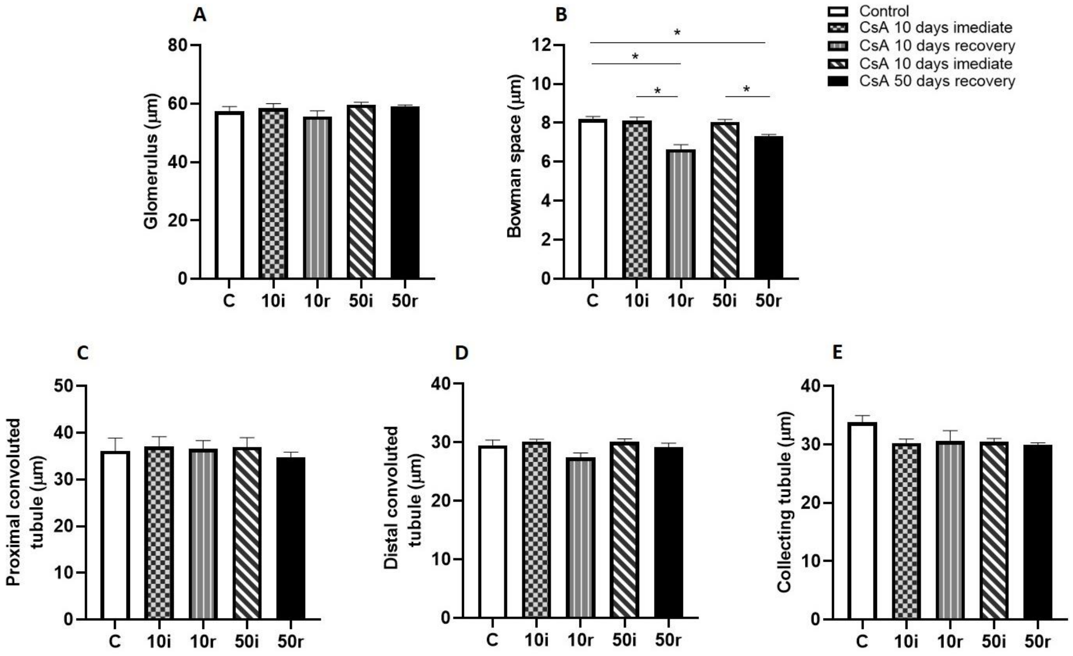
A
B
Control
CsA 10 days imediate
CsA 10 days recovery
CsA 10 days imediate
CsA 50 days recovery
Glomerulus (µm)
80
60
40
20
0
C
10i
10r
50i
50r
Bowman space (µm)
12
10
8
6
4
2
0
*
*
*
*
C
10i
10r
50i
50r
C
D
E
Proximal convoluted tubule (µm)
50
40
30
20
10
0
C
10i
10r
50i
50r
Distal convoluted tubule (µm)
40
30
20
10
0
C
10i
10r
50i
50r
Collecting tubule (µm)
40
30
20
10
0
C
10i
10r
50i
50r

Figure 1.

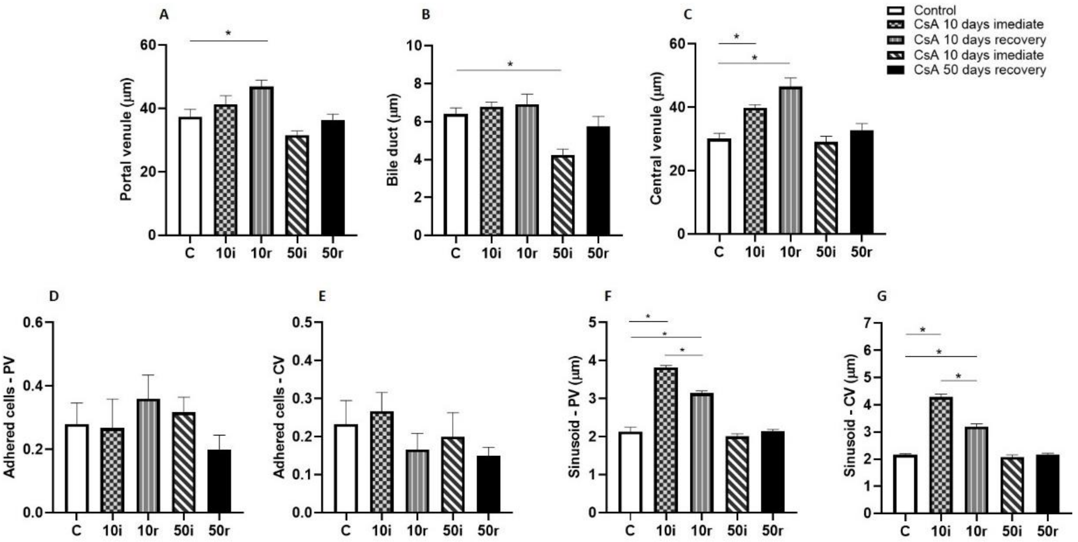
A
B
C
Control
CsA 10 days imediate
CsA 10 days recovery
CsA 10 days imediate
CsA 50 days recovery
Portal venule (µm)
Bile duct (µm)
Central venule (µm)
*
0
20
40
60
0
2
4
6
8
10
C
10i
10r
50i
50r
D
E
F
G
Adhered cells - PV
Adhered cells - CV
Sinusoid - PV (µm)
Sinusoid - CV (µm)
0.0
0.2
0.4
0.6
0.0
0.1
0.2
0.3
0.4
0.5
0
1
2
3
4
5
6
7

Figure 2.

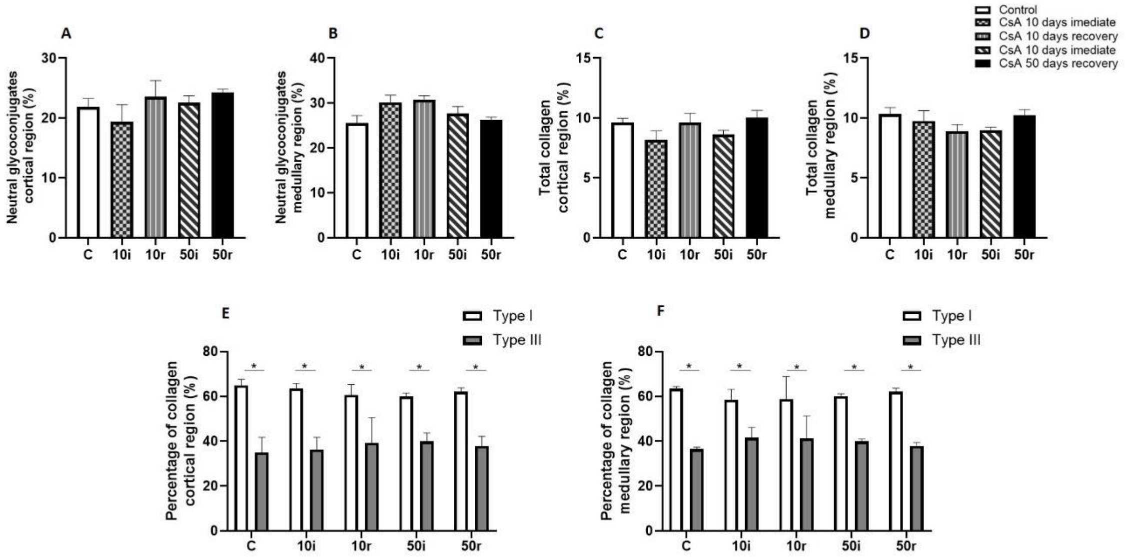
A
Neutral glycoconjugates cortical region (%)
0
10
20
30
C
10i
10r
50i
50r
B
Neutral glycoconjugates medullary region (%)
0
10
20
30
40
C
10i
10r
50i
50r
C
Total collagen cortical region (%)
0
5
10
15
C
10i
10r
50i
50r
D
Total collagen medullary region (%)
0
5
10
15
C
10i
10r
50i
50r
Control
CsA 10 days imediate
CsA 10 days recovery
CsA 10 days imediate
CsA 50 days recovery
E
Type I
Type III
Percentage of collagen cortical region (%)
0
20
40
60
80
*
*
*
*
*
C
10i
10r
50i
50r
F
Type I
Type III
Percentage of collagen medullary region (%)
0
20
40
60
80
*
*
*
*
*
C
10i
10r
50i
50r

Figure 3.

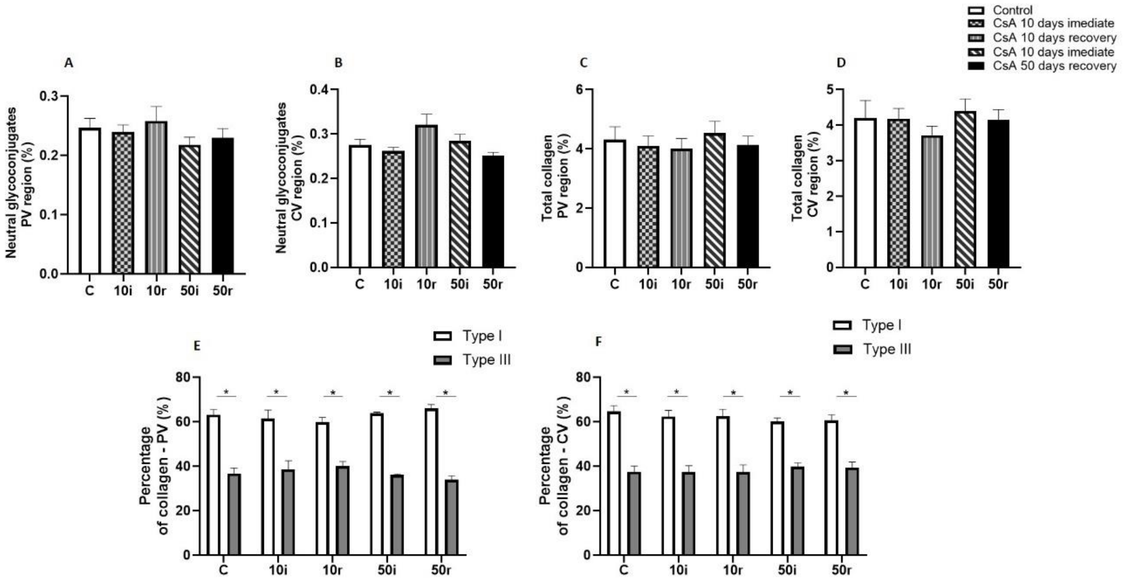
A
B
C
D
Control
CsA 10 days imediate
CsA 10 days recovery
CsA 10 days imediate
CsA 50 days recovery
Neutral glycoconjugates PV region (%)
0.3
0.2
0.1
0.0
Neutral glycoconjugates CV region (%)
0.4
0.3
0.2
0.1
0.0
Total collagen PV region (%)
6
4
2
0
Total collagen CV region (%)
5
4
3
2
1
0
C
10i
10r
50i
50r
E
F
Type I
Type III
Percentage of collagen - PV (%)
Percentage of collagen - CV (%)
80
60
40
20
0
*

Figure 4.

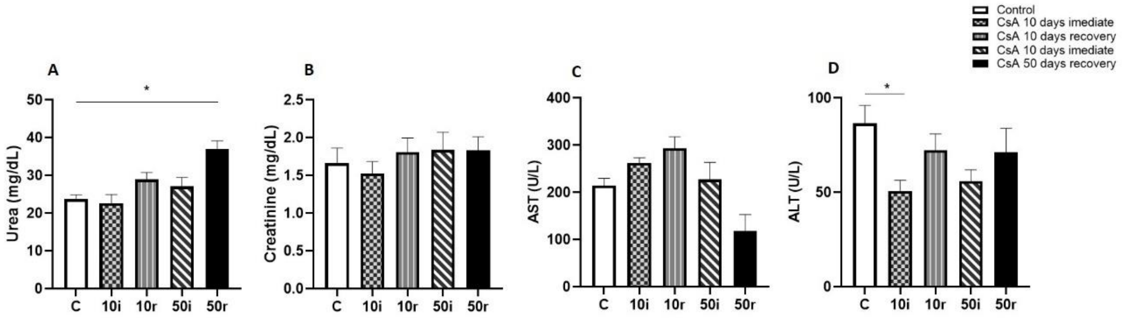
Control
CsA 10 days imediate
CsA 10 days recovery
CsA 10 days imediate
CsA 50 days recovery
A
*
Urea (mg/dL)
0
10
20
30
40
50
C
10i
10r
50i
50r
B
Creatinine (mg/dL)
0.0
0.5
1.0
1.5
2.0
2.5
C
10i
10r
50i
50r
C
AST (U/L)
0
100
200
300
400
C
10i
10r
50i
50r
D
*
ALT (U/L)
0
50
100
C
10i
10r
50i
50r

Figure 5.

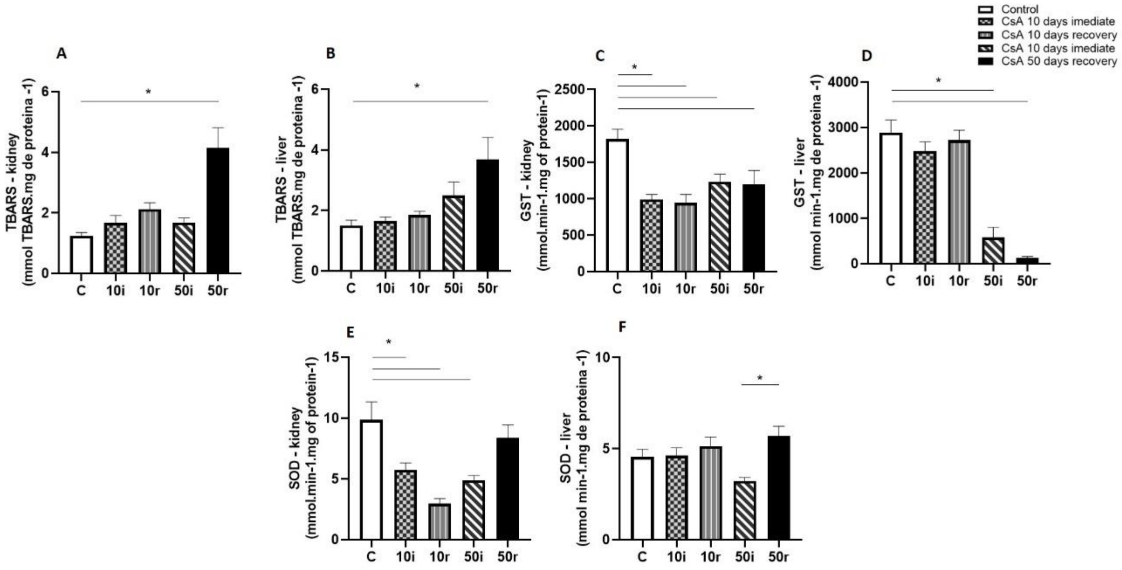
Control
CsA 10 days imediate
CsA 10 days recovery
CsA 10 days imediate
CsA 50 days recovery
A
TBARS - kidney
(mmol TBARS.mg de proteina -1)
0
2
4
6
*
C
10i
10r
50i
50r
B
TBARS - liver
(mmol TBARS.mg de proteina -1)
0
2
4
6
*
C
10i
10r
50i
50r
C
GST - kidney
(mmol.min-1.mg of protein-1)
0
500
1000
1500
2000
2500
*
C
10i
10r
50i
50r
D
GST - liver
(mmol min-1.mg de proteina -1)
0
1000
2000
3000
4000
*
C
10i
10r
50i
50r
E
SOD - kidney
(mmol.min-1.mg of protein-1)
0
5
10
15
*
C
10i
10r
50i
50r
F
SOD - liver
(mmol min-1.mg de proteina -1)
0
5
10
*
C
10i
10r
50i
50r

Figure 6.

5 CONCLUSÃO GERAL

Conclui-se que a exposição as doses de 10 mg/kg e 50 mg/kg de malation no período peripuberal causam danos significativos aos rins, alterando a sua morfologia, além de causar alterações na função hepática e renal. Em relação à exposição a baixa dose de CsA são identificados danos hepáticos de modo imediato e após o período de recuperação, enquanto os rins estas alterações são identificadas apenas após este período.

REFERÊNCIAS

ABBAS, A. K.; LICHTMAN, A. H.; PILLAI, S. Imunologia Celular e Molecular - Abbas 8 ed. **Elsevier Editora Ltda**, n. 8, p. 631–667, 2015.

ABDEL-SALAM, O. M. et al. Preventive effects of cannabis on neurotoxic and hepatotoxic activities of malathion in rat. 2018.

ABOUBAKR, H. M. et al. Therapeutic effects of N -acetylcysteine against malathion-induced hepatotoxicity. v. 6, 2019.

ADU, D. et al. HYPERKALAEMIA IN CYCLOSPORIN-TREATED RENAL ALLOGRAFT RECIPIENTS. **The Lancet**, v. 322, n. 8346, p. 370–372, 13 ago. 1983.

AGARWAL, A.; SAID, T. M. Oxidative stress, DNA damage and apoptosis in male infertility: A clinical approach. **BJU International**, v. 95, n. 4, p. 503–507, 2005.

AHMED FETOUH, F.; AL SHAHAT, A. Hepato-protective effect of green tea extract on cyclosporine a treated rabbits: Histological and ultrastructural study. **Life Science Journal**, v. 10, n. 1, p. 1924–1932, 2013.

AKBEL, E. et al. The subchronic exposure to malathion, an organophosphate pesticide, causes lipid peroxidation, oxidative stress, and tissue damage in rats: The protective role of resveratrol. **Toxicology Research**, v. 7, n. 3, p. 503–512, 8 maio 2018.

AKOOL, E. S. et al. Cyclosporin A and tacrolimus induce renal Erk1/2 pathway via ROS-induced and metalloproteinase-dependent EGF-receptor signaling. **Biochemical Pharmacology**, v. 83, n. 2, p. 286–295, 2012.

AKOOL, E. S. Molecular mechanisms of the protective role of wheat germ oil against cyclosporin A-induced hepatotoxicity in rats. **Pharmaceutical Biology**, v. 53, n. 9, p. 1311–1317, 2015.

AL-ATTAR, A. M. Physiological and Histopathological Investigations on the Effects of α-Lipoic Acid in Rats Exposed to Malathion. **Journal of Biomedicine and Biotechnology**, v. 2010, 2010.

ALANO, C. C.; YING, W.; SWANSON, R. A. Poly(ADP-ribose) Polymerase-1-mediated Cell Death in Astrocytes Requires NAD+ Depletion and Mitochondrial Permeability Transition. **Journal of Biological Chemistry**, v. 279, n. 18, p. 18895–18902, 2004.

ALLEN, W. E. **diFiore’s Atlas of Histology with Functional Correlations (11th Edition)**. [s.l: s.n.]v. 213

ATHER, N. A. et al. ACUTE ORGANOPHOSPHATE INSECTICIDE POISONING. **Journal of Surgery Pakistan**, v. 13, n. 2, p. 71–74, 2008.

BACONI, D. L. et al. Investigation of the toxicity of some organophosphorus pesticides in a repeated dose study in rats. **Romanian Journal of Morphology and Embryology**, v. 54, n. 2, p. 349–356, 2013.

BADR, A. M. Organophosphate toxicity: updates of malathion potential toxic effects in mammals and potential treatments. **Environmental Science and Pollution Research**, v. 27, n. 21, p. 26036–26057, 2020.

BALAH, A.; EZZAT, O.; AKOOL, E. S. Vitamin E inhibits cyclosporin A-induced CTGF and TIMP-1 expression by repressing ROS-mediated activation of TGF-β/Smad signaling pathway in rat liver. **International Immunopharmacology**, v. 65, n. April, p. 493–502, 2018.

BARBOSA, K. B. F. et al. Estresse oxidativo: Conceito, implicações e fatores modulatórios. **Revista de Nutricao**, v. 23, n. 4, p. 629–643, 2010.

BEAUCHESNE, P. R.; CHUNG, N. S. C.; WASAN, K. M. Cyclosporine A: A review of current oral and intravenous delivery systems. **Drug Development and Industrial Pharmacy**, v. 33, n. 3, p. 211–220, 2007.

BINGUL, I. et al. The protective effect of resveratrol against cyclosporine A-induced oxidative stress and hepatotoxicity. **Archives of Physiology and Biochemistry**, v. 0, n. 0, p. 1–6, 2019.

BLOCK, L. H.; SUTTER, P. M.; MIHATSCH, M. J. Cyclosporin a: Pharmacologic activity on the immune system and effects in clinical organ transplantation. **Klinische Wochenschrift**, v. 61, n. 21, p. 1053–1062, 1983.

BOLAND, J. et al. Tissue distribution and toxicity of cyclosporin A in the mouse. **Pathology**, v. 16, n. 2, p. 117–123, 1 jan. 1984.

BOREL, J. F. et al. Biological effects of cyclosporin A: A new antilymphocytic agent. **Agents and Actions**, v. 43, n. 3–4, p. 179–186, 1994.

BOREL, J. F. et al. In Vivo Pharmacological Effects of Ciclosporin and Some Analogues. **Advances in Pharmacology**, v. 35, n. C, p. 115–246, 1996.

BURATTI, F. M.; TESTAI, E. Malathion detoxification by human hepatic carboxylesterases and its inhibition by isomalathion and other pesticides. **Journal of Biochemical and Molecular Toxicology**, v. 19, n. 6, p. 406–414, 2006.

BURDMANN, E. A. et al. Cyclosporine nephrotoxicity. **Seminars in Nephrology**, v. 23, n. 5, p. 465–476, 2003.

CAIRES, A. et al. Endothelin-1 receptor antagonists protect the kidney against the nephrotoxicity induced by cyclosporine-A in normotensive and hypertensive rats. **Brazilian Journal of Medical and Biological Research**, v. 51, n. 2, p. 1–9, 2018.

CAMPISTOL, J. M.; SACKS, S. H. Mechanisms Of Nephrotoxity. p. SS5–SS10, 2000.

CHEN, Y. et al. The Protective Effect of Fluorofenidone against Cyclosporine A-

Induced Nephrotoxicity. **Kidney and Blood Pressure Research**, v. 44, n. 4, p. 656–668, 2019.

CHONG, W. C.; SHASTRI, M. D.; ERI, R. Endoplasmic reticulum stress and oxidative stress: A vicious nexus implicated in bowel disease pathophysiology. **International Journal of Molecular Sciences**, v. 18, n. 4, p. 1–19, 2017.

COBAN, F. K. et al. Boron attenuates malathion-induced oxidative stress and acetylcholinesterase inhibition in rats. **Drug and Chemical Toxicology**, v. 38, n. 4, p. 391–399, 2015.

COLOMBO, D.; AMMIRATI, E. Cyclosporine in transplatation - A history of converging timelines. **Journal of biological regulators and homeostatic agents**, v. 25, n. 4, p. 493–504, 2011.

CZERSKA, M. et al. Today's oxidative stress markers. **Medycyna Pracy**, v. 66, n. 3, p. 393–405, 2015.

DE ARRIBA, G. et al. Cyclosporine A-induced apoptosis in renal tubular cells is related to oxidative damage and mitochondrial fission. **Toxicology Letters**, v. 218, n. 1, p. 30–38, 7 mar. 2013.

DE CHIARA, L. et al. MiR302 regulates SNAI1 expression to control mesangial cell plasticity. **Scientific Reports**, v. 7, n. February, p. 1–14, 2017.

DE FREITAS, K. M. et al. The effects of cyclosporin A And heteropterys tomentosa on the rat liver. **Anais da Academia Brasileira de Ciencias**, v. 87, n. 1, p. 369–379, 2015.

DEHGHANI, M. H. et al. High-performance removal of diazinon pesticide from water using multi-walled carbon nanotubes. **Microchemical Journal**, v. 145, p. 486–491, 1 mar. 2019.

DUMAS, S. J. et al. Phenotypic diversity and metabolic specialization of renal endothelial cells. **Nature Reviews Nephrology**, v. 0123456789, 2021.

EKREMOĞLU, M. et al. An investigation of acute effects at various doses of malathion on glucose homeostasis and insulin resistance in rat liver, pancreas and serum. **Journal of Mind and Medical Sciences**, v. 7, n. 1, p. 85–93, 2020.

ERTHAL, R. P. et al. Exposure to low doses of malathion during juvenile and peripubertal periods impairs testicular and sperm parameters in rats: Role of oxidative stress and testosterone. **Reproductive Toxicology**, v. 96, n. April, p. 17–26, 2020.

ESEN; UYSAL. Protective effects of intravenous lipid emulsion on malathion-induced hepatotoxicity. **Bratisl Med Journal**, v. 119, n. 6, p. 373–378, 2018.

ESPINOZA-NAVARRO, O.; PONCE-LAROSA, C.; BUSTOS-OBREGÓN, E. Organophosphorous Pesticides: Their Effects on Biosentinel Species and Humans. Control and Application in Chile. **International Journal of Morphology**, v. 35, n. 3, p. 1069–1074, 2017.

FAULDS, D.; GOA, K. L.; BENFIELD, P. Cyclosporin. **Drugs**, v. 45, n. 6, p. 953–1040, jun. 1993.

FLORES, C. et al. Lessons to learn from low-dose cyclosporin-A: A new approach for unexpected clinical applications. **Frontiers in Immunology**, v. 10, n. MAR, p. 1–7, 2019.

FOUAD, D.; BADR, A.; ATTIA, H. A. Hepatoprotective activity of raspberry ketone is mediated: Via inhibition of the NF-κB/TNF-α/caspase axis and mitochondrial apoptosis in chemically induced acute liver injury. **Toxicology Research**, v. 8, n. 5, p. 663–676, 2019.

FRANCO, J. L. et al. Zinc reverses malathion-induced impairment in antioxidant defenses. **Toxicology Letters**, v. 187, n. 3, p. 137–143, 2009.

FUJII, H.; KAWADA, N. Inflammation and fibrogenesis in steatohepatitis. **Journal of Gastroenterology**, v. 47, n. 3, p. 215–225, 2012.

GARTNER, L. .; HIATT, J. . **Tratado de Histologia em cores**. [s.l.] Elsevier Health Sciences Brazil, 2017.

GEBHARDT, R.; MATZ-SOJA, M. **Liver zonation: Novel aspects of its regulation and its impact on homeostasisWorld Journal of Gastroenterology**WJG Press, , 14 jul. 2014.

GHAZNAVI, R. et al. Cyclosporine Effects on the Antioxidant Capacity of Rat Renal Tissues. **Transplantation Proceedings**, v. 39, n. 4, p. 866–867, 1 maio 2007.

GOLAN, E. D. **Princípios de farmacologia**. 2. ed. Rio de Janeiro: Guanabara Koogan, 2009.

GUADA, M. et al. Cyclosporine A lipid nanoparticles for oral administration: Pharmacodynamics and safety evaluation. **European Journal of Pharmaceutics and Biopharmaceutics**, v. 101, p. 112–118, 1 abr. 2016.

GUICCIARDI, M. E. et al. Apoptosis and necrosis in the liver. **Comprehensive Physiology**, v. 3, n. 2, p. 977–1010, 2013.

GUPTA, V. K. et al. Anti-Inflammatory and Antioxidative Potential of Aloe vera on the Cartap and Malathion Mediated Toxicity in Wistar Rats. **International Journal of Environmental Research and Public Health**, v. 17, n. 14, p. 5177, 17 jul. 2020.

HAGAR, H. H. The protective effect of taurine against cyclosporine A-induced oxidative stress and hepatotoxicity in rats. **Toxicology Letters**, v. 151, n. 2, p. 335–343, 2004.

HEYMAN, S. N. et al. Cyclosporine A induces endothelin-converting enzyme-1: Studies in vivo and in vitro. **Acta Physiologica**, v. 223, n. 1, 1 maio 2018.

HO, V. The use of ciclosporin in psoriasis: A clinical review. **British Journal of Dermatology, Supplement**, v. 150, n. 67, p. 1–10, 2004.

IGHODARO, O. M.; AKINLOYE, O. A. First line defence antioxidants-superoxide dismutase (SOD), catalase (CAT) and glutathione peroxidase (GPX): Their fundamental role in the entire antioxidant defence grid. **Alexandria Journal of Medicine**, v. 54, n. 4, p. 287–293, 1 dez. 2018.

INCE, S. et al. Taurine alleviates malathion induced lipid peroxidation, oxidative stress, and proinflammatory cytokine gene expressions in rats. **Biomedicine and Pharmacotherapy**, v. 96, n. May, p. 263–268, 2017.

JALILI, C. et al. Resveratrol attenuates malathion-induced renal damage by declining oxidative stress in rats. **International Journal of Pharmaceutical Investigation**, v. 8, n. 4, p. 192, 2018.

JENSEN, I. M.; WHATLING, P. Malathion: A Review of Toxicology. **Hayes' Handbook of Pesticide Toxicology**, p. 1527–1542, 2010.

JUNQUEIRA, L. C.; CARNEIRO, J. **Histologia Básica: texto e atlas**. 13. ed. [s.l.] Guanabara Koogan, 2017.

KAMEL, K. S. et al. Studies to determine the basis for hyperkalemia in recipients of a renal transplant who are treated with cyclosporine. **Journal of the American Society of Nephrology**, v. 2, n. 8, 1992.

KHALIFA, F. K.; ALKHALAF, M. I. Effects of black seed and thyme leaves dietary supplements against malathion insecticide-induced toxicity in experimental rat model. **Journal of King Saud University - Science**, v. 32, n. 1, p. 914–919, 1 jan. 2020.

KIERSZEMBAUM, A. L. **Histologia e Biologia celular: uma introdução à patologia.** 1. ed. Rio de Janeiro: Elsevier, 2004.

KOROLCZUK, A. et al. Ultrastructural examination of renal tubular epithelial cells and hepatocytes in the course of chronic cyclosporin a treatment-a possible link to oxidative stress. **Ultrastructural Pathology**, v. 37, n. 5, p. 332–339, 2013.

KOROLCZUK, A. et al. Oxidative Stress and Liver Morphology in Experimental Cyclosporine A-Induced Hepatotoxicity. **BioMed Research International**, v. 2016, 2016.

KOWALTOWSKI, A. J.; CASTILHO, R. F.; VERCESI, A. E. **Mitochondrial permeability transition and oxidative stressFEBS Letters**FEBS Lett, , 20 abr. 2001.

KRICHEVSKY, A. **Netter'S Histology Flash Cards**. Second Edi ed. [s.l.] Elsevier Inc., 2005. v. 80

KRUEPUNGA, N. et al. Anatomy of rodent and human livers: What are the differences? **Biochimica et Biophysica Acta - Molecular Basis of Disease**, v. 1865, n. 5, p. 869–878, 2019.

KURTZ, A.; DELLA BRUNA, R.; KUHN, K. Cyclosporine A enhances renin secretion and production in isolated juxtaglomerular cells. **Kidney International**, v.

33, n. 5, p. 947–953, 1988.

KWONG, T. C. Organophosphate pesticides: Biochemistry and clinical toxicology. **Therapeutic Drug Monitoring**, v. 24, n. 1, p. 144–149, 2002.

LASRAM, M. M. et al. Association of inflammatory response and oxidative injury in the pathogenesis of liver steatosis and insulin resistance following subchronic exposure to malathion in rats. **Environmental Toxicology and Pharmacology**, v. 38, n. 2, p. 542–553, 2014.

LEE, C. H. et al. Altered Expression of Tight Junction Proteins in Cyclosporine Nephrotoxicity. **American Journal of Nephrology**, v. 33, n. 1, p. 7–16, 2011.

LEE, E. H. et al. Inhibition of PPARα target genes during cyclosporine A-induced nephrotoxicity and hepatotoxicity. **Molecular and Cellular Toxicology**, v. 15, n. 2, p. 185–197, 1 abr. 2019.

LINDHOLM, A. Factors Influencing the pharmacokinetics of cyclosporine in man. **Therapeutic Drug Monitoring**, n. 13, p. 465–477, 1991.

LIU, J.; ERIN, S. Pesticide Exposure and Child Neurodevelopments. **Workplace Health Saf.**, v. 23, n. 1, p. 1–7, 2014.

LIU, Q. feng et al. Klotho mitigates cyclosporine A (CsA)-induced epithelial–mesenchymal transition (EMT) and renal fibrosis in rats. **International Urology and Nephrology**, v. 49, n. 2, p. 345–352, 2017.

LOWE, J. S. .; ANDERSON, P. G. **Stevens & Lowe´s Human Histology**. 4. ed. Philadelphia: Elsevier, 2015.

MAK, K.; PNG, M. The Hepatic Central Vein: Structure, Fibrosis, and Role in Liver Biology. **Anatomical Record**, v. 303, n. 7, p. 1747–1767, 2020.

MATHEW, R. P.; VENKATESH, S. K. Liver vascular anatomy: a refresher. **Abdominal Radiology**, v. 43, n. 8, p. 1886–1895, 2018.

MEHRI, N. et al. Hepatoprotective effect of the root extract of green tea against malathion-induced oxidative stress in rats. **Journal of HerbMed Pharmacology**, v. 5, n. 3, p. 116–119, 2016.

MOON, D.; KIM, J. Cyclosporin A aggravates hydrogen peroxide-induced cell death in kidney proximal tubule epithelial cells. **Anatomy and Cell Biology**, v. 52, n. 3, p. 312–323, 2019.

MOORTHY, A. V.; BLICHFELDT, T. C. Anatomy and Physiology of the Kidney. **Pathophysiology of Kidney Disease and Hypertension**, v. 68, n. 5, p. 1–15, 2009.

MORIDI, H. et al. Protective effect of cerium oxide nanoparticle on sperm quality and oxidative damage in malathioninduced testicular toxicity in rats: An experimental study. **International Journal of Reproductive BioMedicine**, v. 16, n. 4, p. 261–266, 2018.

MUÑOZ-QUEZADA, M. T. et al. Vías de exposición a plaguicidas en escolares de la Provincia de Talca, Chile. **Gaceta Sanitaria**, v. 28, n. 3, p. 190–195, 2014.

MURRAY, B. M.; PALLER, M. S.; FERRIS, T. F. Effect of cyclosporine administration on renal hemodynamics in conscious rats. **Kidney international**, v. 28, n. 5, p. 767–74, nov. 1985.

MUSSON, R.; SMIT, N. Regulatory Mechanisms of Calcineurin Phosphatase Activity. **Current Medicinal Chemistry**, v. 18, n. 2, p. 301–315, 2011.

MUSTAFA, M. et al. Immunopharmacologic Modulation of Experimental Allergic Encephalomyelitis: Low-Dose Cyclosporin-A Treatment Causes Disease Relapse and Increased Systemic T and B Cell-Mediated Myelin-Directed Autoimmunity. **Scandinavian Journal of Immunology**, v. 38, n. 6, p. 499–507, dez. 1993.

NAIR, A.; JACOB, S. A simple practice guide for dose conversion between animals and human. **Journal of Basic and Clinical Pharmacy**, v. 7, n. 2, p. 27, 2016.

NAWATA, C. M.; PANNABECKER, T. L. Mammalian urine concentration: a review of renal medullary architecture and membrane transporters. **Journal of Comparative Physiology B: Biochemical, Systemic, and Environmental Physiology**, v. 188, n. 6, p. 899–918, 2018.

NUR, G. et al. The effect of caffeic acid phenethyl ester (CAPE) on hepatic histopathology and oxidative stress in rats treated with malathion. 2018.

OJEDA, S. R. et al. Recent Advances in the Endocrinology of Puberty. **Endocrine Reviews**, v. 1, n. 3, p. 228–257, 1 jul. 1980.

OZSOY, A. Z. et al. Protective effect of intravenous lipid emulsion treatment on malathion-induced. p. 2425–2434, 2016.

PALLET, N. et al. Response of human renal tubular cells to cyclosporine and sirolimus: A toxicogenomic study. **Toxicology and Applied Pharmacology**, v. 229, n. 2, p. 184–196, 2008.

PENG, C. et al. Biology of Ageing and Role of Dietary Antioxidants. 2014.

PIZZINO, G. et al. Oxidative Stress: Harms and Benefits for Human Health. 2017.

RADI, Z. A. Kidney Pathophysiology, Toxicology, and Drug-Induced Injury in Drug Development. **International Journal of Toxicology**, v. 38, n. 3, p. 215–227, 2019.

RONCHI, J. A.; VERCESI, A. E.; CASTILHO, R. F. Reactive oxygen species and permeability transition pore in rat liver and kidney mitoplasts. [s.d.]

RONCHI, J. A.; VERCESI, A. E.; CASTILHO, R. F. Reactive oxygen species and permeability transition pore in rat liver and kidney mitoplasts. **Journal of Bioenergetics and Biomembranes**, v. 43, n. 6, p. 709–715, 2011.

ROSS, PAWLINA, P. **Histology Ross**. 7. ed. [s.l: s.n.]

SÁNCHEZ-SANTED, F.; COLOMINA, M. T.; HERRERO HERNÁNDEZ, E. Organophosphate pesticide exposure and neurodegeneration. **Cortex**, v. 74, p. 417–426, 2016.

SANDOVAL, L. et al. Effects of chlorpyrifos on cell death and cellular phenotypic specification of human neural stem cells. **Science of the Total Environment**, v. 683, p. 445–454, 15 set. 2019.

SCHELLING, J. R. **Tubular atrophy in the pathogenesis of chronic kidney disease progressionPediatric Nephrology**Springer Verlag, , 1 maio 2016.

SCHREIBER, S. L.; CRABTREE, G. R. The mechanism of action of cyclosporin A and FK506. **Immunology Today**, v. 13, n. 4, p. 136–142, 1992.

SELMI, S. et al. Malathion, an organophosphate insecticide, provokes metabolic, histopathologic and molecular disorders in liver and kidney in prepubertal male mice. **Toxicology Reports**, v. 5, n. August 2017, p. 189–195, 2018.

SETH, V. et al. Pesticide induced alterations in acetylcholine esterase and gamma glutamyl transpeptidase activities and glutathione level in lymphocytes of human poisoning cases. **Clinical Biochemistry**, v. 34, n. 5, p. 427–429, 2001.

SHEHATA, M. et al. **Increased platelet-derived growth factor in the kidneys of cyclosporin-treated ratsKidney International**. [s.l: s.n.].

SHIROLIKAR, M. et al. Managing a side effect : Cyclosporine-Induced nephrotoxicity Introduction Pathophysiology of Nephrotoxicity Risk Factors for Cyclosporine Nephrotoxicity. n. 1, p. 1–7, 2020.

SIDHU, G. K. et al. Toxicity, monitoring and biodegradation of organophosphate pesticides: A review. **Critical Reviews in Environmental Science and Technology**, v. 49, n. 13, p. 1135–1187, 2019.

SILVEIRA, P. P. et al. Developmental origins of health and disease (DOHaD) Origens desenvolvimentistas da saúde e da doença (DOHaD). 2007.

SINITOX. **Sistema Nacional de Informações Tóxico-Farmacológicas - Sinitox**. Disponível em: <https://sinitox.icict.fiocruz.br/dados-nacionais>. Acesso em: 29 abr. 2021.

SLATTERY, C. et al. Cyclosporine A - induced renal fibrosis: A role for epithelial-mesenchymal transition. **American Journal of Pathology**, v. 167, n. 2, p. 395–407, 2005.

SOLTANINEJAD, K.; ABDOLLAHI, M. Current opinion on the science of organophosphate pesticides and toxic stress: A systematic review. **Medical Science Monitor**, v. 15, n. 3, p. 75–90, 2009.

TAKAHASHI, N.; HASHIZUME, M. A systematic review of the influence of occupational organophosphate pesticides exposure on neurological impairment. **BMJ Open**, v. 4, n. 6, 2014.

ULLAH, S. et al. Malathion induced oxidative stress leads to histopathological and biochemical toxicity in the liver of rohu (Labeo rohita, Hamilton) at acute concentration. **Ecotoxicology and Environmental Safety**, v. 161, n. May, p. 270–280, 2018.

USEPA. **Problem Formulation for the Environmental Fate and Ecological Risk, Endangered Species and Drinking Water Assessments in Support of the Registration Review of Diazinon**. [s.l: s.n.].

VERSCHUREN, E. H. J. et al. Sensing of tubular flow and renal electrolyte transport. **Nature Reviews Nephrology**, v. 16, n. 6, p. 337–351, 2020.

VIJAYA KUMAR, S. et al. Current review on organophosphorus poisoning. **Archives of Applied Science Research**, v. 2, n. 4, p. 199–215, 2010.

WAISER, J. et al. **Cyclosporine A up-regulates the expression of TGF-β1 and its receptors type I and type II in rat mesangial cellsNephrology Dialysis Transplantation**, 2002. .

WANG, C. e. et al. Association of CYP3A4*1B genotype with Cyclosporin A pharmacokinetics in renal transplant recipients: A meta-analysis. **Gene**, v. 664, p. 44–49, 2018.

WANG, H. et al. Visualizing liver anatomy, physiology and pharmacology using multiphoton microscopy. **Journal of Biophotonics**, v. 10, n. 1, p. 46–60, 2017.

WHO. Clinical Management of Acute Pesticide Intoxication: Prevention of Suicidal Behaviours. p. 1–25, 2008. Disponível em: <https://www.who.int/mental_health/prevention/suicide/pesticides_intoxication.pdf>.

WOLF, A. et al. Cyclosporine A-induced oxidative stress in rat hepatocytes. **Journal of Pharmacology and Experimental Therapeutics**, v. 280, n. 3, p. 1328–1334, 1997.

WOLF, G. Renal injury due to renin-angiotensin-aldosterone system activation of the transforming growth factor-β pathway. **Kidney International**, v. 70, n. 11, p. 1914–1919, 2006.

YOKOTA, K. et al. Nephrotic syndrome and acute kidney injury induced by malathion toxicity. **BMJ Case Reports**, v. 2017, p. bcr-2017-220733, 9 nov. 2017.

YOUSEF, A. et al. PEG-SOD attenuates the mitogenic ERK1/2 signaling cascade induced by cyclosporin A in the liver and kidney of albino mice. **Chemico-Biological Interactions**, v. 330, n. July, p. 109245, 2020.

YU, W. et al. Cyclosporine A suppressed glucose oxidase induced P53 mitochondrial translocation and hepatic cell apoptosis through blocking mitochondrial permeability transition. **International Journal of Biological Sciences**, v. 12, n. 2, p. 198–209, 2016.

YÜCE, A.; ATEŞŞAHIN, A.; ÇERIBAŞI, A. O. Amelioration of cyclosporine A-induced renal, hepatic and cardiac damages by ellagic acid in rats. **Basic and**

Clinical Pharmacology and Toxicology, v. 103, n. 2, p. 186–191, 2008.

ZHAO, J. H. **Mesangial Cells and Renal Fibrosis**. [s.l.] Springer Singapore, 2019. v. 1165

ZHU, X. D. et al. MicroRNA-377 Mediates Cardiomyocyte Apoptosis Induced by Cyclosporin A. **Canadian Journal of Cardiology**, v. 32, n. 10, p. 1249–1259, 1 out. 2016.

ZIDAN, N. E. H. A. Hepato-and nephrotoxicity in male albino rats exposed to Malathion and spinosad in stored wheat grains. **Acta Biologica Hungarica**, v. 66, n. 2, p. 133–148, 2015.

1 APÊNDICES

Apêndice A – Documentação fotográfica referente ao estudo com Malation (Artigo 1)

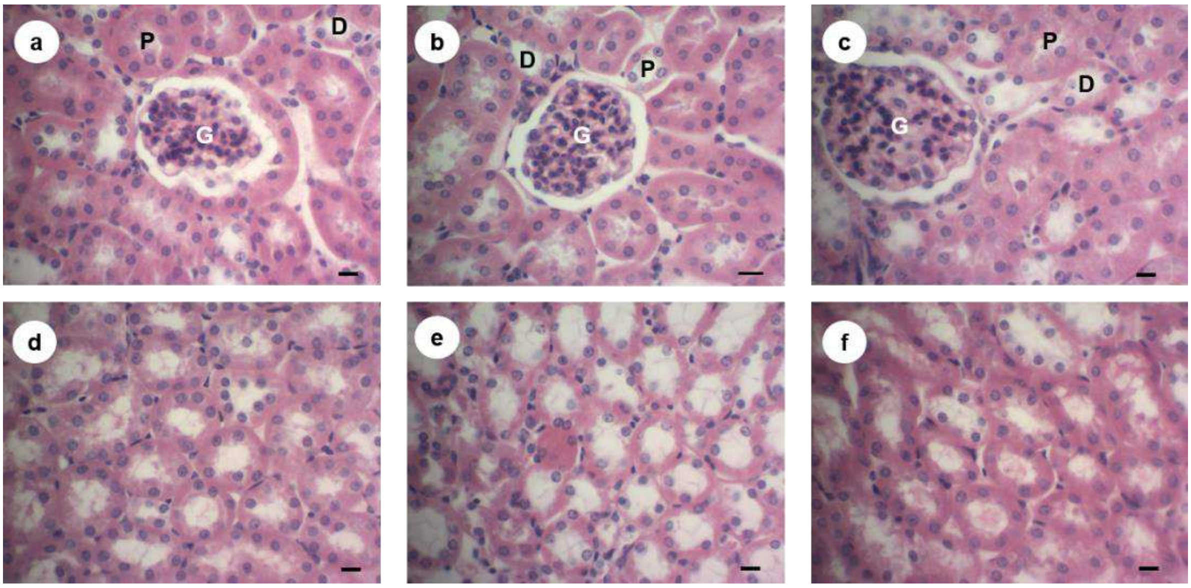

Figura 1. Histologia renal - Hematoxilina e Eosina – Fotomicrografia no aumento de 400x, evidenciando o corpúsculo renal (a, b, c) e túbulos coletores (d, e, f). Grupos: controle (a, d) Malation 10 mg/kg (b, e) e Malation 50 mg/kg (c, f). Glomérulo (G), túbulo contorcido proximal (P) e distal (D); barra = 10 µm.

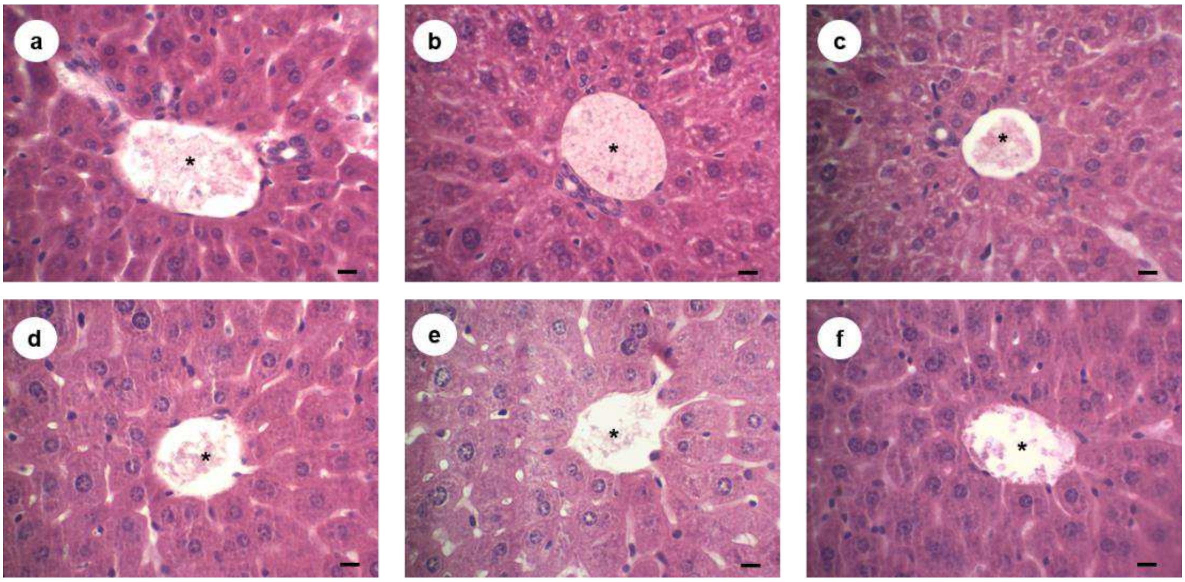

Figura 2. Histologia hepática - Hematoxilina e Eosina Fotomicrografia da coloração de HE no aumento de 400x, evidenciando as vênulas centrolobulares (a, b, c) e portas (d, e, f). Grupos: controle (a, d) Malation 10 mg/kg (b, e) e Malation 50 mg/kg (c, f). Luz dos vasos (*); barra = 10 µm.

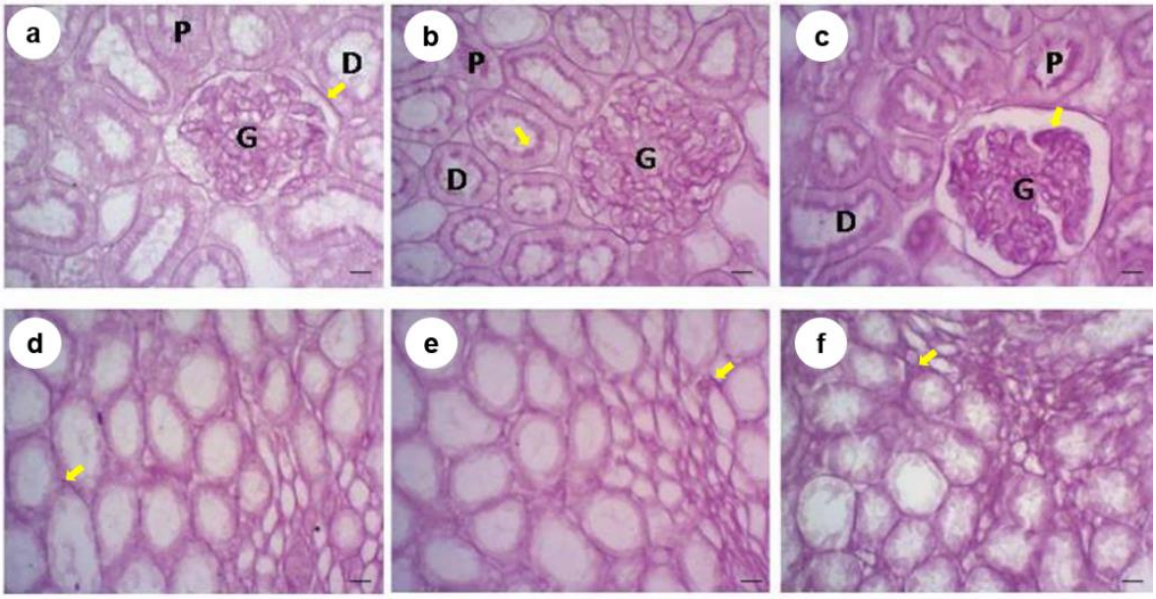

Figura 3. **Histologia renal - Ácido periódico de Schiff (PAS)** Fotomicrografia da coloração de PAS no aumento de 400x, evidenciando a área cortical (a, b, c) e medular (d, e, f) do rim. Glomérulo (G), túbulo contorcido proximal (P) e distal (D). Área marcada positivamente para glicoconjugados neutros (seta amarela). barra = 10 µm. Luz dos vasos (*).

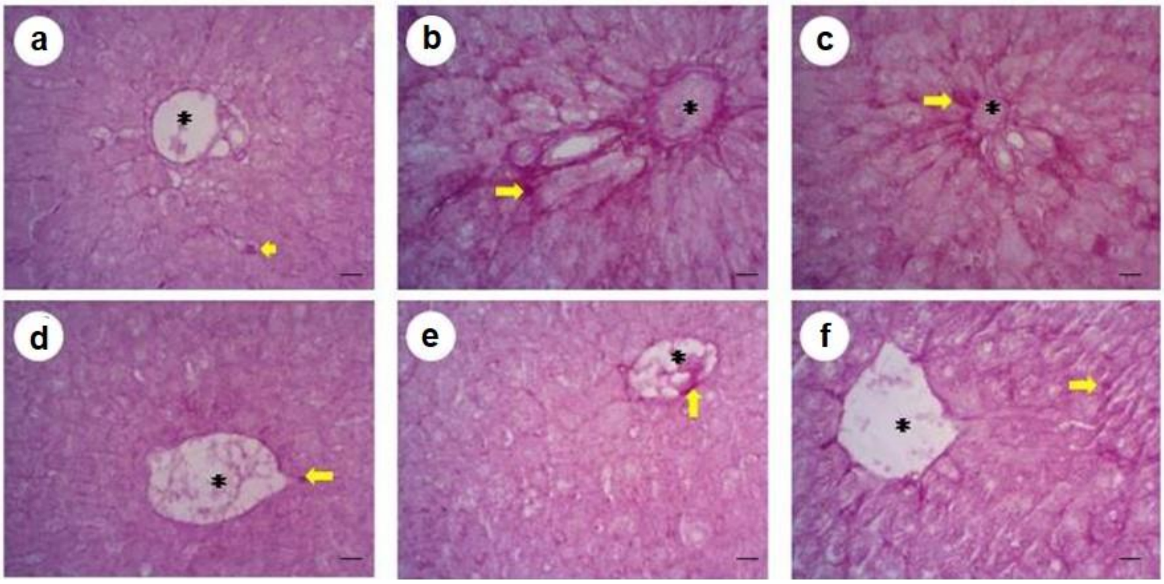

Figura 4. Histologia Hepática - Ácido periódico de Schiff (PAS) Fotomicrografia da coloração de PAS no aumento de 400x evidenciando as vênulas portas (a, b, c) e centrolobulares (d, e, f). Área marcada positivamente para glicoconjugados neutros (seta amarela). barra = 10 µm. Luz dos vasos (*).

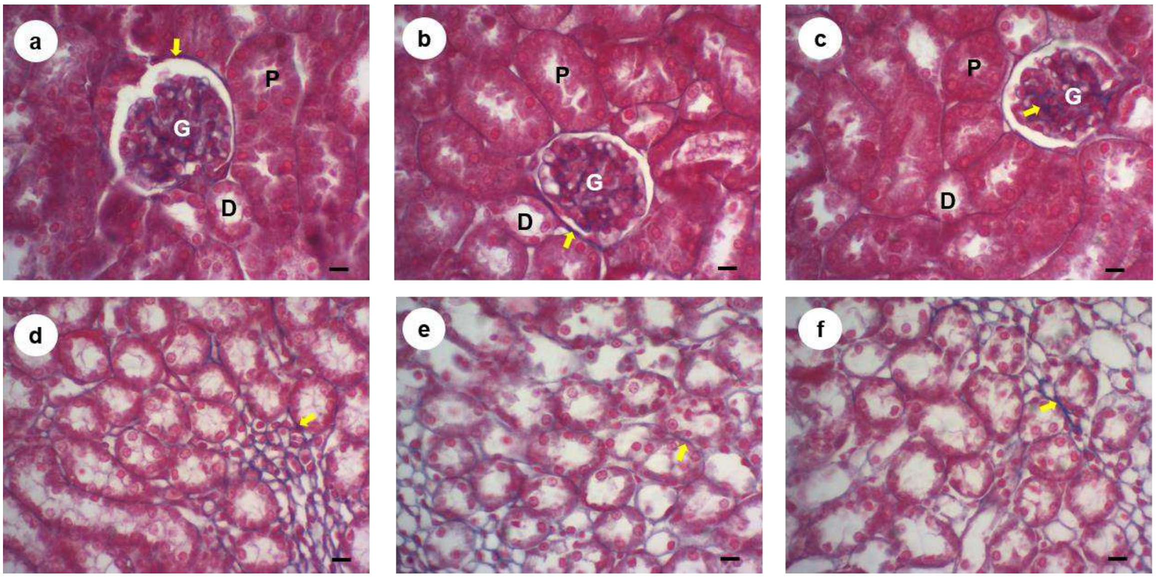

Figura 5. Histologia renal - tricrômico de Azan Heidenhain Fotomicrografia da coloração de Tricrômico de Azan Heidenhain no aumento de 400x evidenciando o colágeno total, presente na área cortical (a, b, c) e medular (d, e, f) do rim. Grupos: controle (a, d) Malation 10 mg/kg (b, e) e Malation 50 mg/kg (c, f). Colágeno total (seta amarela).

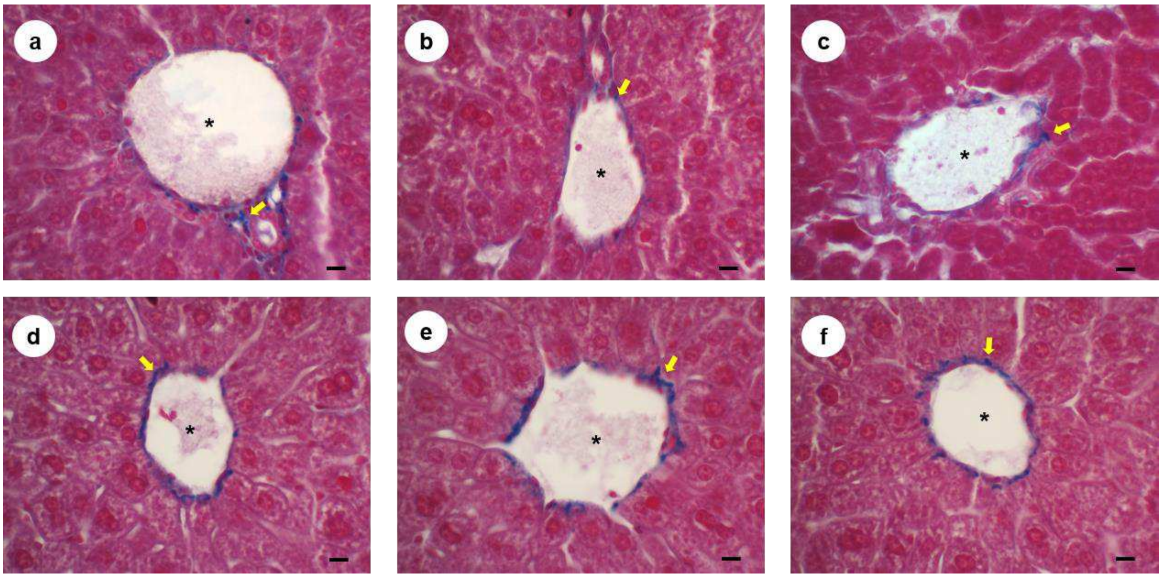

Figura 6. Histologia renal - tricrômico de Azan Heidenhain - Fotomicrografia da coloração de Tricrômico de Azan Heidenhain no aumento de 400x evidenciando o colágeno total, presente as vênulas portas (a, b, c) e centrolobulares (d, e, f). Grupos: controle (a, d) Malation 10 mg/kg (b, e) e Malation 50 mg/kg (c, f). Colágeno total (seta amarela). Colágeno total (seta amarela) e luz da vênula (*).

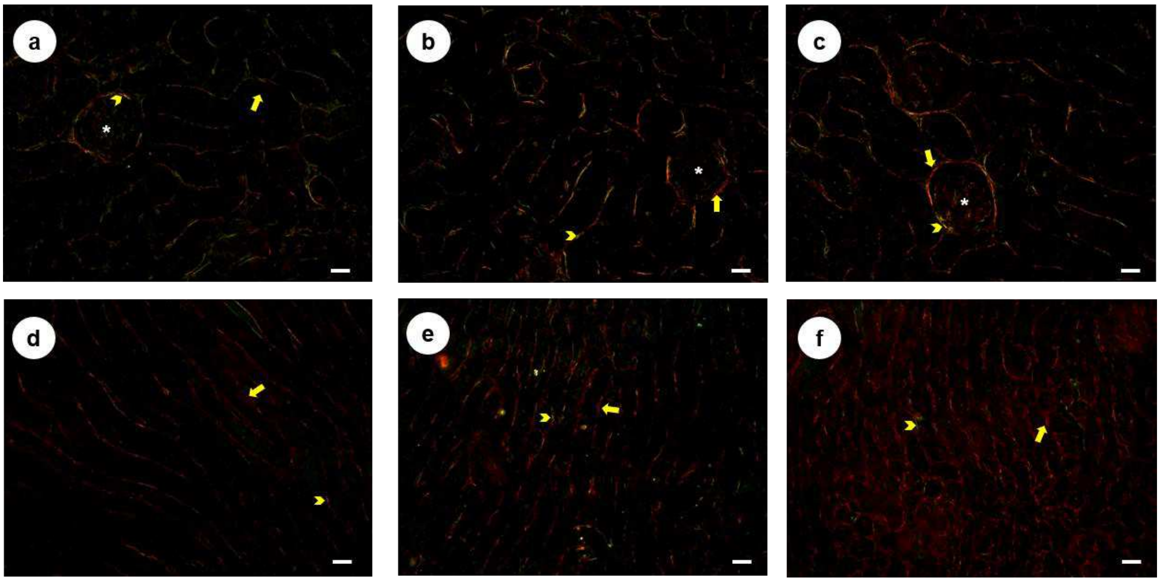

Figura 7. Histologia renal – Picrosirius Red - Fotomicrografia da região cortical polarizada (a,b,c) e região medular polarizada (b, d, f) em aumento de 400x na coloração de Picrosirius Red. Grupos: controle (a, d) Malation 10 mg/kg (b, e) e Malation 50 mg/kg (c, f). Colágeno do tipo I (seta amarela), colágeno do tipo III (ponta da seta) e luz da vênula (*).

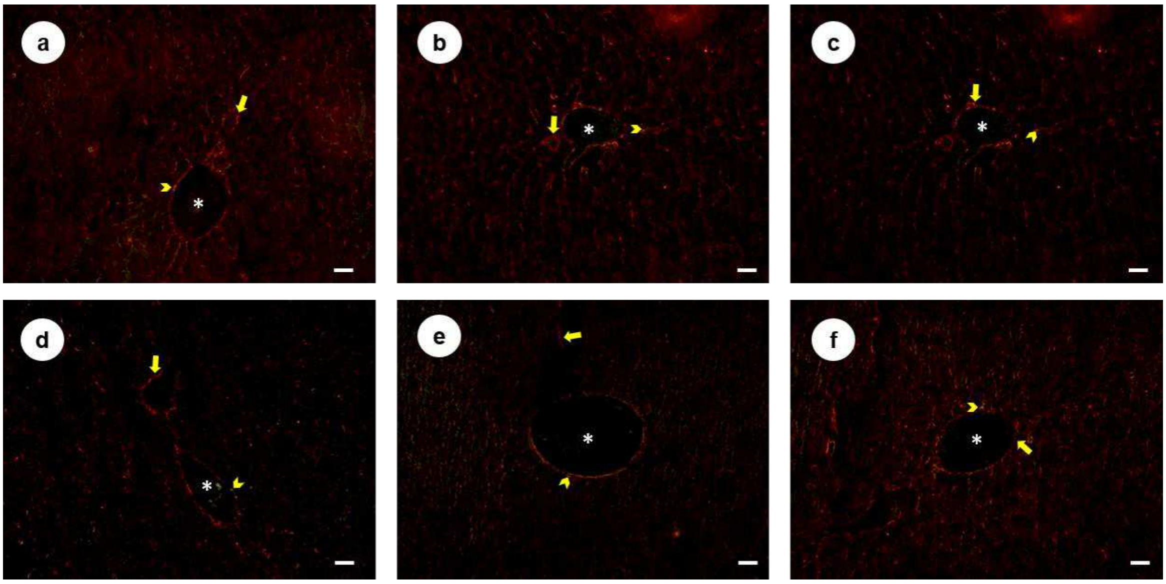

Figura 8. Histologia renal – *Picrosirius Red* Fotomicrografia das vênulas portas polarizadas (a, b, c) e vênulas portas polarizadas (d, e, f) em aumento de 400x na coloração de *Picrosirius Red*. Grupos: controle (a, d) Malation 10 mg/kg (b, e) e Malation 50 mg/kg (c, f). Colágeno do tipo I (seta amarela), colágeno do tipo III (ponta da seta) e luz da vênula (*).

Apêndice B - Documentação fotográfica referente estudo com Ciclosporina A (Artigo 2)

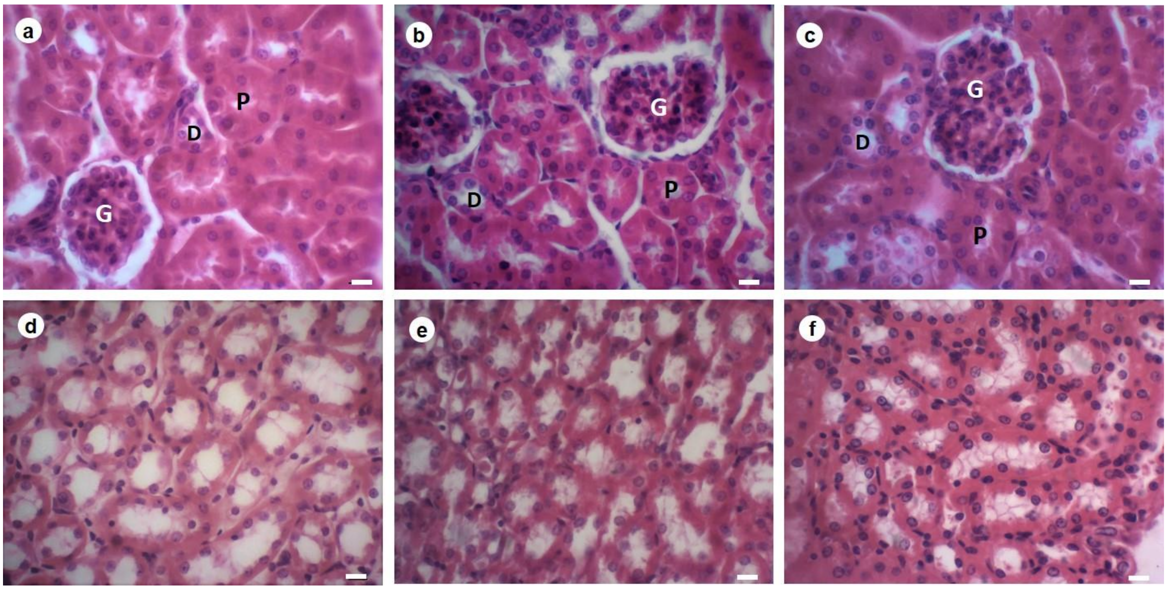

Figura 1. Histologia renal - Hematoxilina e Eosina - Fotomicrografia da região cortical (a, b, c) e da região medular (d, e, f). Coloração: hematoxilina e eosina. Grupos: controle (a, d), CsA10I (b, e) CsA10R (c, f). Glomérulo (G), túbulo contorcido proximal (P) e distal (D), barra: 10 μm. Fonte: o próprio autor.

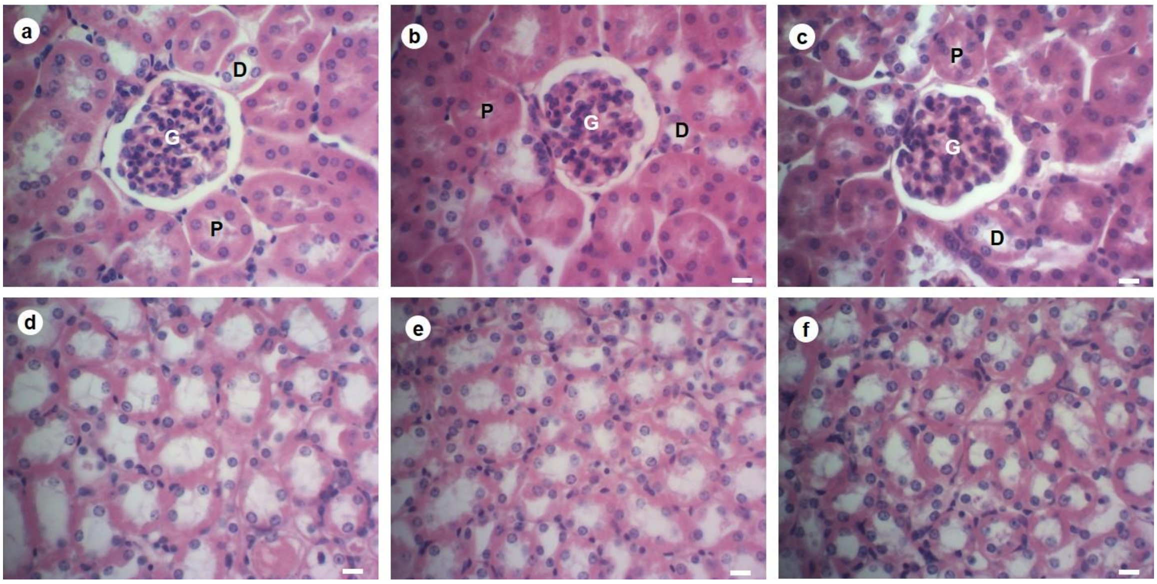

Figura 2. Histologia renal - Hematoxilina e Eosina - Fotomicrografia da região cortical (a, b, c) e da região medular (d, e, f). Grupos: controle (a, d), CsA50I (b, e) CsA50R (c, f). Glomérulo (G), túbulo contorcido proximal (P) e distal (D), barra: 10 μm. Fonte: o próprio autor.

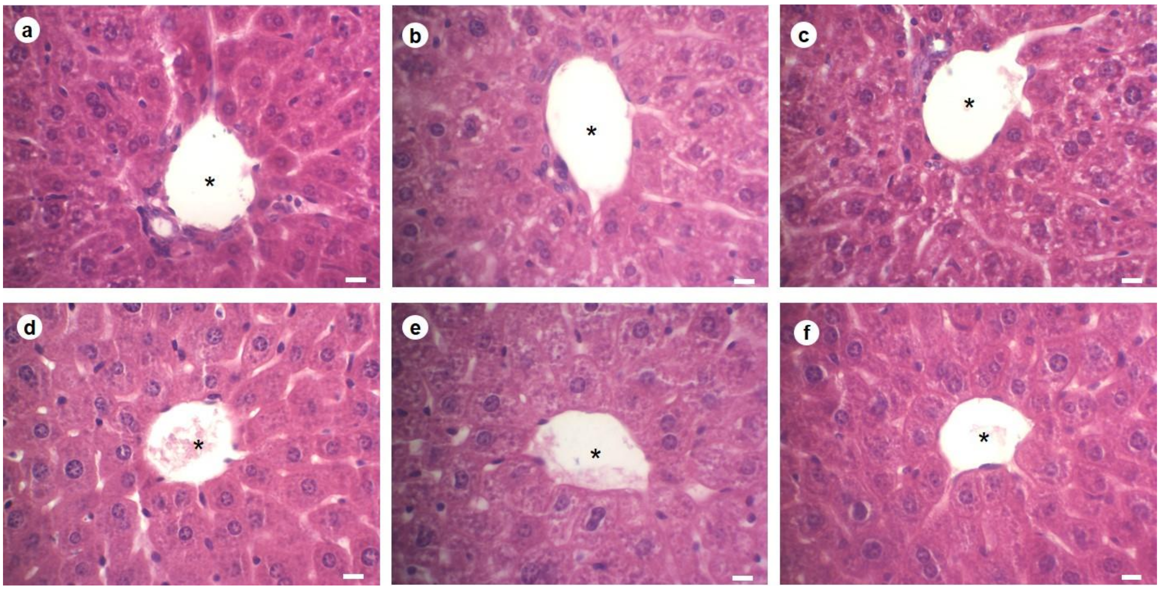

Figura 3. Histologia hepática - Hematoxilina e Eosina - Fotomicrografia da região do espaço porta (a, b, c) e da vênula centrolobular (d, e, f). Grupos: controle (a, d), CsA10I (b, e) CsA10R (c, f). Luz do vaso sanguíneo (asterisco), barra = 10 µm.

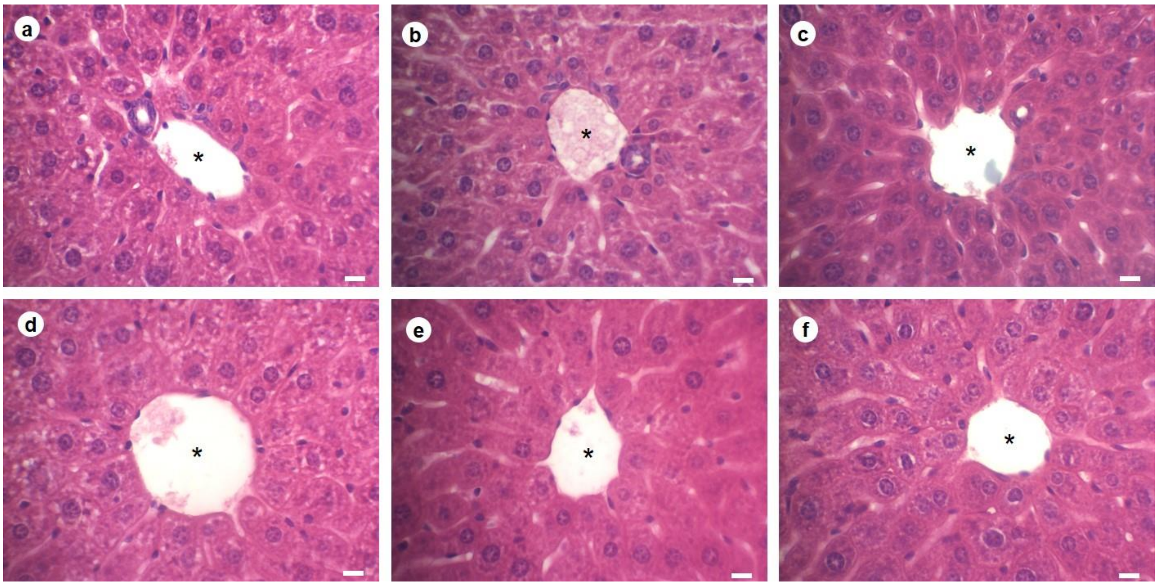

Figura 4. Histologia hepática - Hematoxilina e Eosina - Fotomicrografia da região do espaço porta (a, b, c) e da vênula centrolobular (d, e, f). Grupos: controle (a, d), CsA50I (b, e) CsA50R (c, f). Luz do vaso sanguíneo (asterisco), barra = 10 µm.

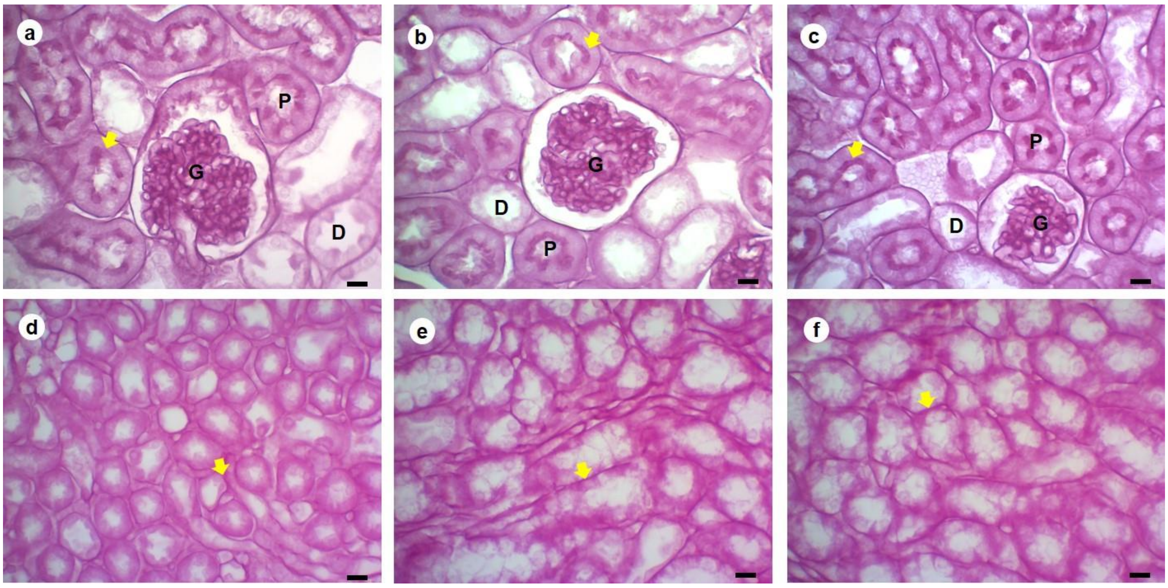

Figura 5. Histologia renal - Ácido periódico de Schiff (PAS) - Fotomicrografia da região cortical (a, b, c) e da região medular (d, e, f) do rim. Grupos: controle (a, d), CsA50I (b, e) CsA50R (c, f). Glomérulo (G), túbulo contorcido proximal (P) e distal (D), marcação positiva para glicogênio (Seta) barra: 10 µm.

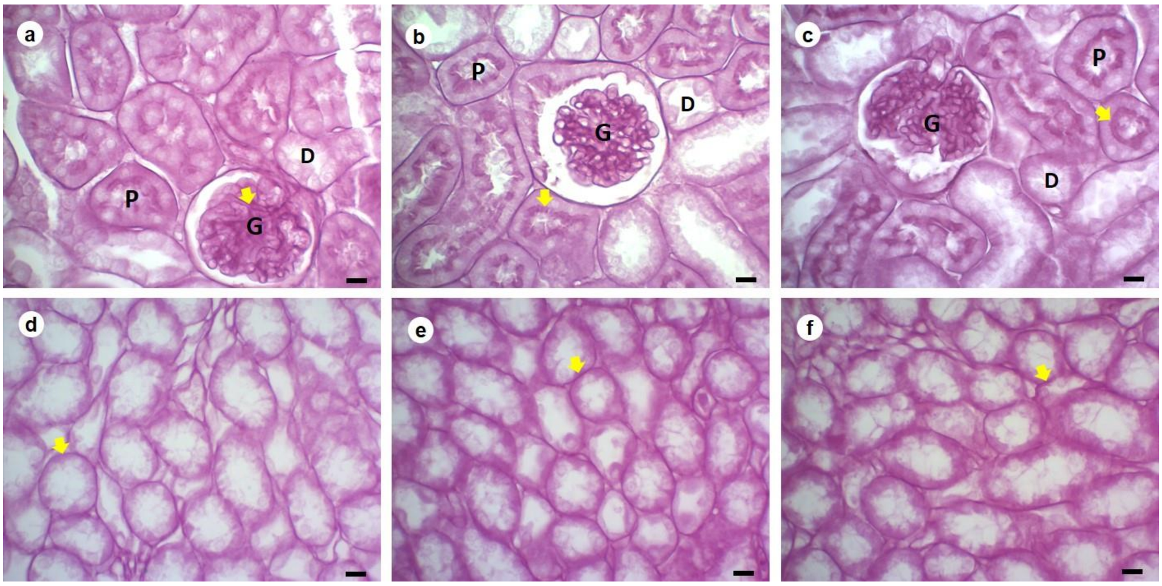

Figura 6. Histologia renal - Ácido periódico de Schiff (PAS) – Fotomicrografia da região cortical (a, b, c) e da região medular (d, e, f) do rim de camundongos *Swiss* machos. Grupos: controle (a, d), CsA50I (b, e) CsA50R (c, f). Glomérulo (G), túbulo contorcido proximal (P) e distal (D), marcação positiva para glicogênio (Seta) barra: 10 µm.

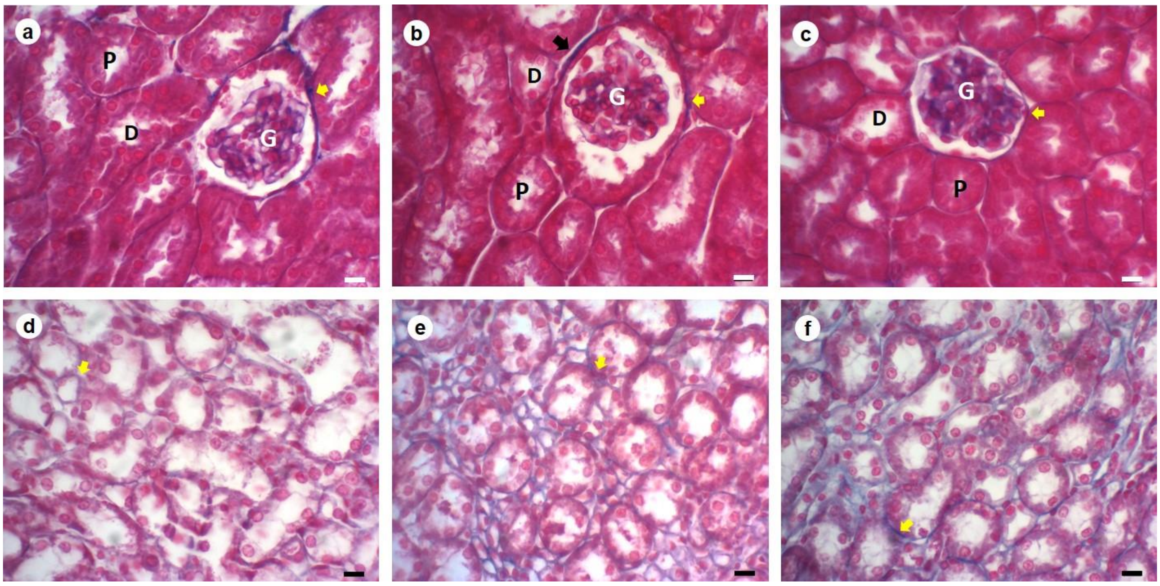

Figura 7. Histologia renal - tricrômico de Azan Heidenhain . Fotomicrografia da região cortical (a, b, c) e da região medular (d, e, f) do rim de camundongos *Swiss* machos. Grupos: controle (a, d), CsA10I (b, e) CsA10R (c, f). Glomérulo (G), túbulo contorcido proximal (P) e distal (D), marcação positiva para colágeno (seta) barra: 10 µm

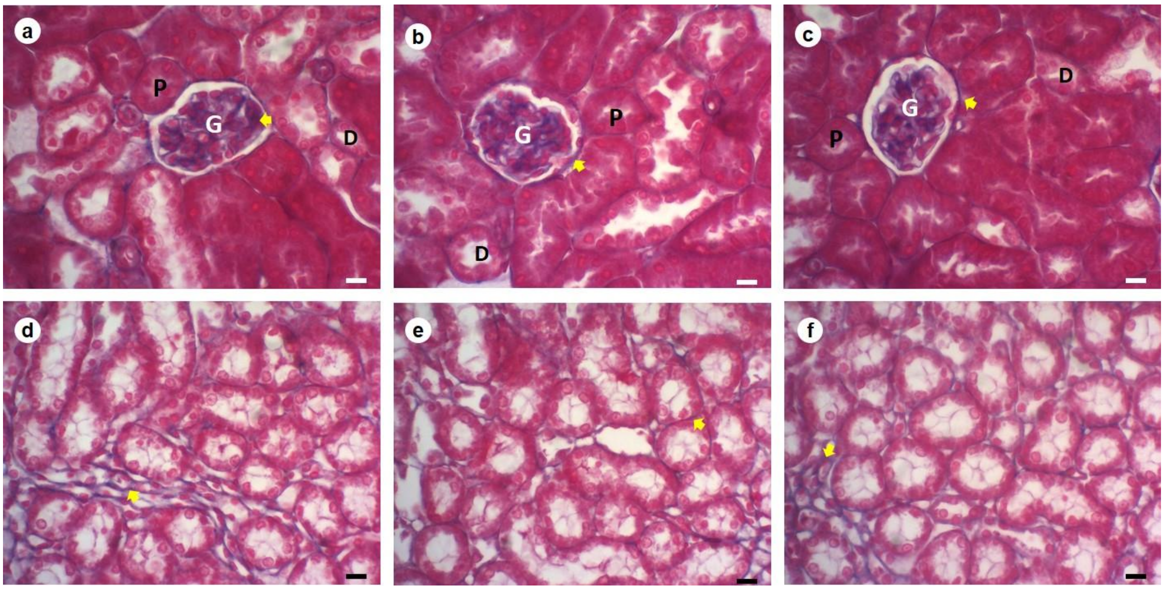

Figura 8. Histologia renal - Tricrômico de Azan Heidenhain -Fotomicrografia da região cortical (a, b, c) e da região medular (d, e, f) do rim de camundongos *Swiss* machos. Grupos: controle (a, d), CsA50I (b, e) CsA50R (c, f). Glomérulo (G), túbulo contorcido proximal (P) e distal (D), marcação positiva para colágeno (seta) barra: 10 µm.

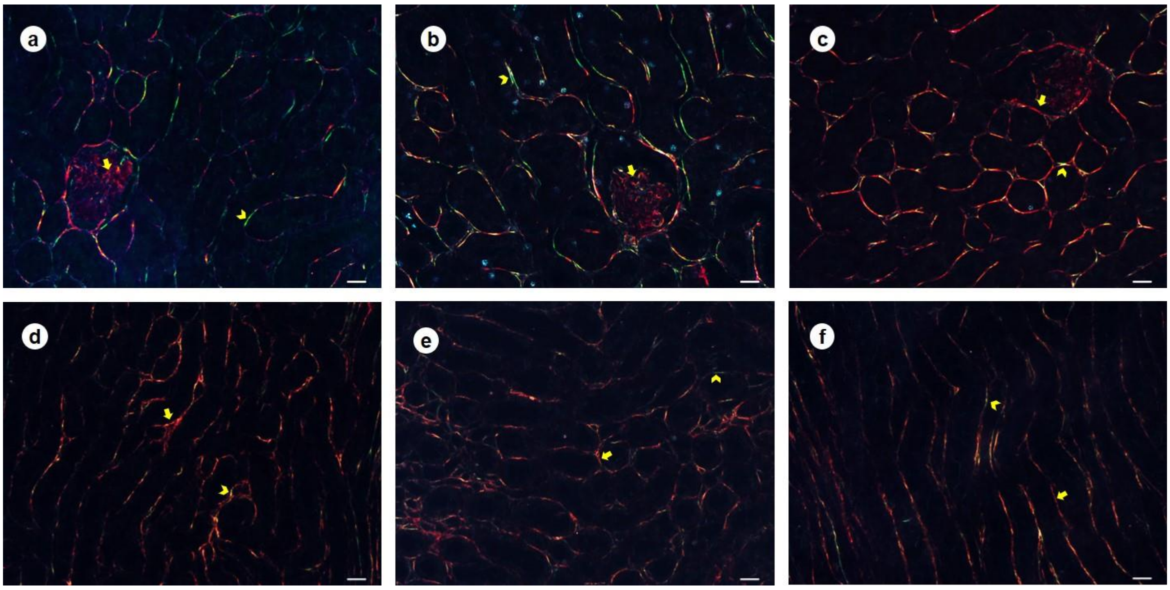

Figura 9. Histologia renal - Picrosirius Red - Fotomicrografia em luz polarizada, da região cortical (a, b, c) e da região medular (d, e, f) do rim de camundongos *Swiss* machos. Grupos: controle (a, d), CsA10I (b, f) CsA10R (c, f). Marcação positiva para colágeno tipo I (cabeça de seta); marcação positiva para colágeno tipo III (seta), barra: 10 µm.

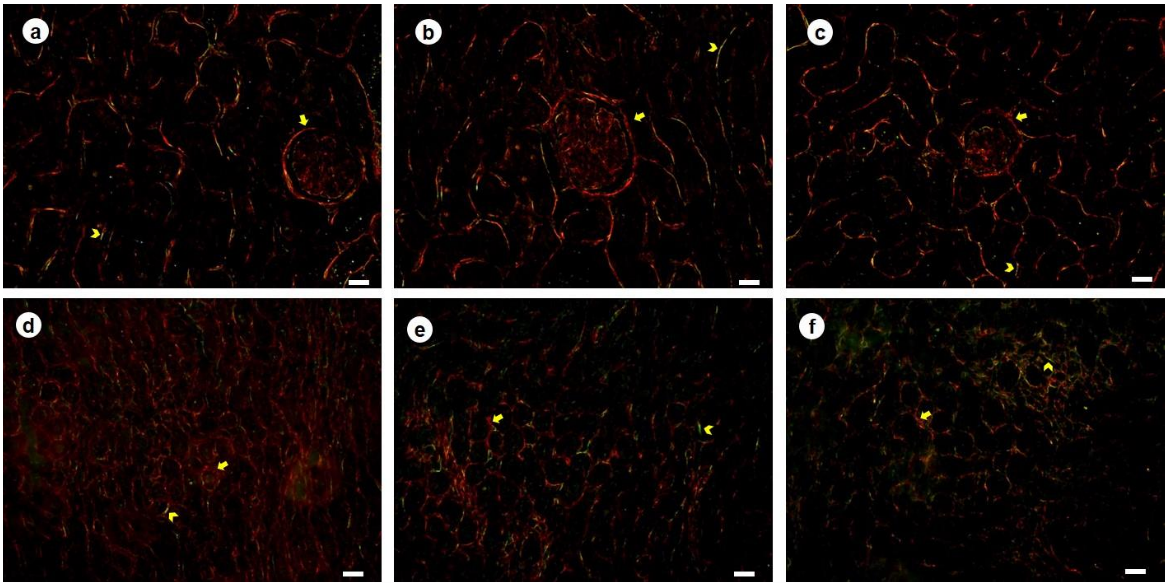

Figura 10. Histologia renal - ***Picrosirius Red*** – Fotomicrografia em luz polarizada, da região cortical (a, b, c) e da região medular (d, e, f) do rim de camundongos *Swiss* machos. Grupos: controle (a, d), CsA50I (b, e) CsA50R (c, f). Marcação positiva para colágeno tipo I (cabeça de seta); marcação positiva para colágeno tipo III (seta), barra: 10 µm.

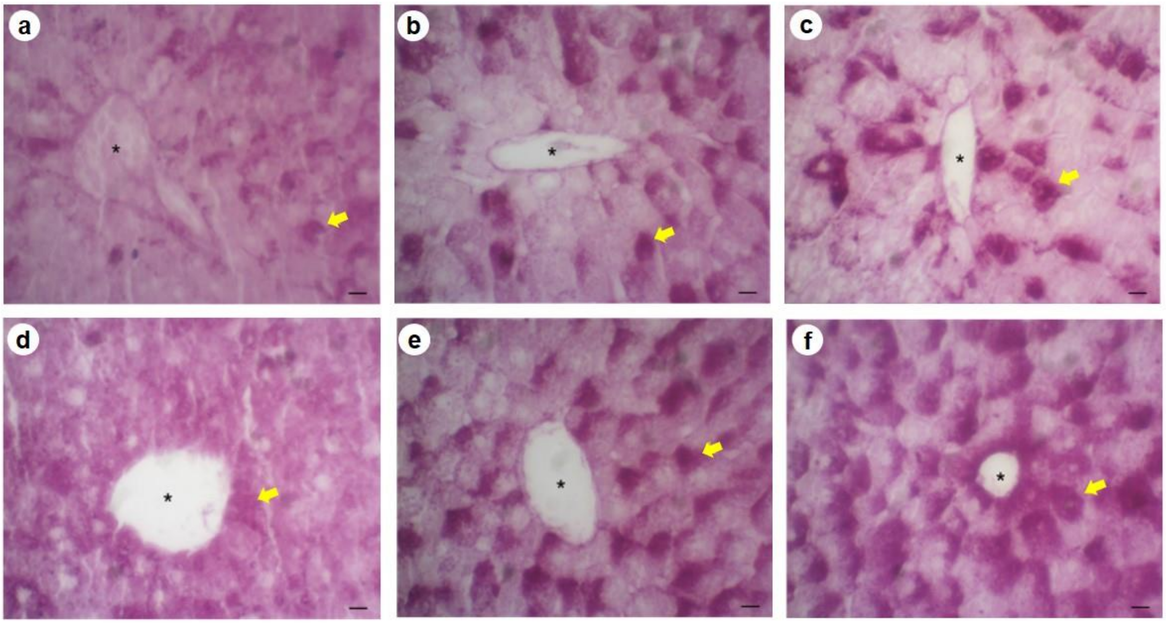

Figura 11. Histologia hepática - Ácido periódico de Schiff (PAS) - Fotomicrografia da região do espaço porta (a, b, c) e da vênula centrolobular (d, e, f) do fígado de camundongos *Swiss* machos. Grupos: controle (a, d), CsA10I (b, e) CsA10R (c, f). Luz do vaso sanguíneo (asterisco); marcação positiva para glicogênio (cabeça de seta), barra = 10 µm.

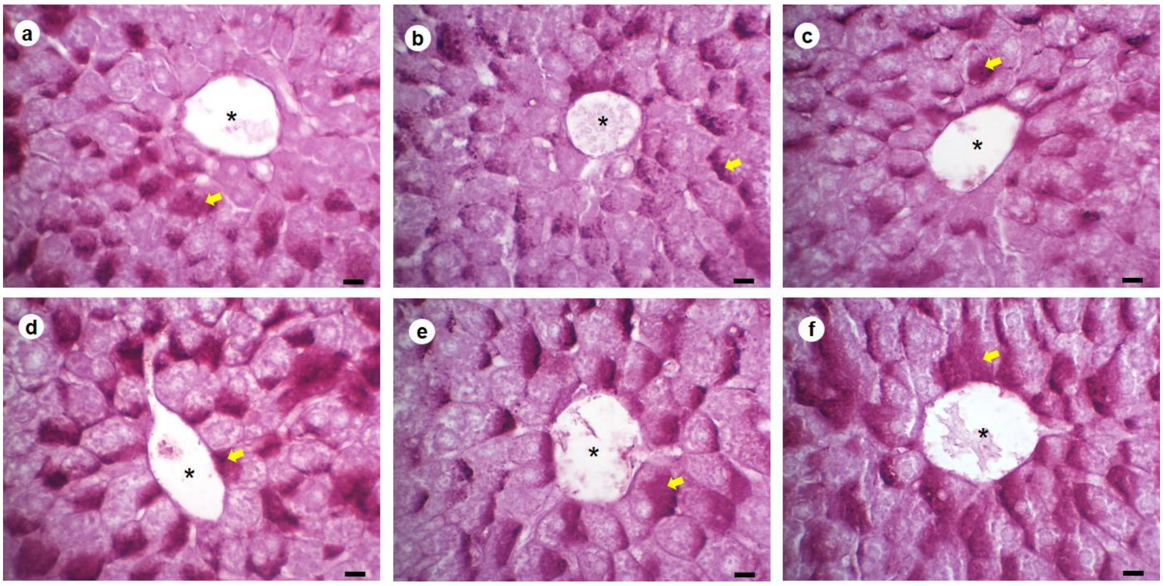

Figura 11. Histologia hepática - Ácido periódico de Schiff (PAS) - Fotomicrografia da região do espaço porta (a, b, c) e da vênula centrolobular (d, e, f) do fígado de camundongos *Swiss* machos. Grupos: controle (a, d), CsA50I (b, e) CsA50R (c, f). Luz do vaso sanguíneo (asterisco); marcação positiva para glicogênio (cabeça de seta), barra = 10 µm.

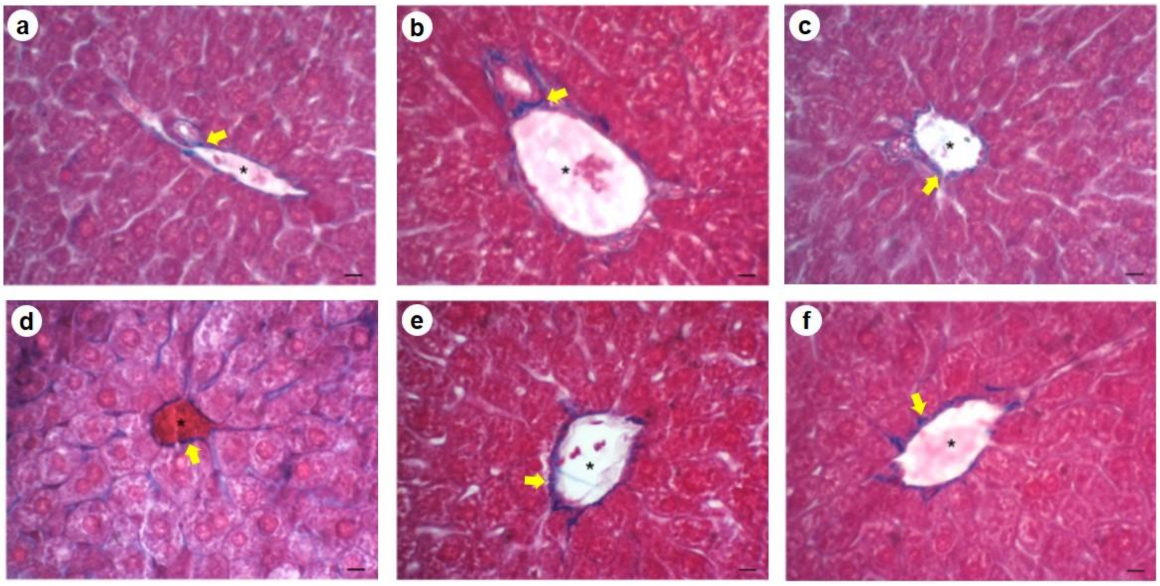

Figura 13. Histologia hepática - Tricrômico Azan Heidenhain - Fotomicrografia da região do espaço porta (a, b, c) e da vênula centrolobular (d, e, f) do fígado de camundongos *Swiss* machos. Grupos: controle (a, d), CsA10I (b, e) CsA10R (c, f). Luz do vaso sanguíneo (asterisco); marcação positiva para colágeno (cabeça de seta), barra = 10 µm.

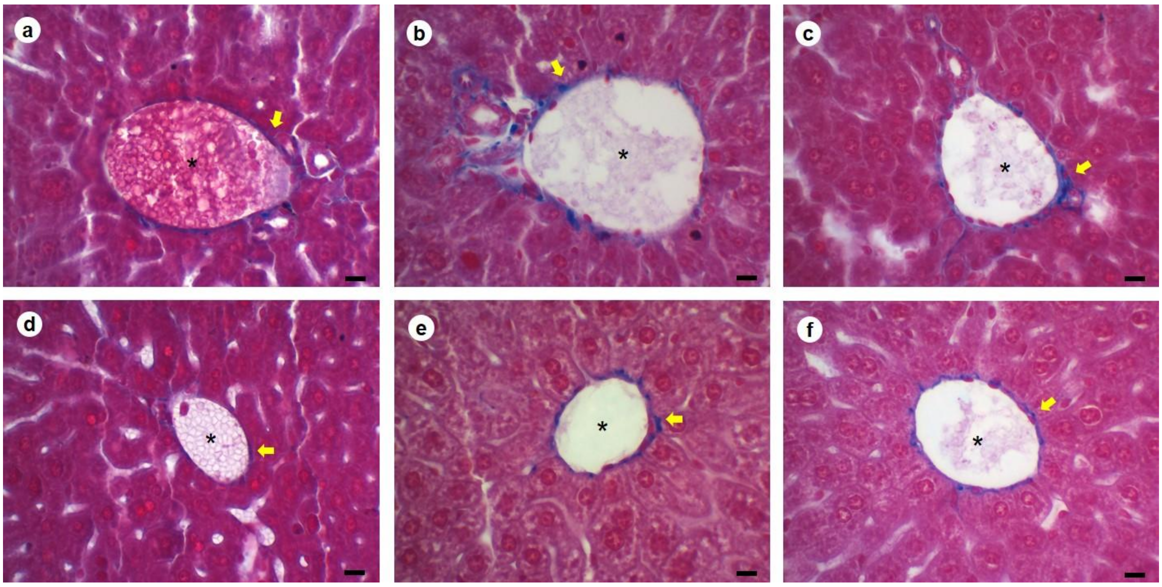

Figura 14. Histologia hepática - Tricrômico Azan Heidenhain - Fotomicrografia da região do espaço porta (a, b, c) e da vênula centrolobular (d, e, f) do fígado de camundongos *Swiss* machos. Grupos: controle (a, d), CsA50I (b, e) CsA50R (c, f). Luz do vaso sanguíneo (asterisco); marcação positiva para colágeno (cabeça de seta), barra = 10 µm.

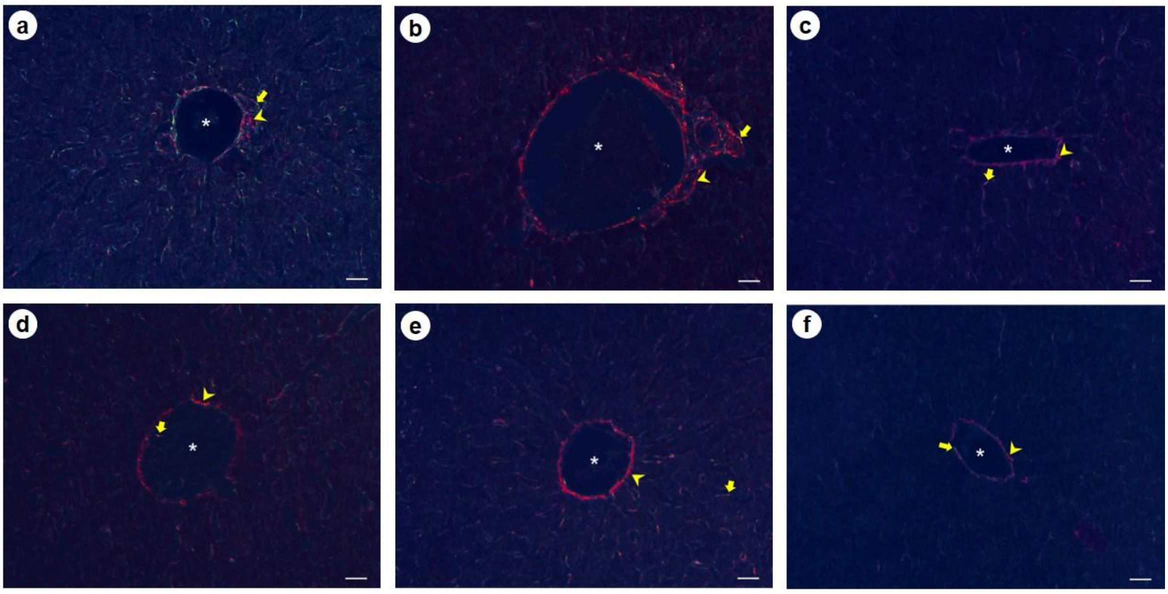

Figura 15. Histologia hepática - Picrosirius red - Fotomicrografia com luz polarizada, da região do espaço porta (a, b, c) e da vênula centrolobular (d, e, f) do fígado de camundongos *Swiss* machos. Grupos: controle (a, d), CsA10I (b, e) CsA10R (c, f). Luz do vaso sanguíneo (asterisco); marcação positiva para colágeno tipo I (cabeça de seta); marcação positiva para colágeno tipo III (seta), barra = 10 µm.

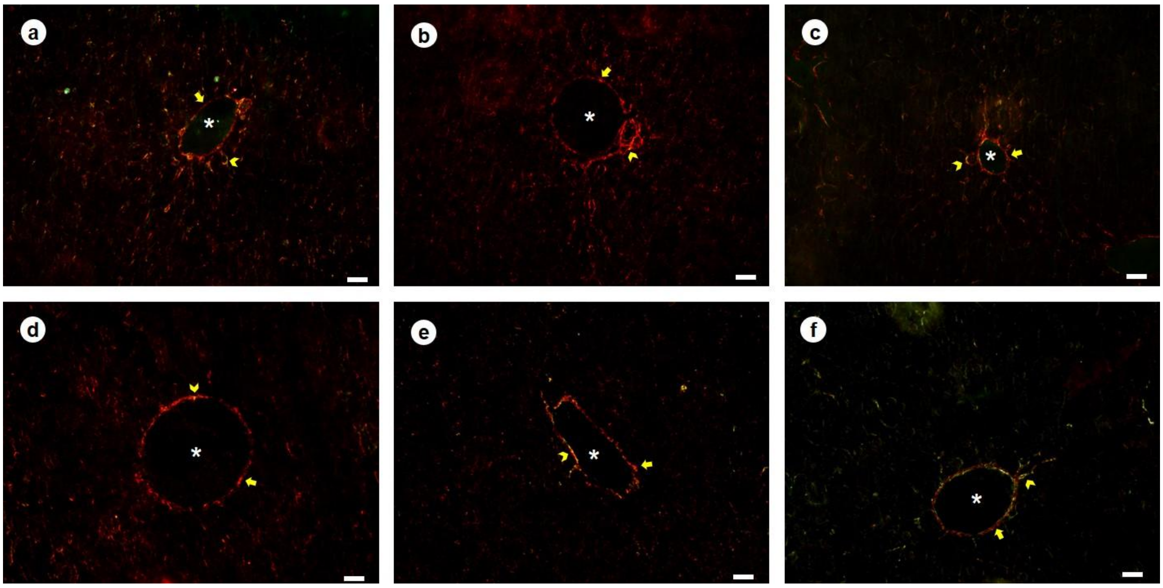

Figura 16. Histologia hepática - Picrosirius red - Fotomicrografia com luz polarizada, da região do espaço porta (a, b, c) e da vênula centrolobular (d, e, f) do fígado de camundongos *Swiss* machos. Grupos: controle (a, d), CsA50I (b, e) CsA50R (c, f). Luz do vaso sanguíneo (asterisco); marcação positiva para colágeno tipo I (cabeça de seta); marcação positiva para colágeno tipo III (seta), barra = 10 µm.

1 ANEXOS

Anexo A

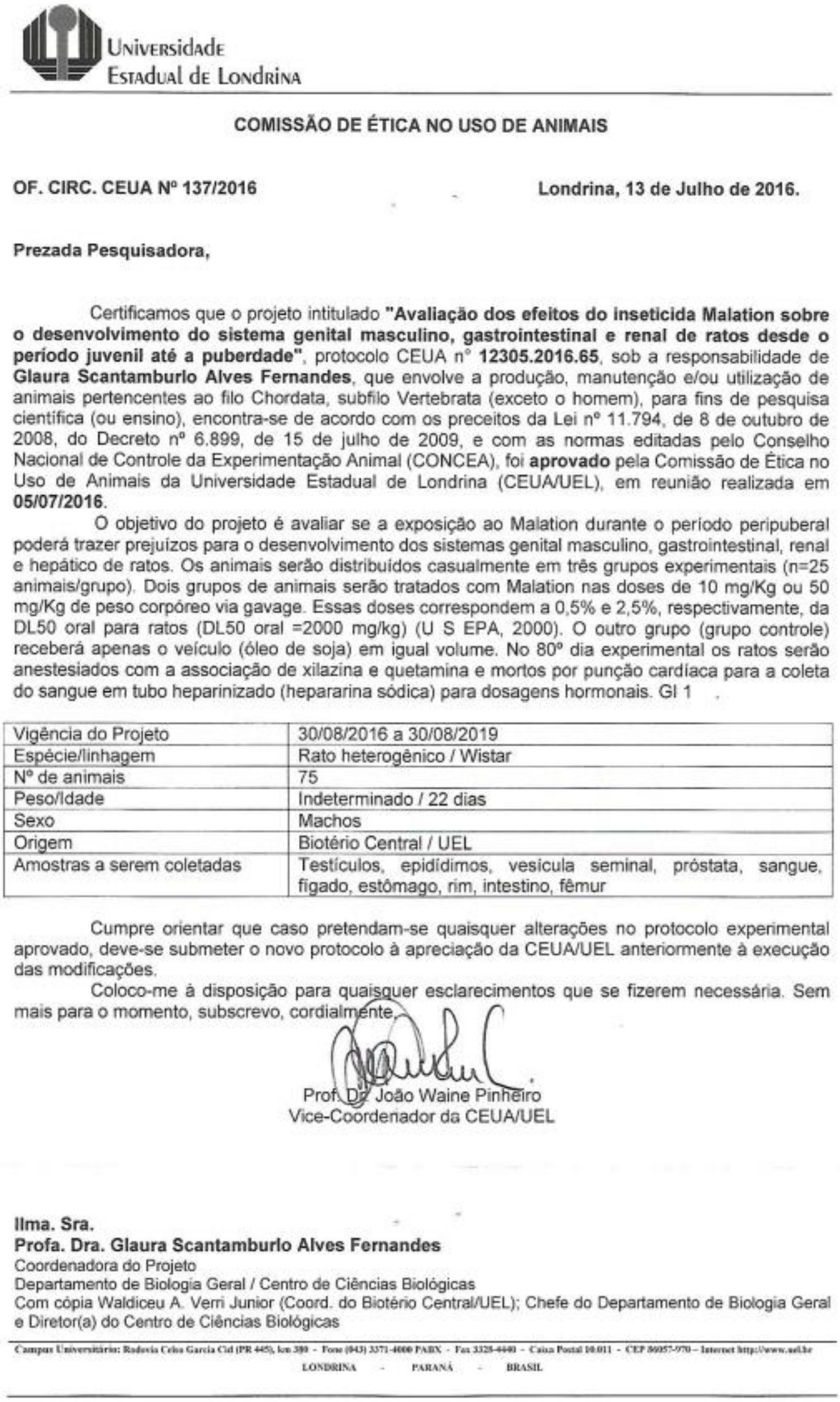

Universidade
Estadual de Londrina

COMISSÃO DE ÉTICA NO USO DE ANIMAIS

OF. CIRC. CEUA Nº 137/2016 **Londrina, 13 de Julho de 2016.**

Prezada Pesquisadora,

Certificamos que o projeto intitulado **"Avaliação dos efeitos do inseticida Malation sobre o desenvolvimento do sistema genital masculino, gastrointestinal e renal de ratos desde o período juvenil até a puberdade"**, protocolo CEUA nº **12305.2016.65**, sob a responsabilidade de **Glaura Scantamburlo Alves Fernandes**, que envolve a produção, manutenção e/ou utilização de animais pertencentes ao filo Chordata, subfilo Vertebrata (exceto o homem), para fins de pesquisa científica (ou ensino), encontra-se de acordo com os preceitos da Lei nº 11.794, de 8 de outubro de 2008, do Decreto nº 6.899, de 15 de julho de 2009, e com as normas editadas pelo Conselho Nacional de Controle da Experimentação Animal (CONCEA), foi **aprovado** pela Comissão de Ética no Uso de Animais da Universidade Estadual de Londrina (CEUA/UEL), em reunião realizada em **05/07/2016**.

O objetivo do projeto é avaliar se a exposição ao Malation durante o período peripuberal poderá trazer prejuízos para o desenvolvimento dos sistemas genital masculino, gastrointestinal, renal e hepático de ratos. Os animais serão distribuídos casualmente em três grupos experimentais (n=25 animais/grupo). Dois grupos de animais serão tratados com Malation nas doses de 10 mg/Kg ou 50 mg/Kg de peso corpóreo via gavage. Essas doses correspondem a 0,5% e 2,5%, respectivamente, da DL50 oral para ratos (DL50 oral =2000 mg/kg) (U S EPA, 2000). O outro grupo (grupo controle) receberá apenas o veículo (óleo de soja) em igual volume. No 80º dia experimental os ratos serão anestesiados com a associação de xilazina e quetamina e mortos por punção cardíaca para a coleta do sangue em tubo heparinizado (heparina sódica) para dosagens hormonais. GI 1

Vigência do Projeto	30/08/2016 a 30/08/2019
Espécie/linhagem	Rato heterogênico / Wistar
Nº de animais	75
Peso/Idade	Indeterminado / 22 dias
Sexo	Machos
Origem	Biotério Central / UEL
Amostras a serem coletadas	Testículos, epidídimos, vesícula seminal, próstata, sangue, fígado, estômago, rim, intestino, fêmur

Cumpre orientar que caso pretendam-se quaisquer alterações no protocolo experimental aprovado, deve-se submeter o novo protocolo à apreciação da CEUA/UEL anteriormente à execução das modificações.

Coloco-me à disposição para quaisquer esclarecimentos que se fizerem necessária. Sem mais para o momento, subscrevo, cordialmente,

Prof. Dr. João Waine Pinheiro
Vice-Coordenador da CEUA/UEL

Ilma. Sra.
Profa. Dra. Glaura Scantamburlo Alves Fernandes
Coordenadora do Projeto
Departamento de Biologia Geral / Centro de Ciências Biológicas
Com cópia Waldiceu A. Verri Junior (Coord. do Biotério Central/UEL); Chefe do Departamento de Biologia Geral e Diretor(a) do Centro de Ciências Biológicas

Anexo B

Universidade
Estadual de Londrina

COMISSÃO DE ÉTICA NO USO DE ANIMAIS

OF. CIRC. CEUA Nº 68/2017 **Londrina, 31 de maio de 2017.**

Prezado (a) professor (a)

Certificamos que o projeto intitulado: " **Avaliação dos efeitos da Ciclosporina A como contraceptivo masculino em camundongos,"** protocolo CEUA **n°10952.2017.79**, sob a responsabilidade de **Glaura Sacatambulo Alves Fernandes**, que envolve a produção, manutenção e/ou utilização de animais pertencentes ao filo Chordata, subfilo Vertebrata (exceto o homem) para fins de pesquisa científica (ou ensino), encontra-se de acordo com os preceitos da Lei nº 11.794, de 8 de outubro de 2008, do Decreto nº 6.899, de 15 de julho de 2009, e com as normas editadas pelo Conselho Nacional de Controle da Experimentação Animal (CONCEA), foi **aprovado** pela Comissão de Ética no Uso de Animais da Universidade Estadual de Londrina (CEUA/UEL), em reunião realizada em **30/05/2017.**

O Objetivo é investigar Diante da relevância clínica e social do assunto e também pela falta de informações precisas na literatura especializada, os objetivos deste estudo são: (1) avaliar se a Ciclosporina A possui efeitos contraceptivos em camundongos machos adultos; (2) analisar se estes efeitos são reversíveis, mesmo após tratamentos mais longos; (3) avaliar as consequências do uso desta droga a longo prazo para o sistema genital masculino; (4) avaliar se a dose utilizada apresenta efeitos hepatotóxicos e nefrotóxicos. Grau invasividade=2

Vigência do Projeto	01/07/2017 a 31/06/2020
Espécie/linhagem	Camundongo Heterogênico / Swiss
Nº de animais	104
Peso/Idade	50 dias
Sexo	Machos
Origem	Biotério Central da Universidade Estadual de Londrina/UEL
Amostras a serem coletadas	Sangue, Punção cardíaca, Testículos e epidídimos, Ductos deferentes, Fígado e Rim.

Cumpre orientar que caso pretendam-se quaisquer alterações no protocolo experimental aprovado, deve-se submeter o novo protocolo à apreciação da CEUA/UEL anteriormente à execução das modificações.

Coloco-me à disposição para quaisquer esclarecimentos que se fizerem necessária. Sem mais para o momento, subscrevo, cordialmente,

Prof. Dr. João Waine Pinheiro
Vice-Coordenador da CEUA/UEL

Ilmo.(a) Sr.(a)
Prof. (a) Dr (a). Glaura Scantambulo Alves Fernandes
Responsável pelo projeto
Departamento de Biologia Geral/CCB

C/C para a Chefia do Depto de Biologia Geral/CCB
C/C para o Biotério do CCB da UEL
C/C para a Direção de Centro do CCB

Campus Universitário: Rodovia Celso Garcia Cid (PR 445), km 380 - Fone (043) 3371-4000 PABX - Fax 3328-4440 - Caixa Postal 10.011 - CEP 86057-970 - Internet http://www.uel.br
LONDRINA - PARANÁ - BRASIL

Anexo C

Guia para autores:

Acta Histochemica: https://www.elsevier.com/journals/acta-histochemica/0065-1281/guide-for-authors

Human & Experimental Toxicology: https://journals.sagepub.com/author-instructions/HET